Fundamental Study on Novel Synthetic Polymer Systems for Fine Particles Settling

by

Han Lu

A thesis submitted in partial fulfillment of the requirements for the degree of

Master of Science

in

Chemical Engineering

Department of Chemical and Materials Engineering

University of Alberta

Abstract

In this study, Random copolymers poly[(2-aminoehtyl methacrylamide hydrochloride)-*st*-(5-methacrylamido-1,2-benzoboroxole)-*st*-(*N*-isopropylacrylamide)] (PAMN) and glycopolymer poly (2-lactobionamidoethylmethacrylamide) (PLAEMA) with various molecular weights were synthesized via conventional free radical polymerization method. The effect of temperature, pH, molecular weight and polymer dosage on the kaolin particle settling rate, turbidity of supernatant, mud-line position, solid volume fraction of sediment, and solid content of sediment were evaluated to determine the flocculation performance. Temperature and pH responsive polymer PAMN was considered as the most efficient flocculant as compared with poly[(2-aminoethyl methacrylamide hydrochloride)-*st*-(*N*-isopropylacrylamide)] (PAN) and Poly(N-isopropylacrylamide) (PNIPAAm). Furthermore, highly compact sediment can be achieved through increasing pH to 11 due to the cationic/anionic transfer property of PAMN. For the study of PLAEMA, large molecular weight has been proved to possess the positive effect on flocculating kaolin fine particles. The adhesive force, polymer

conformation, and other property characterization were determined by several instruments, including surface forces apparatus (SFA), atomic force microscopy (AFM), dynamic light scattering (DLS), and gel permeation chromatography (GPC). Strong adhesion was measured between mica surface and polymers in the case of PAMN and high molecular weight PLAEMA, resulting from benzoboroxole-hydroxyl complexation, electrostatic interaction, hydrogen bonding and flexible polymer chains. The roughness change of polymer coated mica surface is also an evidence of polymer adsorption and aggregation, contributing to the enhanced flocculation behavior. The results in this thesis provide insight into the development of novel polymer flocculants and basic interaction mechanisms between polymer flocculants and fine particles.

Preface

Chapter 3 of this thesis has been published as Lu, H.; Wang, Y.; Li, L.; Kotsuchibashi, Y.; Narain, R.; Zeng, H. "Temperature- and pH-Responsive Benzoboroxole-Based Polymers for Flocculation and Enhanced Dewatering of Fine Particle Suspensions." *ACS Appl. Mater. Interfaces* **2015**, *7* (49), 27176–27187.

Chapter 4 of this thesis will be submitted for publication as Lu, H.; Xiang, L.; Cui, X.; Liu, J.; Wang, Y.; Narain, R.; Zeng, H. "Effect of Molecular Weight of Synthesized Poly (2-lactobionamidoethylmethacrylamide) on Flocculation and Dewatering."

For the work of these two chapters, I was responsible for the design of experiment procedure, data collection and organization, and writing the manuscripts. Wang, Y. and Li, L. assisted with the revision of manuscript. Cui, X. contributed to the Atomic Force Microscopy (AFM) image. Xiang, L. contributed to the Surface Forces Apparatus (SFA) measurement. Liu, J. helped to measure the particle size distribution by Mastersizer. Dr. Zeng, H. and Dr. Narain, R. are corresponding authors and involved with the manuscript and experiment.

Acknowledgement

Table of Content

List of Tables

List of Figures

List of Symbols

A	Hamaker constance, J
D	Separation distance between surfaces, m
$\Delta Dapplied$	Distance that moved by micrometers, m
$\Delta Dmeans$	Actual distance, m
$\Delta Djump$	Jump distance, m
e	The charge of one electron
F (D)	Normal force at distance D, N
H	Height of original suspension, m
h_f	Height of sediment, m
K	Spring constant, N/m
k_B	Boltzmann constant
m_f	Mass of sediment, g
m_s	Mass of solid in the sediment, g
M_n	Number average molecular weight, kDa

M_w	Weight average molecular weight, kDa
P_B	Probability of polymers cover on particles
R_1, R_2	Radius of spherical particle, m
R_H	Hydrodynamic radius, m
T	Absolute temperature, K
V_e	Elution volume, ml
V_f	Sediment volume, ml
x	Distance from the position of stern layer, m
z	Ion valency
ρ_i	ion density in bulk
ρ_s	Density of mineral solid, g/cm^3
η	Viscosity of solution, cP
θ	Surface coverage by flocculants in one particle
φ_f	Solid volume fraction of sediment
ε_0	Permittivity of the vacuum, F/m

ε	Dielectric constant
ψ	Electrostatic potential, mV
ζ	Zeta-potential, mV
μ_E	Electrophoretic mobility

List of Acronyms

ACVA	4',4-azobis (4-cyanovaleric acid)
AEMA	2-aminoethyl methacrylamide hydrochloride
AFM	Atomic force microscope
CHWE	Clark hot water extraction
CT	Composite tailing
CCC	Critical coagulant concentration
DLS	Dynamic light scattering
DMF	Dimethylformamide
DP	Repeating unite number
ELS	Electrophoretic light scattering
FECO	Fringes of equal chromatic order
GPC	Gel permeation chromatography
ISR	Initial settling rate
LAEMA	(2-lactobionamidoethylmethacrylamide)

LCST	Lower critical solution temperature
MAAmBo	5-methacrylamido-1,2-benzoboroxole
MBI	Multiple beam interference
MFT	Mature fine tailings
NMR	Nuclear magnetic resonanc
NTU	Nephelometric turbidity units
PAMN	P(AEMA51-st-MAAmBo76-st-NIPAM381)
PAN	P(AEMA57-st-NIPAM509)
PBA	Phenylboronic acid
PDI	Polydispersity of molecular weight
PEO	Poly (ethylene oxide)
PLAEMA177	PLAEMA with molecular weight of 83 kDa
PLAEMA397	PLAEMA with molecular weight of 186 kDa
PLAEMA975	PLAEMA with molecular weight of 456 kDa
PNIPAAm	Poly (N-isopropylacrylamide)

PVA	Poly (vinyl alcohol)
SAGD	Steam-assisted gravity-drainage
SFA	Surface forces apparatus
SLS	Static light scattering
TEMED	N,N,N', N'-tetra- methylenediamine
TFT	Thin fine tailings
VDW	Van der Waals

Chapter 1 Introduction

1.1 Fundamentals of oil sands

In the past decades, the Canadian economy is mainly fueled by its oil sands industry. The oil sands deposit located in Northern Alberta has been proven to be one of the largest oil deposits in the world. The main deposits of Canada are located in three positions, including Athabasca region, Peace River, and Cold Lake, with reserves of 170 billion barrels of bitumen which is potentially to be capable of supplying crude oil worldwide over 200 years.[1-3] Even though, bitumen extraction from oil sands is more costly than the conventional crude oil, the increasing demand of resource and the technological advance triggered the fast development of oil sands industry. The daily production of crude oil in 2013 is about 3.4 million barrels in Canada, and from which 1.9 million barrels were from oil sands extraction. The daily production of crude oil from oil sands in Canada is able to increase up to 4.8 million barrels in 2030 as expected.[4] However, the issue of local fresh water protection has become a severe challenge along with the rapid expansion of oil sands industry.[5-9] Recently, Clark Hot Water Extraction (CHWE) and Steam-Assisted Gravity-Drainage (SAGD) are the two most significant methods for bitumen extraction,[10-14] and the flow diagrams of the both bitumen extraction technologies were shown in Figure 1.1 and Figure 1.2.
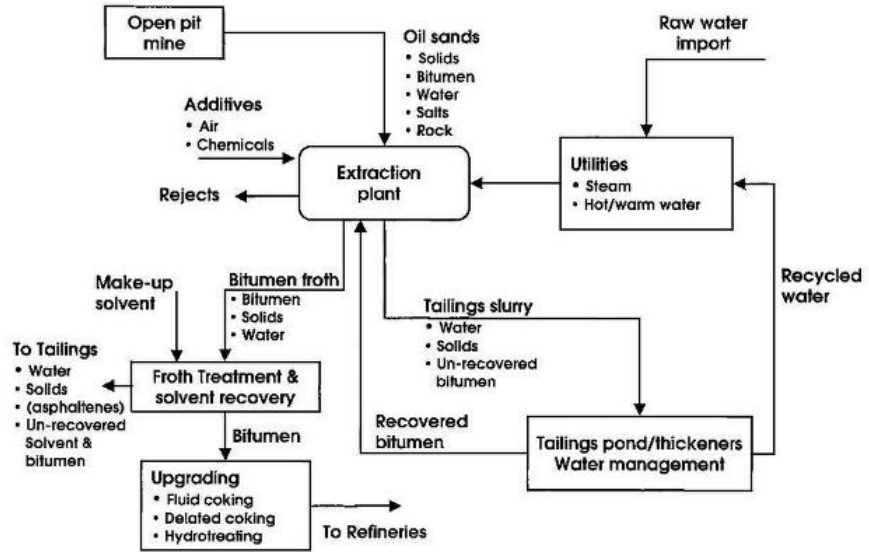
Figure 1.1. Flow chat of Clark Hot Water Extraction (CHWE).[3]
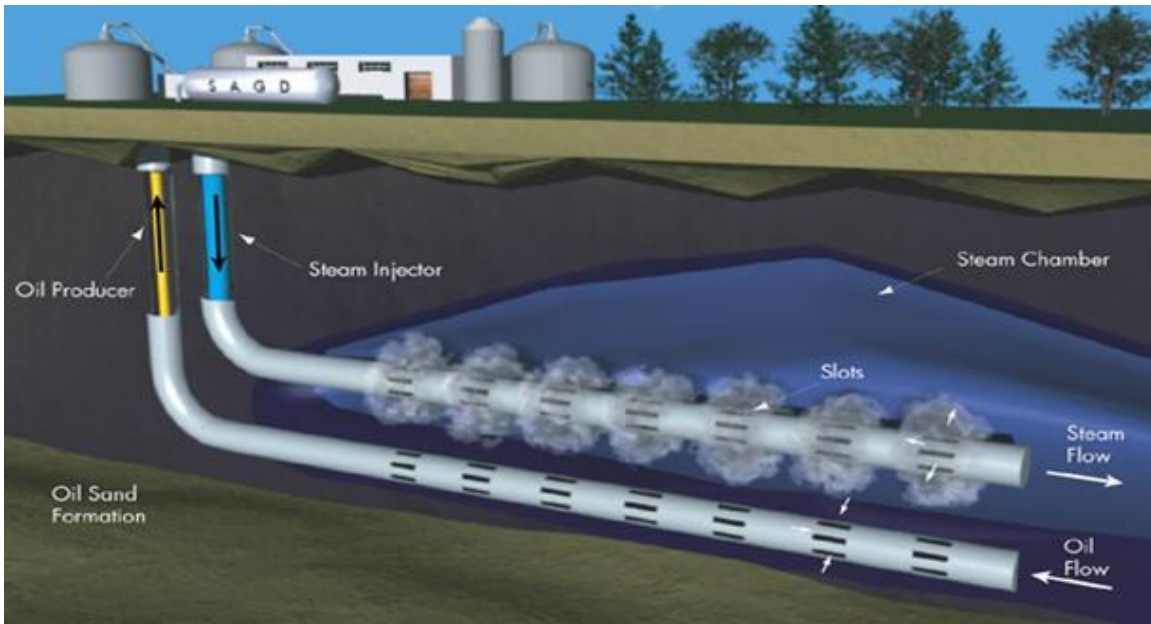
Figure 1.2. Scheme diagram of steam assisted gravity drainage (SAGD).

1.2 Review of the tailing property and tailing management

CHWE is a technique using hot water, steam, and soda caustic to separate the

bitumen from oil sands, along with the production of the alkaline aqueous by-product

(tailing) composed with residual bitumen, sands, fine particles (<44 μm).[15] The oil sands tailing system is difficult to investigated, attributed to the composition varies with ore quality, sources, extraction process, etc. However, the general composition is ~70 - 80 wt% water, ~20 - 30 wt% solid and fine particles, and ~1 - 3 wt% unrecovered bitumen. Initially, fine clays, sands, and residual bitumen flow with alkaline water to the tailings pond at a solid content of ~8 wt% to form the so-called Thin Fine Tailings (TFT), which will consolidates to approximately 20 wt% solid content in a few weeks.[16-17] After several years of consolidation, the solid content of the sediment will reach ~30 - 35 wt% to form the Mature Fine Tailings (MFT),[18-20] as shown in Figure 1.3, which suffers from extremely slow settling rate and remains the fluid-like state for decades due to the residual bitumen on the particle surface. The viscosity of MFT increases up to about 5000 cP with the deposit time. From work previously reported[15], about 3 cubic meter of water is trapped in the tailings with the production of 1 cubic meter of bitumen. The poor consolidation is attributed to the electrostatic repulsion arisen from the enhanced negatively charged clay surfaces in the basic condition. In addition, a total area of 130 km^2 has been occupied by tailings pond. From both perspectives of the environment and economy, improvement of tailing management is a critical and necessary task.
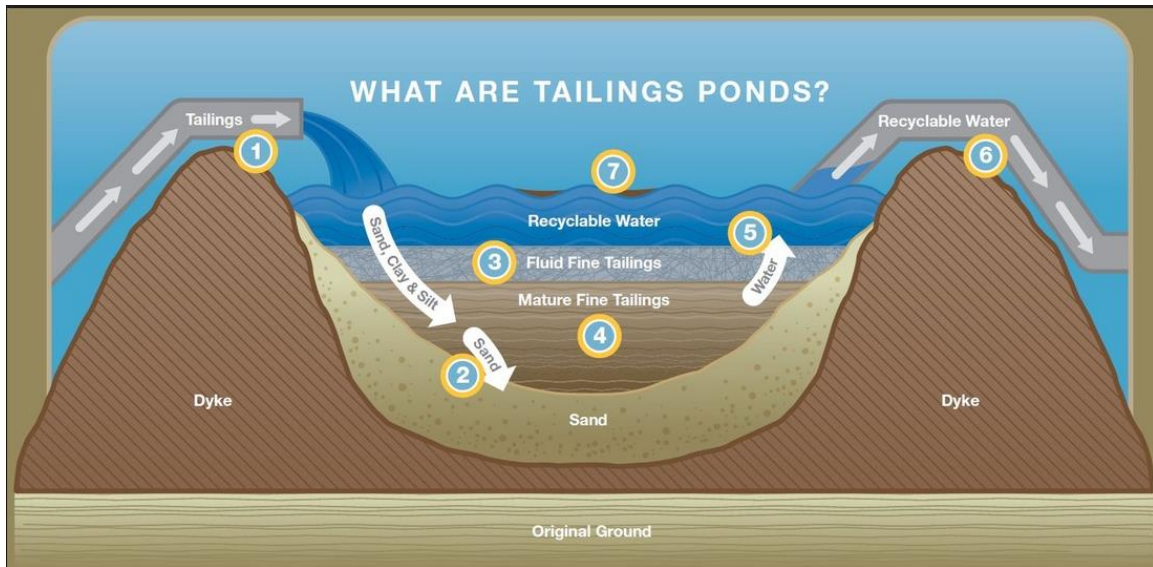
Figure 1.3. The formation mechanism of mature fine tailings (MFT).

Several technologies have been developed to increase the settling rate and to enhance the consolidation of tailings, among which only a few have been applied in commercial scale. For the Physical Process, filtration is one of the most traditional and broadly used method to obtain high recovery of process water and compact dry tailings, using pressure or vacuum force. However, the dry tailing can be only transported by vehicles, coupled with the operation of filtration equipment, leading to higher cost to recycle process water. Thermal drying MFT is a method based on thermal energy, which is able to remove much more water than any other techniques. The moisture of tailings is reduced by the high temperature provided by oven or kiln, but leading to huge energy cost. Electric treatment is put into use to increase settling rate by appling the electrical field directly to the high solid content MFT. Under the electrokinetic effect, negatively charged clays migrate toward the positively charged electrode, contributing to the higher velocity of settling and

enhanced consolidation.[21] Other techniques include, centrifugation, Composite Tailing (CT), freeze/thaw etc.

For the chemical tailing management, Reduce Dispersion of Fines in Process is a new technique to reduce the dispersion of fine clays through developing the novel processes different from the established Clark Hot Water Extraction (CHWE). For example, a non-caustic bitumen extraction process has been developed in order to decrease the difficulty of clay aggregation and consolidation. By changing the pH of slurry, the surface activity will be reduced and the card-house structure of clays and flocs will collapse.[22-24] Thus, In-situ Chemical Treatment is used to increase the consolidation efficiency through injecting chemical reagents, which is able to change pH or facilitate coagulation/flocculation, into MFT in-situ. In-situ Biological Treatment is a method contributing to enhance the bacterial action, resulting in the consolidation of MFT.[25] In addition to the techniques mentioned above, Thickened Tailing and Consolidated Tailing (CT) techniques are two most significant and widely used chemical tailing treatment methods. CT is a technique through mixing gypsum with tailing slurry to reduce the activity of particle surface, in order to increase the probability of collision and aggregation of particle.[26,27] However, the introduction of calcium ions into process water has a negative effect on bitumen extraction. TT technology is also known as paste technology, in which flocculant that aid for aggregating fine particles and accelerating settling rate, is added to the tailing slurry to reuse the water back to bitumen extraction

process without much thermal energy loss. Moreover, as compared with CT technology, polymer flocculant possesses the advantage of less side effect on the chemistry of reused process water. The CT and TT technologies are mainly based on the mechanism of coagulation and flocculation, which will be discussed in details later.

1.3 Coagulation and flocculation

In suspension, individual fine particles are dispersed by various repulsion. The long range electrostatic repulsion was caused by electrical double-layer on particle surface. For example, kaolinite crystal is composed with alumina octahedral and silica tetrahedral layers, which enable the particles to be negatively charged in caustic condition.[28, 29] Steric repulsion arises from the loops and tails of the non-ionic polymers that are fully covered on the particle surfaces due overdose of flocculant. For the hydration repulsion case, excess energy is required for the particles to be brought into close proximity, resulting from the existence of hydrated ions on the particle surface. Coagulation is aimed to depress or eliminate the effect of repulsions mentioned above through mixing or adding chemical agents, such as cationic ions or polyelectrolyte, to the suspension or slurry. By doing this, the predominated van der Waal force is able to increase the probability of particle collision and aggregation. As we mentioned, gypsum is often used as coagulant to mix with tailing slurry, in order to neutralize the surface charge of particle. High salt concentration also has a positive effect on the compression of electrical double layer, reducing energy barrier that hinders the approach of particles.[30] The optimal dosage of

coagulant, which results in the most rapid aggregation and settling, is known as critical coagulant concentration (CCC), at which the energy barrier is reduced to zero. Through the method to control pH value, potential determining ions (hydrogen and hydroxyl) are introduced to help adjust zeta potential of clays in oil sands tailings, avoiding the use of calcium ions which is detrimental to the efficiency of bitumen extraction.

The settling mechanism of flocculation relies on bridging particles by polymer chain, forming flocs large enough to settle down under the effect of gravity. Regardless reduction of repulsion force, long polymer chain is able to reach out of the range of electrical double layer repulsion to adsorb on multiple particle surfaces. The flocculant dosage is a significant factor for efficient bridging and settling due to well dispersion is beneficial for polymer to diffuse to the particle surface and bridge fine particles by extended loops and tails. Overdose will lead to stiff polymer backbones and steric force which does harm to the flocculation and settling. In general, settling rate will reach the highest value when about half of the particle surfaces are covered by flocculant. Moderate charge density of cationic/anionic segment in the polymer chain has a positive effect on the extension of polymer chain in the suspension due to intramolecular electrical double layer repulsion, which also increases the adhesion of polymer on the particle surfaces. In addition, the counter-ionic (cationic) polymers possesses the function of neutralizing charge of particles, facilitating the collision and aggregation of particles (coagulation). The charge density of anionic polymer will hinder its adhesion with

negatively charged surface. However, some work reported previously showed that, salt concentration of the tailings affects the settling and adhesion results, attributed to that high salt concentration is beneficial to compress the electrical double layer, resulting in less repulsion of polymer on the particle surface.[30] Under the effect of hydrogen bonding and Van der Waals force, high molecular weight anionic flocculant is effect to aggregate particles. Non-ionic polymers like PEO and PVA are also widely studied and used as effective flocculant due to the existence of hydrogen bonding and Van der Waals force. Due to the presence of electrical double layer repulsion, coupled with the covered polymer strings, the structure of formed flocs and aggregates are relatively loose, as compared to the coagulation method, trapping large amount of water in the interval of sediment. To overcome these limitations, temperature responsive polymers have been proven as efficient flocculant to induce rapid settling and compact sediment, among which poly (N-isopropylacrylamide) (PNIPAAm) is a typical representative, whose lower critical solution temperature (LCST) is about 32 °C.[31-35] Above LCST, PNIPAAm transfers from hydrophilic to hydrophobic and aggregates in the water solution. Adding PNIPAAm to the tailings at temperature lower than LCST, polymer will adsorb on particle surface due to hydrogen bonding and van der Waals force. Then increasing temperature higher than LCST results in the growth of flocs with aggregation of PNIPAAm, attributed to hydrophobic interaction which will reduce by lowering temperature. Removing stimulus results in the breakup of big flocs, facilitating the

sediment consolidate well. In order to induce faster settling rate, cationic residues were introduced in the PNIPAAm homopolymer to increase the adhesive force of polymer to particles. The incorporation of charged (hydrophilic) groups in the PNIPAAm will increase the LCST of copolymers, and incorporation of hydrophobic segment will do the opposite.

1.4 Intermolecular and surface force

Polymer are popular to be used as effective flocculant or coagulant in tailing management. The polymer-polymer and polymer-particle interaction are highly significant to achieve a deep understanding of flocculation mechanism and to optimize technology of tailing treatment.

1.4.1 Hydrogen bonding and Van der Waals force

Hydrogen bonding is always existing between a hydrogen atom and a strongly electronegative atom which closes to another electronegative atom, and bonding by a lone electrons pair. In general, hydrogen bonding is stronger than ordinary dispersion and dipole-dipole forces and about tenth strength of average covalent bonds. The hydrated layer of hydrophilic particle results from that the charge on the surface of particle facilitates water to form hydrogen bonding with the oxygen atoms at the oxide particles. One water molecule are potentially able to form hydrogen bonding with four other nearby water molecules, resulting in its relatively high boiling point as compared to some other

solvent.

The forces used to describe intermolecular interaction among molecules are generally called Van der Waals (VDW) forces, which was named after the Dutch scientist Johannes Diderik van der Waals, including dipole-dipole force (Keesom force), dipole-induced dipole force (Debye force), and London Dispersion force. For the Keesom force case, polar molecules with permanent electric dipole moments attract/repel the charged end of another polar molecule with its charged end, depending on the mutual orientation. The molecules have permanent dipole moment are also able to polarized molecules without dipole, making a little shift of the electric charge distribution and inducing a dipole. The induced dipole will attracted by the permanent dipole. The location of electron is uncertain of the time since that they move all the time. However, the temporary dipole of non-polarized molecule is formed when all the electron located at the same area at once and formed a negatively charged end. The momentary dipole will induce the surrounding molecules to have instant induced dipoles to interact with the negatively charged end. This phenomenon is called London Dispersion Force. The energy of Van der Waals force follows the distance tendency that the potential energy decreases with $\frac{1}{D^6}$, since all the molecule interaction mentioned above have the same distance tendency. The Van der Waals force between two spheres of radius R is determined by the equation as $F = -\frac{AR}{6D^2}$. For the case of two crossed cylinders, the formula is expressed as $F = -\frac{A}{6D^2}\sqrt{R_1 R_2}$. A represents Hamaker constant, D is the distance between two

surfaces. R_1, R_2 is the radii of two cylinder respectively.

1.4.2 Electrical double layer and electrostatic force

Surfaces in the water are always charged since that ions are readily to adsorb on or dissociate from surface due to the high dielectric constant of water. Amino groups, for instance, can easily be protonated in water to show positive charge, and oxide always shows negative charge resulting from the proton dissociation of exposed hydroxyl groups. The electric field caused by the charged surface attracts ions with opposite charge, forming the electrical double layer. The simplest model of electrical double layer was put forward by Helmholtz in 1850, which suggests that the ions held on the surface will redistribute the concentration and the surface will remain neutral due to the neutralization of counter ions in the bulky solution. Afterwards, Gouy and Chapman proposed the new model of electrical double layer which named as "Gouy-Chapman model", explained that the concentration of ions is a function of distance away from surface. In this model, the electric attraction from the counter-ions and the repulsion from the co-ions are considered, combined with some other forces, the order arisen from electric force is disturbed. In equilibrium situation, counter-ions have large probability to present near the surface as compared to the co-ions. Electrical double layer is formed with stern layer and diffusive layer. Stern layer is between the charged surface and the plane formed with the adsorbed counter-ions centers. The electric potential energy in stern layer decreases linearly with the distance away from surface. Both of the counter-ions and co-ions exist in diffusive

layer and the electric potential energy decrease exponentially with the increase of distance and be described by Poisson-Boltzman Equation as:

$$\frac{d^2\psi}{dx^2} = -\sum_i \left(\frac{z_i e \rho_i}{\varepsilon \varepsilon_0}\right) e^{-\frac{z_i e \psi}{kT}}$$

where ε and ε_0 represent the dielectric constant and permittivity of vacuum respectively, z represents the valence of ions, ψ represents the electric potential, ρ_i represents the ion density in bulk, x is the distance from the position of stern layer.

The counter-ions in the shear plane (in the diffusive layer) move with the particles, attributed to the Coulomb force of ions to the particle surface. Since surface potential and stern potential are both difficult to be measured, zeta potential is always obtained by equipment to character the electric property of particles. The particles in the solution move towards the electron with opposite charge under the influence of applied electric field. In contrary, the fluid viscous force is in the opposite direction as compared to electric force. When the equilibrium of the two forces is achieved, the ratio of particle velocity and the strength of applied electric field determines electrophoretic mobility μ_E, which can be used to calculate zeta potential by the Smoluchowski equation as

$$\mu_E = \frac{2\varepsilon\varepsilon_0\zeta f(\kappa\alpha)}{3\eta}$$

Where f ($\kappa\alpha$) is Henry's function, ζ and η are zeta potential and viscosity of solution respectively.

1.4.3 Bridging force and steric force

One polymer chain adsorb on and bridge multiple particles to promote the particles aggregation and floc growth, increasing the rate of settling, which is the fundamental mechanism of the so-called paste technology of tailing management. In general, high molecular weight flocculant provides more loops and tails to bridge particles, resulting in larger bridging force. Polymer dosage is a critical factor that affect the flocculation performance. Too small amount of polymer might not provide sufficient bridging force for particle aggregation. However, overdose of polymer will also do harm to flocculation due to less bare space of particle surface for the loops and tails to attach on. The overlapping of polymer mushroom and brush also stabilize the particles due to steric force. As the particles approach closer, the mutual penetration of those adsorbed polymer chains requires extra energy for the polymers to dehydrate, thus leading to the repulsive steric force. Since Van der Waals attractive force decreases with distance, the thick of polymer layer plays a significant role of dispersing particles in the suspension. Thicker polymer layer is required to stabilize particles with large size as compared with small ones, resulting from that Van der Waals attractive force is proportional to the radii of particle.

1.5 Reference

(1) Timilsina, G. R.; Prince, J. P.; Czamanski, D.; LeBlanc, N. Impacts of Crude Oil Production from Alberta Oil Sands on the Canadian Economy. In *EcoMod 2005 International Conference on Policy Modeling, Istanbul, June*; 2005.

(2) Berkowitz, N.; Speight, J. G. The Oil Sands of Alberta. *Fuel* **1975**, *54* (3), 138–149.

(3) Masliyah, J.; Zhou, Z. J.; Xu, Z.; Czarnecki, J.; Hamza, H. Understanding Water-Based Bitumen Extraction from Athabasca Oil Sands. *Can. J. Chem. Eng.* **2004**, *82* (4), 628–654.

(4) Söderbergh, B.; Robelius, F.; Aleklett, K. A Crash Programme Scenario for the Canadian Oil Sands Industry. *Energy Policy* **2007**, *35* (3), 1931–1947.

(5) Kelly, E. N.; Schindler, D. W.; Hodson, P. V.; Short, J. W.; Radmanovich, R.; Nielsen, C. C. Oil Sands Development Contributes Elements Toxic at Low Concentrations to the Athabasca River and Its Tributaries. *PNAS* **2010**, *107* (37), 16178–16183.

(6) Kelly, E. N.; Short, J. W.; Schindler, D. W.; Hodson, P. V.; Ma, M.; Kwan, A. K.; Fortin, B. L. Oil Sands Development Contributes Polycyclic Aromatic Compounds to the Athabasca River and Its Tributaries. *Proceedings of the National Academy of Sciences* **2009**, *106* (52), 22346–22351.

(7) Rogers, V. V.; Wickstrom, M.; Liber, K.; MacKinnon, M. D. Acute and Subchronic Mammalian Toxicity of Naphthenic Acids from Oil Sands Tailings. *Toxicol. Sci.* **2002**, *66* (2), 347–355.

(8) El-Din, M. G.; Fu, H.; Wang, N.; Chelme-Ayala, P.; Pérez-Estrada, L.; Drzewicz, P.; Martin, J. W.; Zubot, W.; Smith, D. W. Naphthenic Acids Speciation and Removal during Petroleum-Coke Adsorption and Ozonation of Oil Sands Process-Affected Water. *Science of the Total Environment* **2011**, *409* (23), 5119–5125.

(9) Beynon, B. M.; Pemberton, S. G.; Bell, D. D.; Logan, C. A. Environmental Implications of Ichnofossils from the Lower Cretaceous Grand Rapids Formation, Cold Lake Oil Sands Deposit. **1988**.

(10) Liu, J.; Xu, Z.; Masliyah, J. Interaction between Bitumen and Fines in Oil Sands Extraction System: Implication to Bitumen Recovery. *The Canadian Journal of Chemical Engineering* **2004**, *82* (4), 655–666.

(11) Humphreys, R. D. *Tar Sands Extraction Process*; Google Patents, 1999.

(12) Filby, J.; Aviezer, S.; Tannenbaum, E. *Oil Sands Extraction*; Google Patents, 2010.

(13) Shin, H.; Polikar, M.; others. Optimizing the SAGD Process in Three Major Canadian Oil-Sands Areas. In *SPE Annual Technical Conference and Exhibition*; Society of Petroleum Engineers, 2005.

(14) Butler, R.; others. SAGD Comes of Age! *Journal of Canadian Petroleum Technology* **1998**, *37* (07).

(15) Masliyah, J.; Czarnecki, J.; Xu, Z. Handbook on Theory and Practice of Bitumen Recovery from Athabasca Oil Sands. *Vol. I. Theoretical basis* **2010**.

(16)Kasperski, K. L. A Review of Properties and Treatment of Oil Sands Tailings. *AOSTRA Journal of Research* **1992**, *8*, 11–11.

(17)Allen, E. W. Process Water Treatment in Canada's Oil Sands Industry: I. Target Pollutants and Treatment Objectives. *Journal of Environmental Engineering and Science* **2008**, *7* (2), 123–138.

(18)Xu, Y.; Dabros, T.; Kan, J. Filterability of Oil Sands Tailings. *Process Safety and Environmental Protection* **2008**, *86* (4), 268–276.

(19)Revington, A. P.; Omotoso, O.; Wells, P. S.; Hann, T. C.; Weiss, M. H.; Bugg, T.; Eastwood, J.; Young, S. J.; O'neill, H. R.; Sanchez, A. C.; et al. *Process for Flocculating and Dewatering Oil Sand Mature Fine Tailings*; Google Patents, 2010.

(20)Penner, T. J.; Foght, J. M. Mature Fine Tailings from Oil Sands Processing Harbour Diverse Methanogenic Communities. *Can. J. Microbiol.* **2010**, *56* (6), 459–470.

(21)Powter, C. B.; Biggar, K. W.; Silva, M. J.; McKenna, G. T.; Scordo, E. B. Review of Oil Sands Tailings Technology Options. In *Tailings and Mine Waste*; 2011; Vol. 10.

(22)Permien, T.; Lagaly, G. The Rheological and Colloidal Properties of Bentonite Dispersions in the Presence of Organic Compounds V. Bentonite and Sodium Montmorillonite and Surfactants. *Clays and Clay Minerals* **1995**, *43* (2), 229–236.

(23)Oster, J. D.; Shainberg, I.; Wood, J. D. Flocculation Value and Gel Structure of Sodium/calcium Montmorillonite and Illite Suspensions. *Soil Science Society of America Journal* **1980**, *44* (5), 955–959.

(24) McFarlane, A.; Bremmell, K.; Addai-Mensah, J. Improved Dewatering Behavior of Clay Minerals Dispersions via Interfacial Chemistry and Particle Interactions Optimization. *Journal of colloid and interface science* **2006**, *293* (1), 116–127.

(25) Allen, E. W. Process Water Treatment in Canada's Oil Sands Industry: II. A Review of Emerging Technologies. *Journal of Environmental Engineering and Science* **2008**, *7* (5), 499–524.

(26) Renault, S.; Lait, C.; Zwiazek, J. J.; MacKinnon, M. Effect of High Salinity Tailings Waters Produced from Gypsum Treatment of Oil Sands Tailings on Plants of the Boreal Forest. *Environmental Pollution* **1998**, *102* (2), 177–184.

(27) Chalaturnyk, R. J.; Scott, J. D.; Özüm, B. Management of Oil Sands Tailings. *Petroleum Science and Technology* **2002**, *20* (9-10), 1025–1046.

(28) Murray, H. H. Applied Clay Mineralogy Today and Tomorrow. *Clay minerals* **1999**, *34* (1), 39–39.

(29) Hu, Y.; Liu, X.; Xu, Z. Role of Crystal Structure in Flotation Separation of Diaspore from Kaolinite, Pyrophyllite and Illite. *Minerals Engineering* **2003**, *16* (3), 219–227.

(30) Ji, Y.; Lu, Q.; Liu, Q.; Zeng, H. Effect of Solution Salinity on Settling of Mineral Tailings by Polymer Flocculants. *Colloids and Surfaces A: Physicochemical and Engineering Aspects* **2013**, *430*, 29–38.

(31) Zhu, X.; Yan, C.; Winnik, F. M.; Leckband, D. End-Grafted Low-Molecular-Weight PNIPAM Does Not Collapse above the LCST. *Langmuir* **2007**, *23* (1), 162–169.

(32) Ohya, S.; Nakayama, Y.; Matsuda, T. Thermoresponsive Artificial Extracellular Matrix for Tissue Engineering: Hyaluronic Acid Bioconjugated with Poly (N-Isopropylacrylamide) Grafts. *Biomacromolecules* **2001**, *2* (3), 856–863.

(33) Lutz, J.-F.; Akdemir, Ö.; Hoth, A. Point by Point Comparison of Two Thermosensitive Polymers Exhibiting a Similar LCST: Is the Age of Poly (NIPAM) Over? *Journal of the American Chemical Society* **2006**, *128* (40), 13046–13047.

(34) Kawaguchi, H.; Fujimoto, K.; Mizuhara, Y. Hydrogel Microspheres III. Temperature-Dependent Adsorption of Proteins on Poly-N-Isopropylacrylamide Hydrogel Microspheres. *Colloid and Polymer Science* **1992**, *270* (1), 53–57.

(35) de las Heras Alarcón, C.; Farhan, T.; Osborne, V. L.; Huck, W. T.; Alexander, C. Bioadhesion at Micro-Patterned Stimuli-Responsive Polymer Brushes. *Journal of Materials Chemistry* **2005**, *15* (21), 2089–2094.

Chapter 2 Experimental Techniques

2.1 Surface forces apparatus (SFA)

2.1.1 Development of SFA

Before the first version of surface forces apparatus showed up, Derjaguin and co-workers found that a repulsive force of non-electrostatic origin existed between the surfaces at high electrolyte concentrations when they used two crossed polarized metal wires to measure the potential barrier between the wires in electrolyte solutions.[1]

After that, the first apparatus was described by Tabor and Winterton in 1969, which was able to measure the forces between two surfaces for separation distance as low as 5–30 nm with a 3 Å distance resolution in the air,[2] followed by several update versions with improved techniques.[3-5]

SFA Mk I was then described by Israelachvili and Adams to measure the forces in the liquid media, but not in the air. A motor-driven micrometer and a piezoelectric crystal was used in SFA Mk I, resulted in that the two mica surfaces were able to move toward or apart from each other in a range of control from the micrometer to the ångstrom level.[6,7] Some significant attachments were added to SFA Mk II for more interfacial phenomenon study. The single cantilever was replaced by the double cantilever in the new apparatus. By doing this, the strength was increased to prevent the surfaces from rotating. In addition, the added "friction device" contributed to the lateral direction motion of the

upper surface. The Mk III was developed and tested during the period 1985-1989 and then described by Israelachvili and McGuiggan[5] since SFA was gradually used in more complex system. Due to the "separation chambers" design, the control system in the upper chamber sealed by Teflon was less likely to be degraded due to materials used in various experiments. While, the surfaces and bathing solution was in the lower chamber. By doing this, more stable thermal drift, more linear and larger motion range were achieved.

SFA 2000 was designed to address the drawbacks existed in SFA Mk III. The schematic of the main components of SFA 2000 is shown in Figure 2.1. The main components of this device are micrometers, the main stage with central single-cantilever spring, and the lower and the upper disk holders.
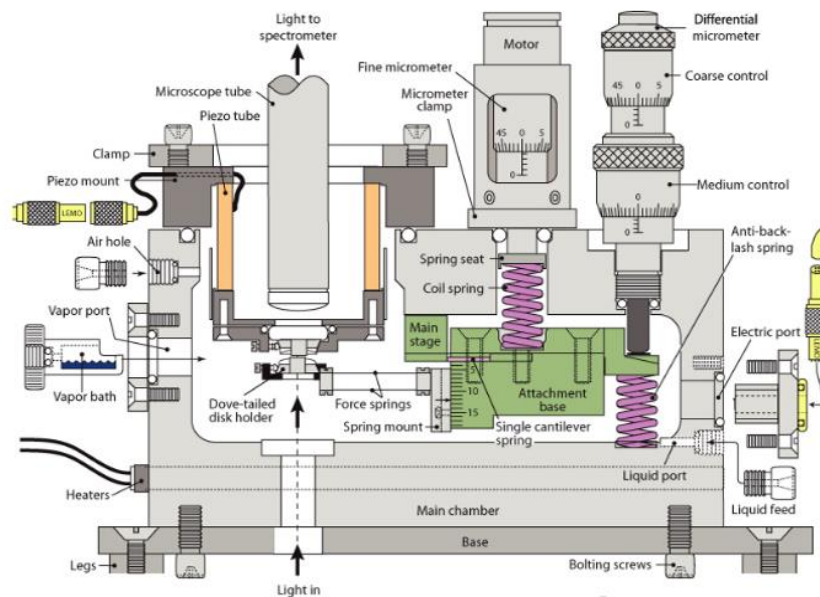
Figure. 2.1. Scheme of surface forces apparatus 2000.[8]

The light path in SFA 2000 was shown in the Figure 2.2. Starting from the white light source, the light beam is reflected by a mirror to go through the two black silvered mica surfaces that glued on two crossed cylinders with the same radius R. Attributed to the function of spectrometer slit, a series of fringes of equal chromatic orders (FECO) are generated and recorded by the video camera.[9-13] The FECO pattern was then used to calculate the absolute distance between two surfaces.
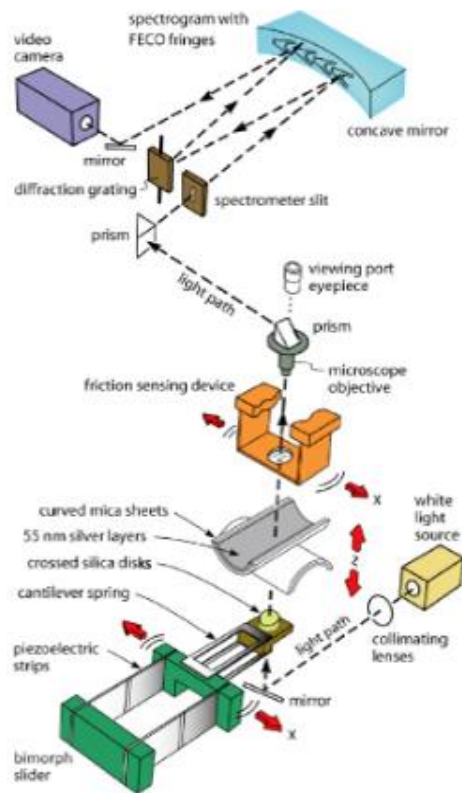
Figure. 2.2. Scheme of surface forces apparatus set up.

2.1.2 The SFA force measurement

The motion of surface at the base of double cantilever was controlled by differential micrometer, motor-driven fine micrometer and/or piezo tube. The distance of this surface

is represented by D_{app}. The absolute distance of two surfaces is donated as D_{mean}, which is measured by multiple beam interference (MBI). When the two surfaces come to a rest at a distance D, the normal force $\Delta F(D)$ between two surfaces is determined by Hooke's law:

$$\Delta F(D) = K(D_{app} - D_{mean})$$

Where K represents the spring constant. When $\partial F(D)/\partial D > K$, the lower surface will jump toward or away from the upper surface due to the mechanism instability. The jump distance (D_{jump}) when two surfaces jump apart from contact is measured to calculate the adhesive force by:

$$F_{adhesive} = K \times \Delta D_{jump}$$

2.2 Gel permeation chromatography (GPC)

2.2.1 Development of GPC

Gel permeation chromatography is a widely used polymer fractionation technique, possessing advantage of good resolution in short time and susceptible to automation. The nomenclature of this separation has been suggested as gel filtration, exclusion chromatography, gel chromatography, restricted diffusion chromatography, molecular sieve chromatography, molecular sieve filtration, and gel permeation chromatography. The nomenclature is far from uniform due to the various experiment and column-packing

materials applied.

The use of gel permeation chromatography dates back at least 1950, which was used primarily with water and buffer solution as solvent. In 1960, the insoluble crosslinked polystyrene with different degrees of swelling was used as medium by Vaughan to demonstrate its ability of molecular weight separation.[14] The application of organic solvent was achieved during the period of 1961-1962. In 1962, Moore made two significant improvement for GPC. Larger molecular weight range could be measured due to the use of highly cross-linked and rigid gel with wide range of permeability. Furthermore, automation of molecular weight distribution measurement was achieved, attributed to the application of differential refractometer as continuous detector.

2.2.2 Mechanism of GPC

A typical gel permeation chromatography was shown in Figure 2.3. The basic elements are a solvent pumping system, a sample injection valve, columns with thermostat, a detector to record the solvent eluted vs. polymer concentration.
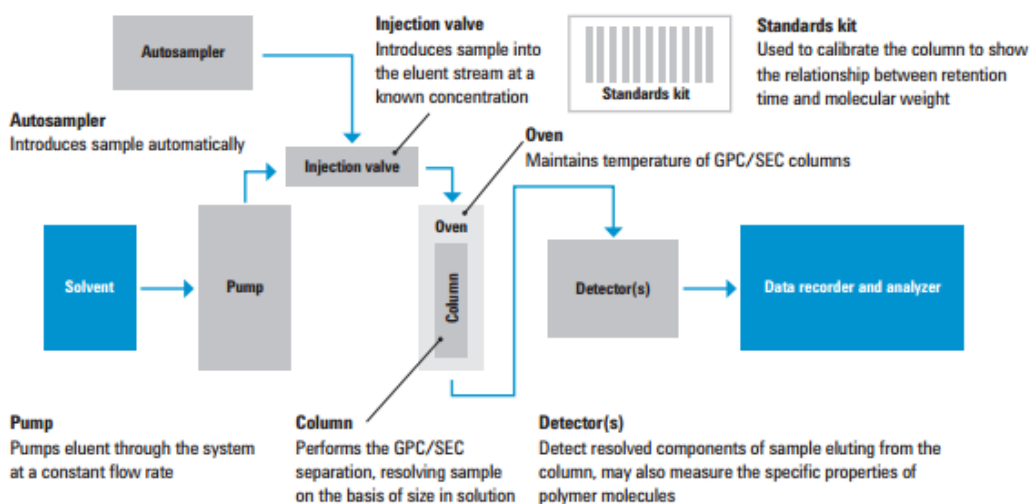
Figure 2.3. The schematic drawing of gel permeation chromatography (GPC).

The columns used in GPC are often ranging from 0.5-3 cm in diameter, and varying from 1-10 m in length[15], and packed with crosslinked gel with different sizes of pores. The polymer dissolved in the solvent is introduced to the head of column and pass through the column with a typical flow rate of 1 ml/min. As shown in the Figure 2.4, during the separation process, the polymer with large molecular weight is able to escape from the column faster than the smaller one, attributed to large molecular weight polymer will be excluded by the pores of gel or solid. However, polymer with small molecular weight will enter the pores, extending the time of leaving the column.[16]
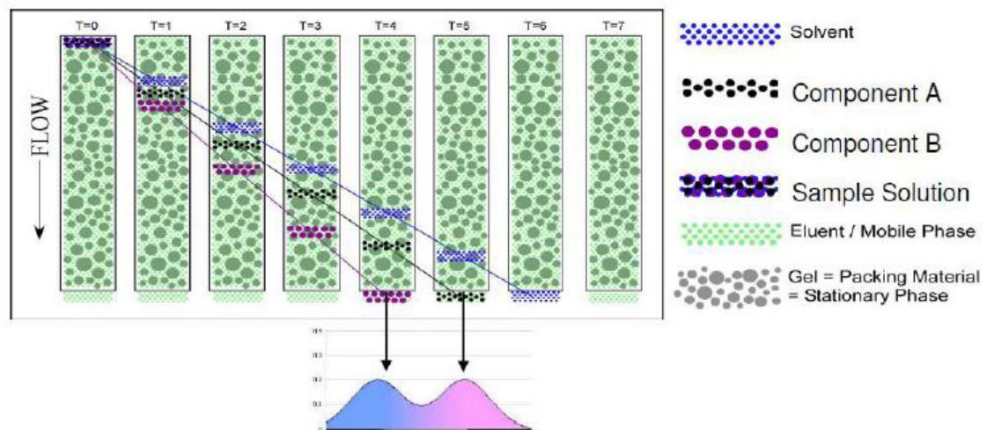
Figure 2.4. The polymer separation mechanism plot of gel-packed column.

The recorder response plot was shown in the Figure (a). The abscissa represents elution time, and ordinate is the refractive index between the reference solvent and the polymer solution. For a variety of polymers, the relationship of elution time and molecular weight is the formula as:

$$V_e = -B \log M + C$$

Where V_e represents the elution volume to the center of peak, M represents molecular weight, B and C are both constant number.

To do the calibration of GPC, the molecular weight of a series narrow molecular weight fraction is required. Molecular weight can be obtained according to the calibration of standard molecular weight (Figure 2.5).
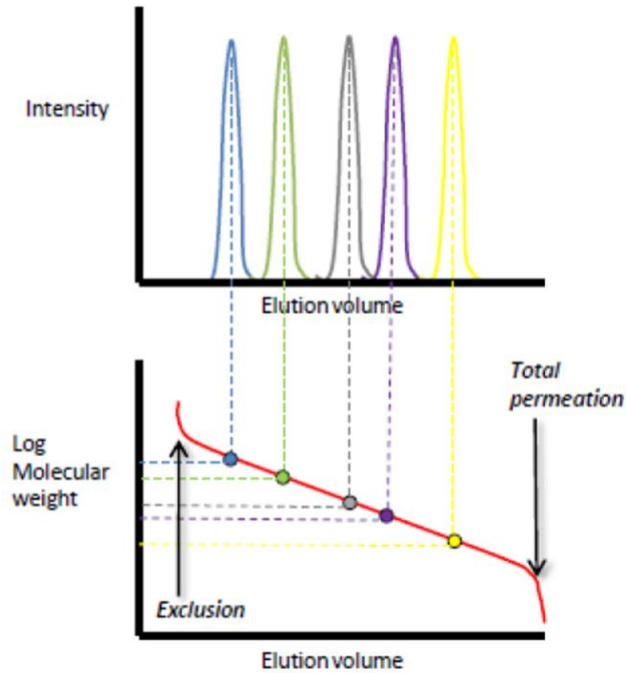
Figure 2.5. The drawing of molecular weight measurement calibration.

2.3 Zetasizer nano

The techniques of dynamic light scattering (DLS), electrophoretic light scattering (ELS), static light scattering (SLS) are respectively used in the Zetasizer nano to measure the particle and molecular size ranging from nanometer to microns, zeta potential and electrophoretic mobility, and molecular weight.

2.3.1 Zeta potential

Particles or molecules have zeta potentials will move towards the electrode under the influence of the field which was applied by using the dip cell (Figure 2.6). The zeta potential is able to be determined by measuring the motion velocity due to speed is proportional to the zeta potential and field strength. Zeta potential can provide

information of the particles or aggregates directly related to the performance of flocculation or coagulation.[17] As shown in the Figure 2.7, zeta potential is the electric potential in the electrical double layer. The potential difference of the bulky medium far away from particle and the stationary layer attached to the particle surfaces.[18]
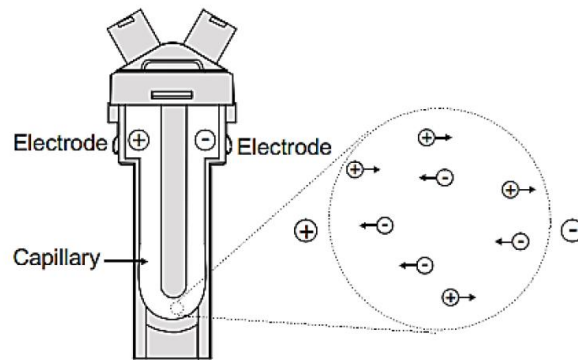
Figure 2.6. Schematic diagram of Dip Cell used for zeta potential measurement.
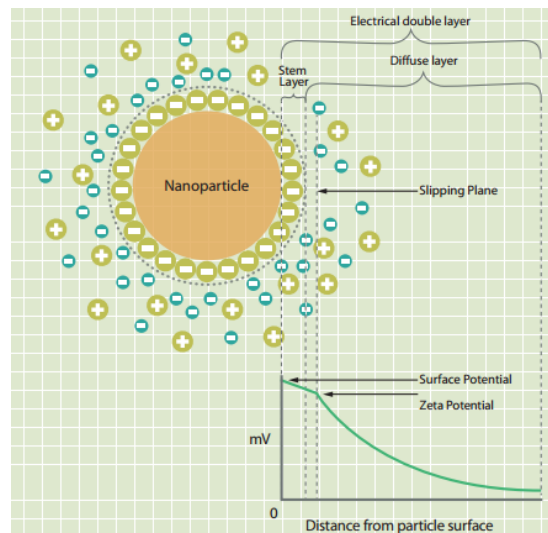
Figure 2.7. Schematic of electrical double layer of negatively charged particle.

2.3.2 Dynamic Light Scattering (DLS)

Dynamic Light Scattering (DLS), also called Photon Correlation Spectroscopy, is a

spectroscopic technique used to characterize the hydrodynamic radius and size distribution of polymer, and colloidal particles in solution or suspension. The particles and molecules are able to diffuse in the liquid due to Brownian motion which is easily influence by temperature. In addition, particle and molecule sizes also determine the speed of Brownian motion, following the principle that the smaller of particle size, the faster particle moves. The relationship velocity and particle size is defined by Stokes Einstein equation:

$$D = \frac{k_B T}{6\pi\eta a}$$

where D is the diffusion constant; k_B is the Boltzman's constant, T is the temperature, η is viscosity of the solution and a is the hydrodynamic radius of the spherical particle.

In order to measure the velocity of diffusion of particles, the techniques of dynamic light scattering (DLS) is used to measure the time dependent light intensity fluctuation of the particles illuminated by laser.[19] A photomultiplier positioned at 90° to the light source was used as the detector to collect light diffracted from the particles. In a typical DLS experiment, dispersions are often filtered before measurement and samples are also diluted to low concentrations, avoiding the existence of unwanted particles and the aggregation of polymers.

2.4 Mastersizer

The Mastersizer uses the technique of laser diffraction to measure particle size distributions. In a laser diffraction measurement, the light was scattered when the laser beam passes through the samples dispersed in the solution. The particles with small size will scatter the light at large angle relative to the laser beam. In contrast, particles with large size scatter the light at small angle, as shown in the Figure 2.8. The intensity of angular change is recorded to obtain the scattering pattern from the particles, which was used to analyze and calculate the particle size distribution using the Mie theory of light scattering assuming a volume equivalent sphere model.[20] Mie theory was used to make a prediction of the direction of light way after the scattering of spherical particles and deal with the way light adsorbed by or passes through the particles.
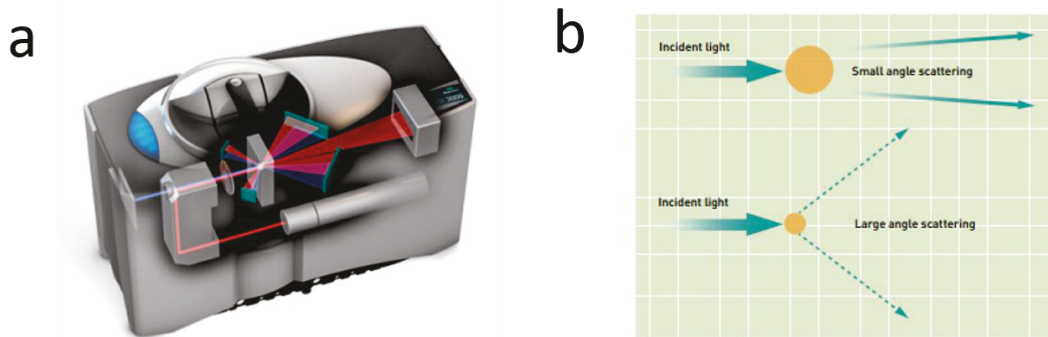
Figure 2.8. (a) Schematic of Mastersizer setup. (b) The light scattering mechanism.

2.5 Reference

(1) Derjaguin, B. V.; Voropayeva, T. N. Surface Forces and the Stability of Colloids and Disperse Systems. *Journal of Colloid Science* **1964**, *19* (2), 113–135.

(2) Tabor, D.; Winterton, R. H. S. The Direct Measurement of Normal and Retarded van Der Waals Forces. In *Proceedings of the Royal Society of London A: Mathematical, Physical and Engineering Sciences*; The Royal Society, 1969; Vol. 312, pp 435–450.

(3) Israelachvili, J. N.; Adams, G. E. Measurement of Forces between Two Mica Surfaces in Aqueous Electrolyte Solutions in the Range 0–100 Nm. *Journal of the Chemical Society, Faraday Transactions 1: Physical Chemistry in Condensed Phases* **1978**, *74*, 975–1001.

(4) Israelachvili, J. N.; McGuiggan, P. M. Adhesion and Short-Range Forces between Surfaces. Part I: New Apparatus for Surface Force Measurements. *Journal of Materials Research* **1990**, *5* (10), 2223–2231.

(5) Israelachvili, J. N.; Adams, G. E. Direct Measurement of Long Range Forces between Two Mica Surfaces in Aqueous KNO3 Solutions. *Nature* **1976**, *262*, 774–776.

(6) Israelachvili, J. Direct Measurements of Forces between Surfaces in Liquids at the Molecular Level. *Proceedings of the National Academy of Sciences of the United States of America* **1987**, *84* (14), 4722.

(7) Israelachvili, J. N. Techniques for Direct Measurements of Forces between Surfaces in Liquids at the Atomic Scale. *Chemtracts Anal. Phys. Chem* **1989**, *1* (1).

(8) Israelachvili, J.; Min, Y.; Akbulut, M.; Alig, A.; Carver, G.; Greene, W.; Kristiansen, K.; Meyer, E.; Pesika, N.; Rosenberg, K.; et al. Recent Advances in the Surface Forces Apparatus (SFA) Technique. *Reports on Progress in Physics* **2010**, *73* (3), 036601.

(9) Chen, Y. L.; Helm, C. A.; Israelachvili, J. N. Measurements of the Elastic Properties of Surfactant and Lipid Monolayers. *Langmuir* **1991**, *7* (11), 2694–2699.

(10) Alig, A. R. G.; Gourdon, D.; Israelachvili, J. Properties of Confined and Sheared Rhodamine B Films Studied by SFA-FECO Spectroscopy. *The Journal of Physical Chemistry B* **2007**, *111* (1), 95–106.

(11) Luengo, G.; TSUCHIYA, M.; HEUBERGER, M.; ISRAELACHVILI, J. Thin Film Rheology and Tribology of Chocolate. *Journal of food science* **1997**, *62* (4), 767–812.

(12) Israelachvili, J. N. Thin Film Studies Using Multiple-Beam Interferometry. *Journal of Colloid and Interface Science* **1973**, *44* (2), 259–272.

(13) Heuberger, M.; Luengo, G.; Israelachvili, J. Topographic Information from Multiple Beam Interferometry in the Surface Forces Apparatus. *Langmuir* **1997**, *13* (14), 3839–3848.

(14) Cantow, M. J. R. *Polymer Fractionation*; Elsevier, 2013.

(15) Giger, W.; Schaffner, C. Determination of Polycyclic Aromatic Hydrocarbons in the Environment by Glass Capillary Gas Chromatography. *Analytical Chemistry* **1978**, *50* (2), 243–249.

(16) Cazes, J. Gel Permeation chromatography—Part 1. *J. Chem. Educ.* **1966**, *43* (7), A567.

(17) Revil, A.; Pezard, P. A.; Glover, P. W. J. Streaming Potential in Porous Media: 1. Theory of the Zeta Potential. *Journal of Geophysical Research: Solid Earth (1978–2012)* **1999**, *104* (B9), 20021–20031.

(18) Eaton, D. R. Outer Sphere Complexes as Intermediates in Coordination Chemistry. *Reviews of chemical intermediates* **1988**, *9* (3), 201–232.

(19) Brar, S. K.; Verma, M. Measurement of Nanoparticles by Light-Scattering Techniques. *TrAC Trends in Analytical Chemistry* **2011**, *30* (1), 4–17.

(20) Apetz, R.; Van Bruggen, P. B. Transparent Alumina: A Light Scattering Model. *Journal of the American Ceramic Society; authors version* **2003**.

Chapter 3 Temperature and pH Responsive Benzoboroxole based Polymers for Flocculation and Enhanced Dewatering of Fine Particle Suspensions

3.1 Introduction

In the past decades, the Canadian economy is fueled by its oil sands industry. However, the environmental issues associated with the oil sands extraction processes and mineral industry can potentially cause significant risks to the ecosystem in northern Alberta. Releasing water trapped in large volumes of tailings (containing large amount of kaolin) from industry is still a major challenge.[1, 2] Flocculation is considered a main method for solid-liquid separation.[3-8] Common polymeric flocculants with high molecular weight can induce the fast settling of suspended solid particles through bridging force or charge neutralization. However, the formation of large flocs and open structures due to strong bridging force may trap a significant amount of water and lead to low solid density of sediment.[2, 9]

Poly(N-isopropylacrylamide) (PNIPAAm) has proved to be an efficient flocculant due to its ability to reversibly switch between hydrophilic and hydrophobic characters as a function of temperature. At temperature below its lower critical solution temperature (LCST), PNIPAAm is soluble in water. However, at temperatures above the LCST, PNIPAAm shows hydrophobicity. PNIPAAm chains adsorbed on particle surfaces are collapsed which cause strong inter-particle interactions due to the hydrophobic

interaction, which is beneficial for increasing the settling rate. If the formed sediment is cooled below LCST after the top height of the so called mud-line barely decreases, the adhesion of the polymers to the particle surfaces was reduced, leading to breakup of the big flocs. Smaller Particles could fill the gaps between flocs formed previously, and enhanced consolidation can thus be achieved.[4, 6, 9-12]As previous study shows, fine particles in the suspension often exhibit stability tending to resist aggregation, which commonly results from electrical charge. Destabilization and floc formation are two principle steps determining the water clarity and settling rate, respectively. Destabilization permits the particles to move close and improve the probability of collision, followed by the floc growth.[13] PNIPAAm homopolymer suffers from the disadvantage of a notable lack of the ability to neutralize surface charges of particles, which may hinder both the destabilization of suspended particles and floc growth, leading to relatively turbid released water and low setting rate.[4] In addition, in order to avoid self-aggregation of polymer chains before particles flocculation, NIPAAm homopolymer cannot be added at temperatures higher than its LCST. To overcome these limitations, different components were introduced to PNIPAAm backbone via copolymerization.[6, 14, 15] For example, Franks et al. synthesized cationic/anionic NIPAAm copolymers which facilitated fast settling rate at 50 °C.[6] Counter-charged polymers were strongly attached on the particle surfaces by electrostatic interaction, combined with hydrophobic interaction, resulting in strong aggregation and fast settling of suspension. However, even

though temperature was reduced lower than the LCST, the formed sediment was difficult to continuously condense under gravity due to strong electrostatic interaction, resulting in the formation of big flocs unable to break up as in the case of NIPAAm homopolymer. On the other hand, the introduction of the hydrophilic cationic/anionic component must be carefully controlled as the LCST of the random copolymers will be dramatically increased as well.[16-19]

To meet these specific challenges, our group has been investigating to develop efficient tailings and mineral flocculant with the functional groups which are able to induce fast settling rate, and meanwhile to consolidate sediment well. In recent years, phenylboronic acid (PBA) and its derives that can reversibly interact with adjacent hydroxyl groups have received increasing attention for various applications such as in the development of biomaterials for treatment of cancer and obesity.[20-22] O-hydroxymethyl phenylboronic acid (benzoboroxole) shows strong interaction with the diols on glycopolymers and sugars at neutral or basic pH condition.[23] Since kaolin clay is an important component in oil sands and mineral tailings, contains hydroxyl groups (Al-OH or Si-OH) at neutral or slightly basic condition,[24,25] it is expected that benzoboroxole based polymers can interact with the hydroxyl groups on kaolin clay in a similar way as they would interact with diols on sugar, hence facilitating the flocculation of the solid particles. On the other hand, the introduction of the hydrophobic benzoboroxole also allows polymer LCST to retain at a temperature near 32 °C,[19] even though hydrophilic amino groups presented on PNIPAAm

backbone. Since bitumen was extracted with hot water (50 ºC – 80 ºC) in oil sand industry, the application of temperature responsive polymer as flocculant was able to take advantage of the thermal energy in high temperature tailings to flocculate particles. Strong adhesion is necessary to form big flocs, which is a critical factor to increase settling rate. However, in order to obtain enhanced consolidation after fast settling, the strong adhesion needs to be reduced to disassemble the big flocs into small particles during consolidation step, which is achievable due to the reversible neutral/anionic transition of benzoboroxole by controlling pH.[10] Under strong basic conditions, kaolin clay is highly negatively charged and seldom does any hydroxyl exist on the particles surface.[26-30] Meanwhile, benzoboroxole groups are also negatively charged and may work as dispersant. The reduced adhesion of polymers onto the particles surfaces would be expected to cause further consolidation of sediment.

In this work, a new type of pH and temperature responsive cationic copolymer has been designed for the solid-liquid separation, viz. flocculation and enhanced dewatering of fine solid suspensions. To the best of our knowledge, this is the first report of copolymers containing benzoboroxole residues used for solid-liquid separation in tailings water treatment. The initial settling rate, supernatant turbidity, sediment solid content, and solid volume fraction were investigated in this study. Previously reported NIPAAm based cationic and homopolymer with similar molecular weight were also synthesized and used to treat kaolin suspension as control groups, comparing the flocculation behavior with the

benzoboroxole based polymer at neutral pH. Zeta potential analyzer, dynamic light scattering (DLS), surface forces apparatus (SFA) were also employed to characterize the intermolecular and surface interactions between the polymers and solid particles, providing insights into the flocculation mechanism.

3.2 Materials and Methods

3.2.1 Materials

2-aminoethyl methacrylamide hydrochloride (AEMA), 5-methacrylamido-1,2-benzoboroxole (MAAmBo), were synthesized following reported procedures.[8, 31] *N*-isopropylacrylamide (NIPAAm) monomer and 4',4-azobis (4-cyanovaleric acid) (ACVA) were purchased from Sigma-Aldrich Chemicals (Oakville, ON, Canada). Organic solvents were purchased from Caledon Laboratories Ltd. (Georgetown, ON, Canada). The kaolin was purchased from Acros Organics. The particle sizes distribution and specific surface area were shown in the Figure S1. The D_{10}, D_{50}, D_{90} of solid particles were 1.94 μm, 6.67 μm, 27.2 μm respectively.

3.2.2 Synthesis of linear statistical benzoboroxole based cationic copolymers.

The random poly[(2-aminoehtyl methacrylamide hydrochloride)-*st*-(5-methacrylamido-1,2-benzoboroxole)-*st*-(*N*-isopropylacrylamide)] was synthesized by conventional free radical polymerization. In a typical procedure, AEMA (70 mg, 0.4 mM) was dissolved in 1 mL of distilled deionized water. ACVA (2.8 mg, 0.01 mM), NIPAM (815 mg, 7.2 mM), MAAmBo (116 mg, 0.4 mM) were dissolved

in 5 mL DMF. The solution above was mixed in a 10-mL Schlenk tube and purged with nitrogen for 30 min. The sealed tube was placed in a preheated 70 °C oil bath. The polymerization was carried out in the inert atmosphere for 24 h. The polymers were purified by dialysis against double distilled deionized water for 4 days. Then the solution was frozen by liquid nitrogen for 10 min and freeze-dried for 2 days. Molecular weight and molecular weight distribution (PDI) were determined by gel permeation chromatography (GPC) (Viscotek model 250 dual detectors system), using DMF containing 0.01 % LiBr as eluent. The flow rate was set to 1.0 mL/min. The resulting polymer was characterized by ^{1}H NMR and the composition was determined as P(AEMA$_{51}$-st-MAAmBo$_{76}$-st-NIPAM$_{381}$) (denoted as PAMN).

3.2.3 Synthesis of linear statistical amine based copolymers

The random poly[(2-aminoethyl methacrylamide hydrochloride)-st-(N-isopropylacrylamide)] was synthesized by conventional free radical polymerization as described above. AEMA (72 mg, 0.4 mM) was dissolved in 1 mL double distilled deionized water. ACVA (2.8 mg, 0.01 mM), NIPAM (928 mg, 8.2 mM) were dissolved in 5 mL DMF. After mixing in a 10-mL Schlenk tube, the solution was degassed by nitrogen gas for 30 min. The tube was sealed with parafilm and heated in the oil bath at 70 °C. Polymerization was proceeded for 24 h under nitrogen. The resulting polymer was purified by dialysis with double distilled deionized water for 4 days followed by freeze drying.   Molecular weight and polydispersity (PDI) were determined

by aqueous GPC, as described above. The obtained polymer was characterized by ^{1}H NMR and was determined as P(AEMA$_{57}$-st-NIPAM$_{509}$) (denoted as PAN).

3.2.4 Synthesis of linear NIPAAm homopolymers

N-isopropylacrylamide was synthesized by conventional free radical polymerization as described above. ACVA (2.8 mg, 0.01 mM), NIPAAm (1 g, 8.9 mM) were dissolved in 6 mL DMF. The solution was degassed by nitrogen for 30 min in a 10-mL Schlenk tube. The tube was sealed with parafilm and heated in the oil bath at 70 °C. Polymerization was proceeded for 24 h under the inert atmosphere. The resulting polymer was purified by dialysis with double distilled deionized water for 4 days followed by freeze drying. Molecular weight and polydispersity (PDI) were determined by aqueous GPC, as described above. The obtained polymer was characterized as PNIPAAm$_{531}$ (denoted as PN).

Lower critical solution temperatures (LCSTs) of polymers were determined using a UV-Vis spectrometer with a heating rate of 0.5 ℃/min. The transmittance at wavelength of 500 nm was recorded at different temperatures.

3.2.5 Settling test

Polymers (2.5, 5, 10 or 20 mg) were mixed with 10 mL double distilled deionized water in 20-mL vials for 24 h to enable complete dissolution before addition to the kaolin suspension. In this study, kaolin suspension was used as a model tailing. To prepare kaolin suspension with solid content of 5 wt%, a mechanical stirrer (IKA® Digital Stirrer

RW20, Fisher Scientific) and a 4 blade stainless steel impeller (blade width 3 cm, Fisher Scientific) were used for stirring kaolin suspension in a 2 L beaker at 700 rpm for 30 min. The pH value of kaolin suspension was adjusted by 0.1 M sodium hydroxide solution and monitored by a pH meter (Accumet 200XL, Fisher Scientific). 90 mL model tailings suspension was transferred into 250-mL baffled beakers by syringe, followed by sealing with the parafilm (Parafilm, Pechiney Plastic Packaging Company, Chicago, Illinois, US). Kaolin suspensions were stirred for 2 min in 250-mL beakers at 300 rpm before dropwise addition of polymer stock solutions at a rate of 0.1 ml/s. The stirring was stopped immediately after complete addition of the polymer solution. The mixture was transferred to 100-mL graduated cylinder. The cylinder was inverted for 5 times vigorously and then left still on the bench at room temperature (25 °C), the height of so-called mud-line (interface of supernatant and sediment) was recorded as a function of time.[3] For batch settling tests at temperature higher than LCST, polymer stock solution was added to kaolin suspension in 250-mL baffled beakers at room temperature with a stirring rate of 300 rpm. After complete addition of polymer solution, the stirring was stopped before transferring the mixture to 100-mL cylinders. Cylinders were inverted 5 times vigorously, and placed in a preheated 50 °C water bath where the suspension rapidly approach the temperature of surrounding water (~ 10 s). The time zero was taken as soon as the cylinder was placed in the hot water bath. The heights of mud-line were recorded as a function of time. All the settling tests were repeated for 3 times.

To investigate the ability of PAMN to improve consolidation of sediment, the pH of the formed sediment was increased from 7 to 11, contributing to the function switch of polymers from flocculants to dispersants after fast settling phase. All but 10 mL supernatant was removed out from cylinder after 30 min of settling (the top height of sediment came to a plateau). Increasing pH of sediment from 7 to 11 by adding 0.1 M sodium hydroxide solution without stirring and then recording the height of mud-line for 72 h. Control test was carried out without any pH change under exactly the same condition specified above.

The initials settling rate (ISR) was determined by the initial slope of plot (height of mud-line vs time). The light transmittance of the supernatant at 500 nm wavelength was monitored by a UV-Vis spectrometer. The turbidity (NTU) of released water was calculated by the equation of NTU $\approx 0.191 + 926.1942 \times [-\log(\%T/100)]$, where $\%T$ is transmittance measured by UV−vis spectrometer.[8] The mass of sediment (m_f) was weighed after removing supernatant from graduated cylinders. The mass of solid clays (m_s) can be obtained by drying the sediment in an oven at 60 °C for 24 h. Solid content of sediment is derived from dividing the mass of solid clays (m_s) by the total mass of sediment (m_f). The final solid volume fraction of sediment φ_f was calculated through equation (1), where: ρ_s represents the density of mineral solid (g/cm^3), V_f represents the final sediment volume recorded after 24 h.

$$\varphi_f = \frac{m_s}{\rho_s \cdot V_f} \quad (1)$$

3.2.6 Zeta potential of solid particles and polymer size

Electrokinetic (zeta) potentials of kaolin powders and polymer/particle aggregates were measured as a function of dosage (ppm) by a Malvern Zetasizer Nano ZSP. Prior to zeta potential measurement, 0.1 wt% kaolin suspension was prepared by dispersing selected amount of kaolin particles in 0.01 M KCl aqueous solution. As the random copolymers PAMN and PAN are pH sensitive, desired pH values of the suspensions were adjusted before zeta potential measurement. The suspension was stirred in a 20-mL vial for 5 min before transferring into an electrophoresis cell for zeta potential measurements.

The hydrodynamic radii of polymers (100 ppm) were also measured using the Malvern Zetasizer Nano ZSP under various pH conditions and at temperatures higher and lower than LCST.

3.2.7 Interaction force measurements between polymers and clay surfaces and imaging of adsorbed polymers.

The interaction forces between polymers and model clay surface mica, were directly measured using a surface forces apparatus (SFA, Surforce LLC, Santa Barbara, CA). The adsorbed polymers were imaged using an AFM (MFP-3D, Asylum, Santa Barbara, CA). The polymer films for surface force measurement and AFM imaging were prepared by drop coating method on mica surface. Several drops of the synthetic polymer solution (1 mg/mL in Milli-Q water) were placed on the mica surface to allow adsorption for 1 h in a

Petri dish saturated with water vapor followed by rinsing the surfaces with a capacious amount of Milli-Q water for several times and then dried in vacuum.

SFA has been widely used for direct measurements of intermolecular and surface forces of many materials, in both vapors and liquid media, with Angstrom resolution for separation distance and nanonewton force precision.[32-36] In a typical SFA experiment, two back-silvered mica sheets with same thickness of 1-5μm were glued on two cylindrical silica disks (radius $R = 2$ cm). The interaction between two cross-cylindrical mounted surfaces is locally equivalent to two spheres of radius $2R$ or a sphere of radius R near a flat surface when the surface separation D was much smaller than R ($D \ll R$). The absolute distance between two surfaces was determined through multiple beam interferometry employing fringes of equal chromatic order (FECO) and the surface forces were measured through Hooke's law by multiplying the spring constant by its deflection.[32, 37] During the force measurements, the reference distance ($D= 0$) was defined at the adhesive contact between two bare mica surfaces in air. Then one of the mica surfaces was drop coated with the polymer. The surface forces measurements were repeated for at least three times for two different pairs of surfaces under each experimental condition to ensure the reproducibility.

Surface morphology of adsorbed polymer layer on mica was characterized using an AFM in tapping mode in air. At least three samples were imaged at different (>3) positions and typical AFM image was presented.

3.3 Results and discussion

3.3.1 Synthesis of polymers

Linear homopolymers and statistical copolymers with various compositions were synthesized by conventional free radical polymerization and their molecular weight were determined by GPC (Figure S2). Monomers, 2-aminoethyl methacrylamide hydrochloride (AEMA) and 5-methacrylamido-1,2-benzoboroxole (MAAmBo) (as shown in Scheme 1), were introduced into the polymers for inducing strong interactions with the particle surface via electrostatic or covalent bonds. The incorporation of the monomers, *N*-isopropylacrylamide (NIPAAm) and 5-methacrylamido-1,2-benzoboroxole (MAAmBo), enabled the polymers to exhibit temperature and pH responsiveness, respectively. Consistent with previous reports, the molecular weights polydispersity (Table 1) of the synthesized polymers via conventional free radical polymerization (Scheme 1) were relatively high.[8, 38, 39] The polymer compositions were determined by ^{1}H NMR and shown in Figure S3. The successful synthesis of PAMN was also determined with infrared spectroscopy as shown in Figure S4. The performance of polymers on settling model tailings (kaolin suspension) were investigated at temperatures below and above the LCST. Light transmittance measurements of NIPAAm homopolymer by UV-Vis shows a transition temperature of 32 °C under each pH conditions (Figure 1), in good agreement with previous reports.[4, 40, 41] LCST of amino-based positively charged PAN were found to vary between 38 ~ 41 °C under various pH conditions, which is a

significant increase as compared to the LCST of NIPAAm homopolymer. As shown in Figure 1, the LCSTs of PAN decreased slightly with the pH increase due to the neutralization of positive charge of amino groups. The LCST of PAMN was found to be around 34-37 °C at pH 7 and 9, due to the presence of the hydrophobic MAAmBo residues. However, at pH 11, the LCST of PAMN was much higher as compared to pH 7 and 9, as a result of the presence of negative charges on the PAMN. The above result also agrees well with previous report that incorporating charged (hydrophilic) moieties can generally increase LCSTs of thermally responsive polymers, while the addition of hydrophobic residues generally decrease the LCSTs of copolymers.[16]
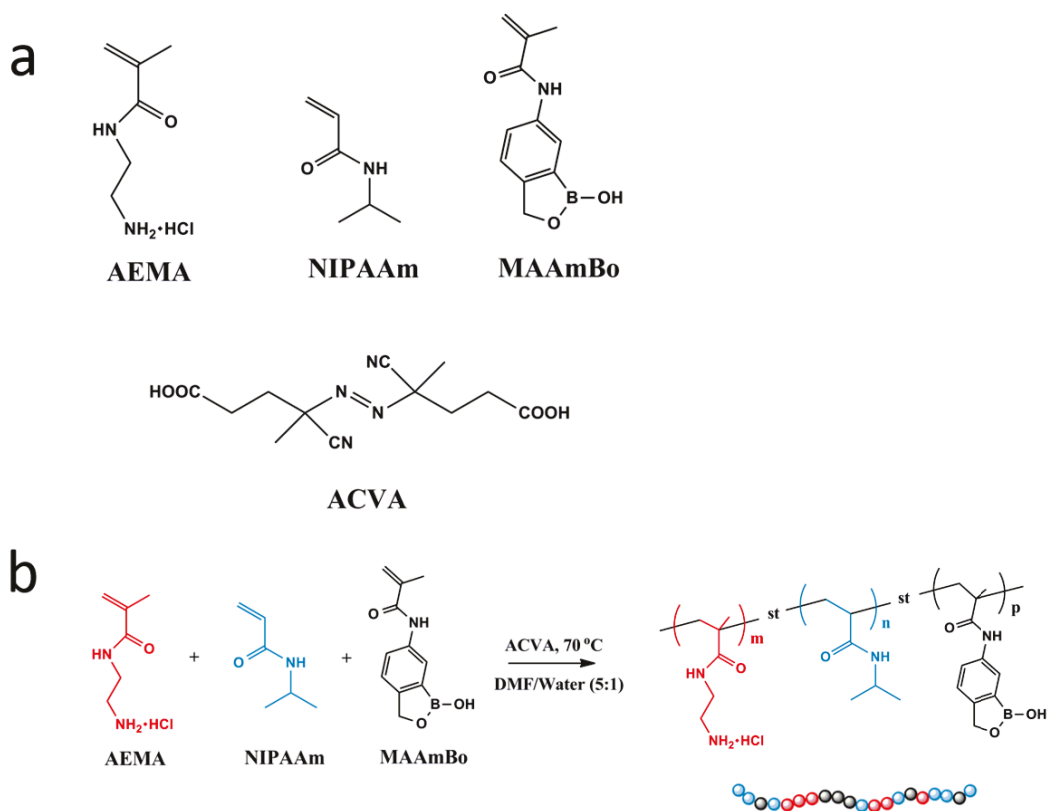
Figure 3.1. (a) Structures of monomers and initiator, and (b) synthesis of random copolymers using 4,4-azobis-(4-cyanovaleric acid) (ACVA) as initiator via conventional free radical polymerization.

Table 3.1. Synthetic parameters, polymer compositions and hydrodynamic sizes of PAMN, PAN, and PNIPAAm.

Polymer denotation	Polymer Compositions	M_n (kDa)	M_w/M_n	Hydrodynamic Size (nm)	
				25 °C	50 °C
PAMN	P(AEMA$_{51}$-st-MAAmBo$_{76}$-st-NIPAAm$_{381}$)	68	3.45	7	43
PAN	P(AEMA$_{57}$-st-NIPAAm$_{509}$)	68	3.71	5	84
PNIPAAm	PNIPAAm$_{531}$	60	3.31	6	126
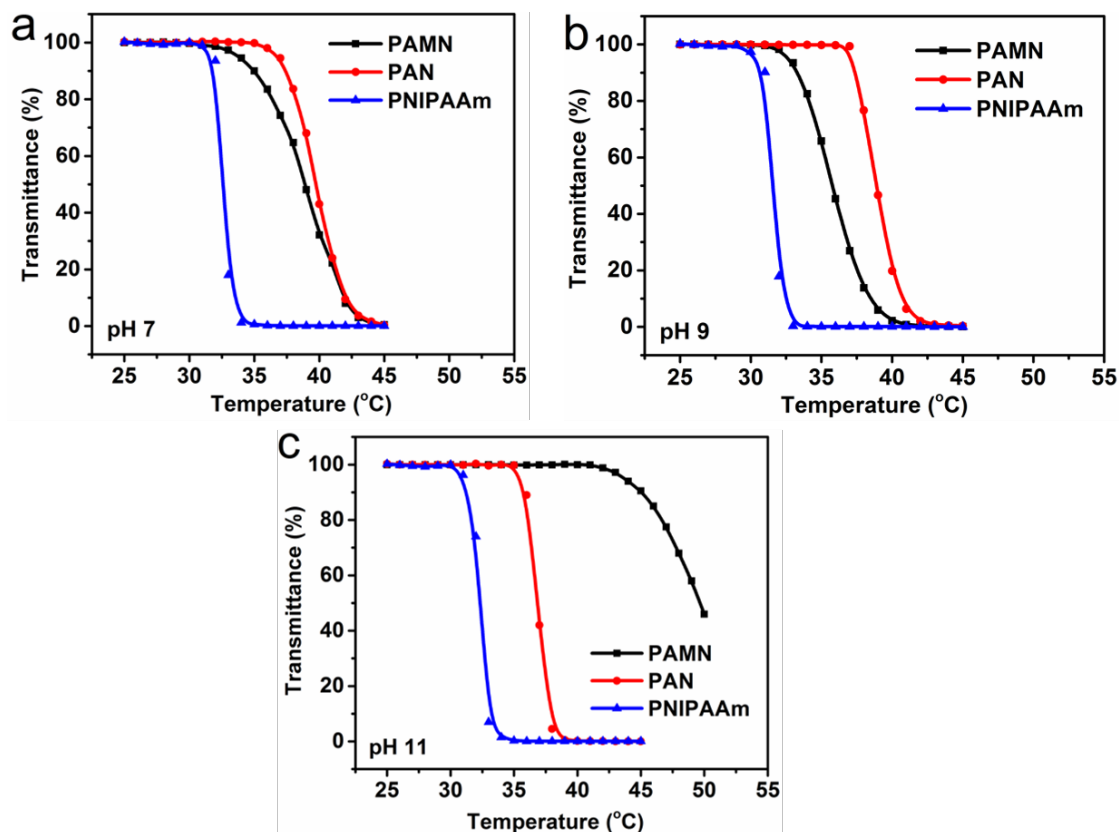
Figure 3.2. Lower critical solution temperatures (LCSTs) of PNIPAAm based copolymers at (a): pH 7, (b): pH 9, (c) pH 11; ■PAMN, ● PAN, ▲ PNIPAAm.

3.3.2 Polymer Aggregation

The hydrodynamic size distribution of the polymers synthesized was studied at different temperatures and pH values as shown in the Figure 2. As expected, with the increasing of temperature, the R_H of PAMN, PAN, and PNIPAAm increased from around 5 nm to 43, 84 and 126 nm at neutral pH, a similar size change was recorded at pH 9. However, at pH 11, PAMN did not show any obvious aggregation after increasing temperature up to 50 °C. In addition, size distribution plot of PAN is similar to that of PNIPAAm at 50 °C. At 25 (C, the R_H of PAMN at pH 11 is doubled as compared to the

results obtained at pH 7 and 9. At pH 11, MAAmBo groups became negatively charged resulting in a dramatic increase of the LCST (> 50 °C) of PAMN as shown in Figure 1c. The highly charged PAMN chains barely aggregated, but were able to swell and extend due to the electrical double layer repulsive force. The significant increase of R_H suggests the formation of bulky aggregates as a result of hydrophobic interaction at temperature higher than LCST. At 50 °C, the R_H of PAN aggregates increased with pH values, which agrees well with LCST result (decreased with pH value), resulting from neutralization of positive charge of amino groups by hydroxide ions in the solution. At pH 7 and 9, PAN formed aggregates with smaller R_H as compared to NIPAAm homopolymer case, due to the electrical double layer repulsion among the positively charged amino groups, which was also due to higher LCST.

Figure 3.3. Distributions of hydrodynamic radius (R_H, nm) of three polymer flocculants in water: PAMN at 25°C (black solid line), PAMN at 50°C (red dash line), PAN at 25°C (blue dot line), PAN at 50°C, (pink dash dot line), PNIPAAm at 25°C (green dash dot line), PNIPAAm at 50°C (blue short dash line) at (a): pH 7, (b): pH 9, (c) pH 11.

3.3.2 Polymer Aggregation

The hydrodynamic size distribution of the polymers synthesized was studied at different temperatures and pH values as shown in the Figure 2. As expected, with the increasing of temperature, the R_H of PAMN, PAN, and PNIPAAm increased from around 5 nm to 43, 84 and 126 nm at neutral pH, a similar size change was recorded at pH 9.

However, at pH 11, PAMN did not show any obvious aggregation after increasing temperature up to 50 °C. In addition, size distribution plot of PAN is similar to that of PNIPAAm at 50 °C. At 25 (C, the R_H of PAMN at pH 11 is doubled as compared to the results obtained at pH 7 and 9. At pH 11, MAAmBo groups became negatively charged resulting in a dramatic increase of the LCST (> 50 °C) of PAMN as shown in Figure 1c. The highly charged PAMN chains barely aggregated, but were able to swell and extend due to the electrical double layer repulsive force. The significant increase of R_H suggests the formation of bulky aggregates as a result of hydrophobic interaction at temperature higher than LCST. At 50 °C, the R_H of PAN aggregates increased with pH values, which agrees well with LCST result (decreased with pH value), resulting from neutralization of positive charge of amino groups by hydroxide ions in the solution. At pH 7 and 9, PAN formed aggregates with smaller R_H as compared to NIPAAm homopolymer case, due to the electrical double layer repulsion among the positively charged amino groups, which was also due to higher LCST.

3.3.3 Initial settling rate

As shown in Figure 3a and b, the initial settling rates (ISR) of kaolin suspensions treated with three different kinds of polymers were different at pH 7. For the suspension treated with PAMN, higher ISR (0.6 m/h and 12 m/h at 25 °C and 50 °C, respectively) at low dosage (~ 25 ppm) was observed as compared to the suspension treated by PAN and PNIPAAm. The relatively lower settling results as compared with commercial flocculant

results from the extremely large difference of molecular weight. We focused on the comparison to the low molecular weight polymer flocculant like PAN and PNIPAAm used in other work to show the significance of introduction of benzoboroxole groups in the polymer to improve settling rate and clarity of supernatant. The settling rate dropped sharply when the dosage of PAMN exceeded 50 ppm. The kaolin clay suspension treated with PAN showed slightly higher ISR as compared to PNIPAAm case due to the electrostatic interaction. When the settling test proceeded at 50 °C (higher than LCSTs), as shown in Figure 3b, the increase of ISR for suspension dosed with PAMN is much more drastically as compared to suspension dosed with PAN due to the LCST of PAMN is lower, contributing larger improvement of hydrophobic force. High temperature also has positive effect on flocculation kinetics, reducing system viscosity to allow a homogeneous distribution of flocculant in the water, which is a benefit to facilitate polymer adsorption and charge neutralization on the particle surface. [42] Flocculation process involves three main steps, among which destabilization of dispersed particles and floc growth determines the turbidity of released water and initial settling rate, respectively.[13] The polymers in this study were unable to provide sufficient bridging force to capture a large amount of particles, due to the short polymer chains. However, the reversible complexation (with a binding constant of around 17 at neutral pH) of MAAmBo to hydroxyl groups on the surface of kaolin particles account for the floc growth and obvious settling for PAMN case.[13,19] It is generally accepted that the ISR will

keep increasing with the addition of flocculants until the suspension is overdosed (almost

half of the surface area of particles are covered by flocculants) according to the equation,

$P_B = \theta(1-\theta)$, P_B represents the probability of polymers cover on particles with a

conformation of loops which is beneficial to particles interaction and θ is the surface

coverage by flocculants in one particle.[42] The probability of flocculation (P_B) is the

largest when θ is equal to 0.5, over which the polymers conformations of mushrooms or

brushes will substitute the loops. As the dosage of PAMN exceeded 50 ppm in the

suspension, the ISR started to decrease, which might be due to more than half of the

surface of kaolin particle was occupied with polymer chains and less free space was left

for polymer attachment. The affinity between the particles were hindered by the steric

force arisen from overlapping mushrooms or brushes.[43] The hydrophobic force arisen

from PNIPAAm segments at 50 °C (>LCSTs), combined with the existing complexation,

hydrogen bonding and electrostatic force, accounted for the improved ISR at pH 7.

3.3.4 Turbidity of supernatant

The turbidity of the supernatant after 24 h of settling at pH 7 is shown in Figure 3c

and d. For the suspension dosed with PAMN, the turbidity of supernatant remained lower

than 240 NTU and 500 NTU at 25 and 50 °C respectively. The released water obtained

from suspension treated by PAN was with similar clarity as that treated by PAMN,

especially at 25 °C. However, the suspension dosed with PNIPAAm suffered from

poorest clarity, suggesting that plenty of fine particles remained in the released water. For

the suspension dosed with PNIPAAm, the turbidity kept increasing up to 2000 NTU with the dosage of polymer. The water clarification problem mostly lies in the destabilization of dispersed particles step. For the PAMN and PAN cases, polymers worked as polyelectrolyte to destabilize the particles by adsorbing and neutralizing the charges on to the negatively charged particle surfaces, which results in extremely low turbidity of supernatant. Cations provided by amino groups not only were able to improve water clarity due to charge neutralization ability, but also to strengthen the adhesion on to particle surface, inducing floc growth and faster settling rate as shown in Figure 3a and b. As previously reported, PNIPAAm with molecular weight < 1 MDa merely work as dispersant in suspension, leading to steric force at room temperature.[44] PNIPAAm homopolymer chains adsorb on the particle surfaces by hydrogen bonding without any charge neutralization. The conformation of tails or mushrooms also account for the enhanced steric force among particles. Thus, particles were dispersed in the supernatant by both electrostatic and steric forces, leading to the lowest supernatant clarity after settling. With increasing polymer dosage, the supernatant clarity was further reduced due to the enhanced steric force.
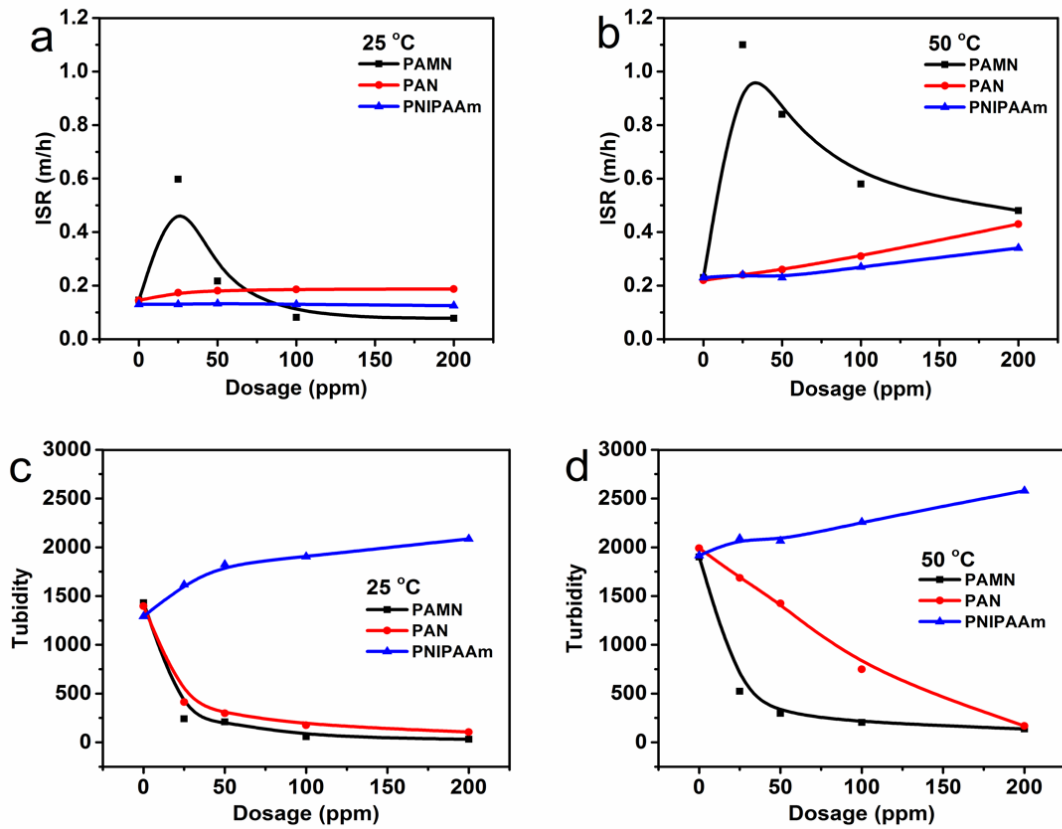
Figure 3.4. Initial settling rates (ISR, m/h) (a and b) and turbidity (c and d) of kaolin suspension (pH 7) dosed with polymers at 25 and 50 °C. ■ PAMN, ● PAN, ▲ PNIPAAm.

3.3.5 Sediment density

Solid content of sediment and sediment solid volume fraction are both used to represent the amount of solid in the sediment (sediment density). Figure 4 illustrates the sediment density at pH 7 after settling at 25 °C and at 50 °C. The suspension treated by PAMN showed the highest settling rate but the lowest solid content of sediment as compared with the PAN and PNIPAAm cases. The low sediment density for the PAMN

case could be due to strong adhesive interaction of polymer on the particle surface, which contributed to the strong sediment, leading to the considerable amount of water trapped in the intervals between the bulky PAMN-particle flocs which could not be further condensed by gravity. Although suffered from low settling rate due to lack of strong adhesion, for PAN and PNIPAAm cases, flocs or particles are small enough to fill into the gaps and squeeze out more water, which also agrees well with the initial settling rate result shown in Figure 3. In Figure 4b and d, suspension was settled at 50 °C for 6 h , and then kept standing at 25 °C. Lowering the temperature after settling phase resulted in an enhanced secondary consolidation of the suspension treated by PNIPAAm, which is mainly due to the absence of hydrophobic interaction of the PNIPAAm chains to effectively bridge the solid particles.[4, 45] However, particles treated by PAMN and PAN did not show such behaviors due to the presence of complexation and electrostatic attraction with the particles at either testing temperature.
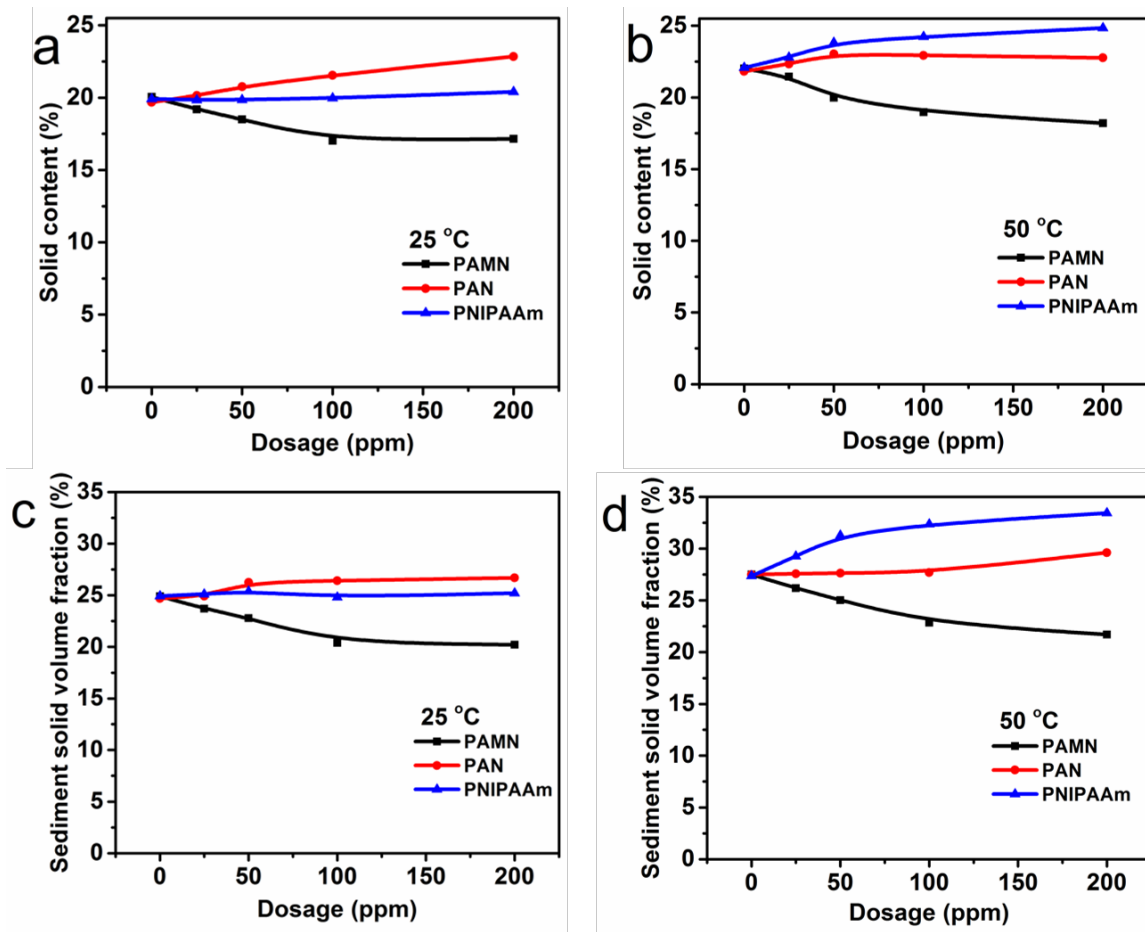
Figure 3.5. Weight percent (a and b) and volume fraction (c and d) of the solid in the sediment after flocculating kaolin suspension (pH 7) dosed with polymers at 25 and 50 °C. ■ PAMN, ● PAN, ▲ PNIPAAm.

3.3.6 The effect of pH on the performance of PAMN in kaolin suspension flocculation and settling

Figures 5a and b illustrated the impact of pH on the initial settling rate of kaolin suspension at 25 and 50 °C, respectively. Figure 5 shows that the initial settling rate of kaolin suspension at pH 9 was the highest among the three pH conditions (i.e. pH 7, 9 and 11). At pH 11, no flocculation or no obvious settling occurred at each temperature

condition, and the supernatant turbidity remained as high as in the case of suspension without polymer treatment (Figures 5c and d). The enhanced flocculation and settling behavior at pH 9 was most likely due to (1) the complexation of charged benzoboroxole groups and the hydroxyl groups on kaolin surfaces, and (2) electrostatic attraction between positive charged amino groups and negatively charged kaolin surfaces. However, it was observed from Figure 5c and d that the turbidity of supernatant after settling at pH 9 was higher as compared to the pH 7 case, which results from the particle surfaces being more ionized due to the higher pH medium, resulted in that the particles were difficult to be destabilized by electrical interaction at the first phase. While higher settling rate was the result of fast flocs growth due to the strong adhesion of benzoboroxole groups to particle surfaces at pH 9. At pH 11, PAMN and kaolin particles were both highly negatively charged, PAMN was not able to destabilize or bridge highly ionized particles, but worked as dispersant in the suspension.
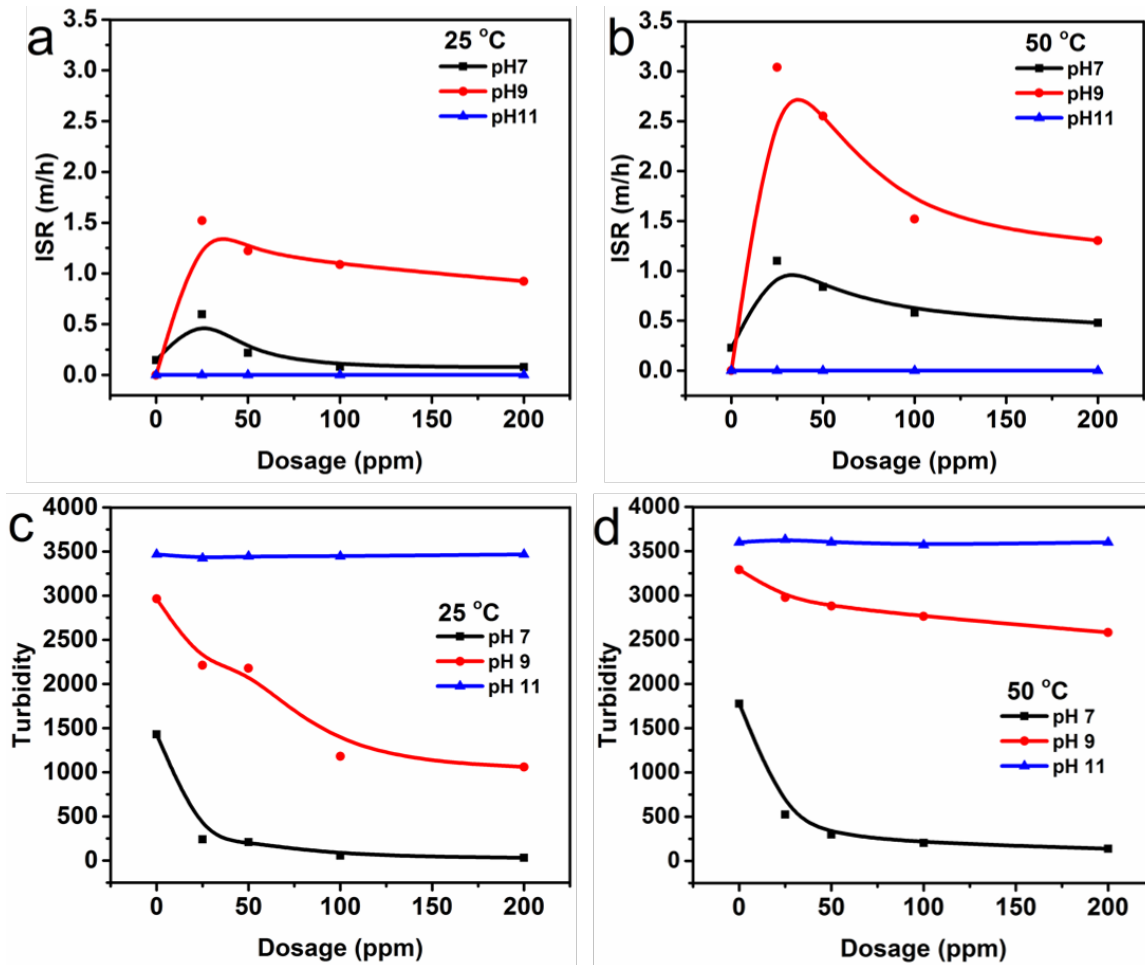
Figure 3.6. Initial settling rates (ISR, m/h) (a and b) and turbidity (c and d) of supernatant of kaolin suspension after dosed with PAMN at 25 and 50 °C. ■ pH 7, ● pH 9, ▲ pH 11.

3.3.7 The effect of pH on the performance of PAMN in sediment condensation

When the sediment height reached a plateau, consolidation behaviors of sediment with polymer dosage were studied at various pH and temperatures. Comparing Figures 6a with b and Figures 6c with d, it was clearly observed that the sediment density for pH 11 case is obviously higher as compared to the other two cases. According to the above

result, pH 11 case suffers from extremely low settling rate and highest turbidity, which suggests negligible flocculation or settling at the initial stage (about one hour). However, extremely small amount of sediment settled just under gravity was of high density, which can be explained by the negligible adhesion between polymers and particles under this condition. The small size particles became more compact than larger ones after settling to the bottom which is beneficial in squeezing out any trapped water to form the most compact structure.
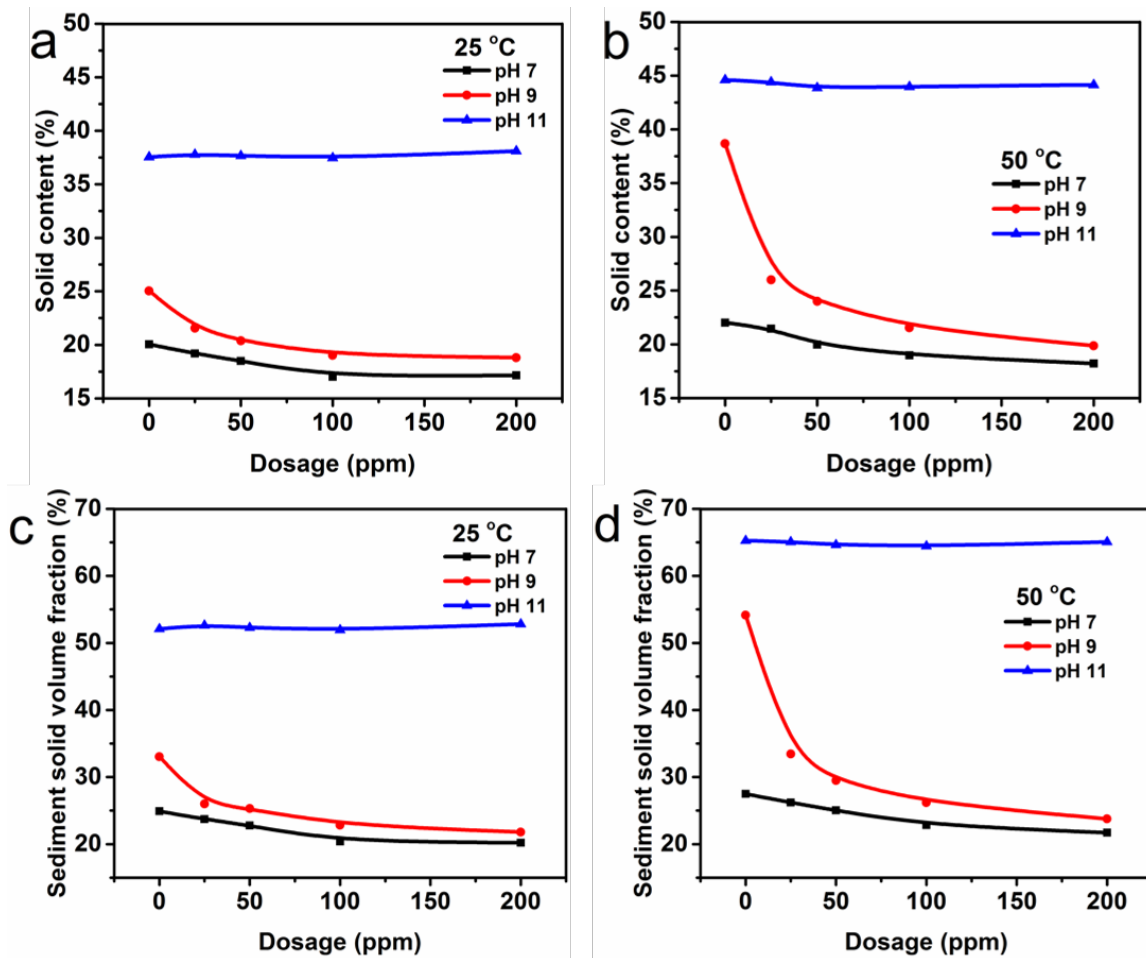
Figure 3.7. Weight percent (a and b) and volume fraction (c and d) of the solid in the sediment after flocculating kaolin suspension dosed with PAMN at 25 and 50 °C. ■ pH 7, ● pH 9, ▲ pH 11.

3.3.8 Second-step consolidation

As the batch settling experiments proceed, settling rate decreased gradually and the top height of sediment came gradually to a plateau. Continuous consolidation of sediment was hindered by strong attractive interaction and stable network set up with the PAMN-particle aggregates. As shown in Figure 7a and b, at each temperature conditions, sediment can be further condensed under gravity due to the pH switchover from 7 to 11 after 30 minutes. Since the introduction of pH sensitive benzoboroxole moieties, PAMN was negatively charged at pH 11, which resulted in the breakup of flocs in the sediment due to absence of complexation and electrostatic attraction. For the control test without pH switchover, no further condensation was observed after 72 h of settling, due to the stable network set up by particle-PAMN aggregates. Figure 7c shows that for the case with pH switchover after settling step, the sediment continuously condensed to nearly 50 % with respect to the sediment solid volume fraction as compared to 30 % for the pH 7 case. As shown in Figure 8A (a and c), the so called mud-lines of sediment with pH switchover (left) were much lower than the ones without pH increase (right), which also suggests that increasing pH after the settling step contributes to enhanced secondary consolidation of sediment. As shown in Figures 8A (b and d), in the pH 7 case, the sediment was stable like a gel. However, the solids in the sediment were readily to drift for the pH 11 case, due to the absence of strong adhesion between particles, provided an evidence of the substitution of attractive force by repulsive force. As the flocculation

mechanism shown in Figure 8B, it is noted that different flocculation and settling behavior at various pH are attributed to the changing of interaction of PAMN on the particle surface. Complexation of benzoboroxole to hydroxyl groups of particle, electrostatic interaction, and bridging force induced by hydrogen bonding are the main driving force of PAMN to adsorb on kaolin particle surface. At pH 9, adhesive interaction was dominated by interaction between benzoboroxole and hydroxyl groups, which is stronger than the dominative bridging force at pH 7. Except for providing adhesive force, electrostatic interaction induced by cationic amino groups to negatively charged particles are also responsible for charge neutralization and reverse, which contributing to the particle collision and aggregation. The reduced electrical repulsive force, combined with strong attractive force, are attributed to fast settling rate and low turbidity of supernatant. To enhance the solid density in the sediment, strong attractive force was reduced through increasing pH, reduced positive charge provided by amino groups and inducing the benzoboroxole groups carrying negative charge. The attractive/repulsive force transition allowed the breakup of flocs, which was beneficial for enhancing consolidation and releasing water, as smaller size particles were able to fill the gaps between previous

aggregates, and much water was released from the interspace of the network.
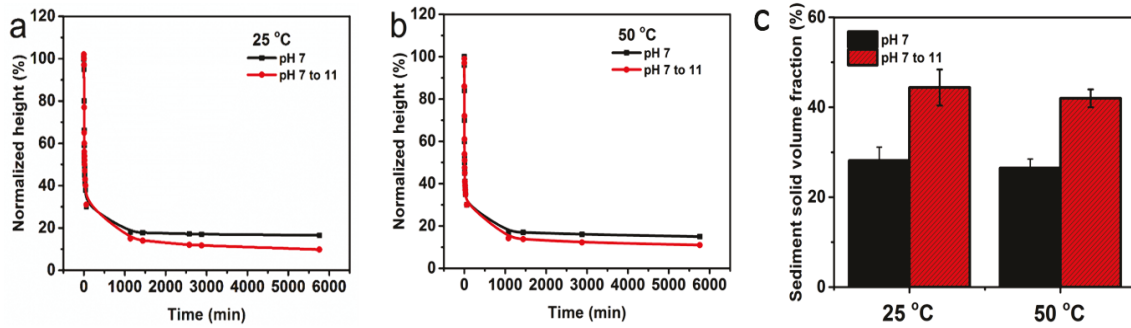
Figure 3.8. Height of interface between sediment and clarified supernatant as a function of time for PAMN at 25 (a) and 50°C (b), sediment solid volume fraction of kaolin sediment after settling of 72 h (c). The black color represents suspension flocculated at pH 7; red color represents suspension flocculated at pH 7 for 30 minutes, then adjusted to pH 11.
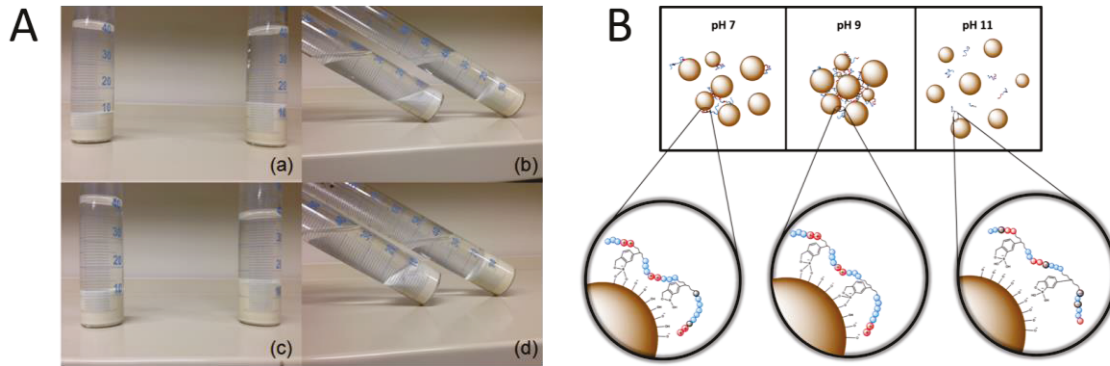
Figure 3.9. (A) Photographs of heights and conformations of sediment after settling by PAMN for 72 h at 25 (a and b) and 50 °C (c and d). The cylinders on the left in each photo represent sediments without pH change, and the right ones represent sediments with pH changing from 7 to 11 after 30 min of settling. (B) Flocculation mechanism of PAMN on the kaolin particle surface at pH 7, 9, 11.

3.3.9 Zeta potential measurements

Zeta potential measurements of 0.1 mg/mL kaolin clay suspension under various pH conditions were studied as a function of polymer dosages. As illustrated in Figure 9a, at 25 °C, zeta potentials for PAN case are almost the same at pH 7 and 9. However, for PAMN case, zeta potentials measured at pH 9 were slightly lower at either test temperature as compared to the pH 7 case. At 50 °C, as shown in Figure 9b, zeta potentials of kaolin treated by PAN were lower than that treated by PAMN at pH 7 and 9. For the pH 11 case, at either test temperature, kaolin suspension dosed with PAMN remains highly negative zeta potential at all dosages, due to a majority of benzoboroxole groups in PAMN turned to negatively charged (hydrophilic) form and the primary amine of AEMA segments (with a pKa of about 9) were neutralized by hydroxyl groups.[46, 47] NaCl was produced with the neutralization of amino groups under high basic condition, contributing to the compressed electrical double layer as shown in Figure 9a and b. For PAMN case, the lower zeta potentials (closer to zero) at pH 9 as compared to pH 7 case were attributed to the partial transfer of benzoboroxole moieties to their negatively charged form, accounting for affinity between particles, which was also beneficial to the complexation of benzoboroxole groups to hydroxyl on the particle surfaces, agreeing well with the initials settling rate result in Figure 5. Also, at pH 7 and 9, the surface charge of clay/PAMN aggregate switched from negative to positive when the polymer dosage

increased over 50 ppm, with an isoelectric point occurring at 25 ppm (Figure 9a), which agrees well with the settling results that the highest ISR was achieved at 25 ppm.

3.3.10 Interaction between polymer and kaolin particles

To better understand the mechanism of PAMN mediated particle flocculation, the interaction between negatively charged mica surface and PAMN coated surface was investigated using a surface forces apparatus (SFA) in deionized water. The interaction of PAMN on particle surface is mainly arisen from electrostatic force and adhesive interaction of benzoboroxole groups with hydroxyl groups. Mica and kaolin crystal both are composed of octahedral and silicon tetrahedral layers allowing negative charge and hydroxyl groups exist on the particle surface.[48] Thus we use mica to substitute kaolin in this force test. A typical force-distance profile is shown in Figure 9c, where one mica surface and one mica surface coated with PAMN were first brought in contact and then separated apart. A confined PAMN thickness of around 25 nm indicates the successful coating of PAMN onto mica surface. During separation, a strong adhesion was measured between PAMN and the mica surface, and the PAMN layer was stretched a few nm before the two surfaces jumped apart, which indicate the strong bridging attraction of PAMN to mica, arising from the combination of electrostatic attraction and the complexation between benzoboroxole on PAMN and hydroxyl groups on mica. A typical AFM image of PAMN layer coated on mica is shown in Figure 9d which also confirms the adsorption of PAMN on the clay surface.
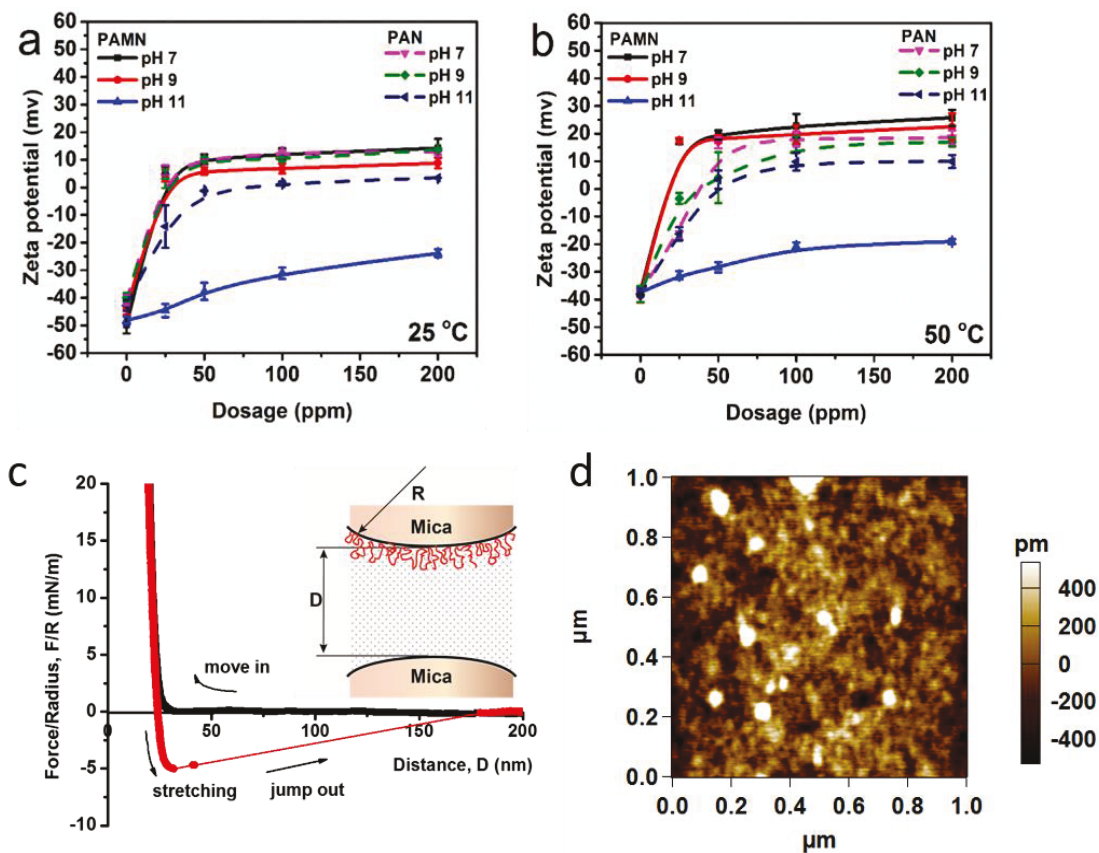
Figure 3.10. Zeta potentials of kaolin polymer aggregates measured as a function of pH and dosage of flocculants (solid line represents PAMN, and dash line represents PAN) at 25 (a) and 50 °C (b). Force vs distance profile between a mica surface and a PAMN layer coated on mica in Milli-Q water at 25 °C (c), and AFM image of PAMN coating deposited on mica (d).

3.4 Conclusions

This work reports the first example of using benzoboroxole-based copolymers poly[(2-aminoethyl methacrylamide hydrochloride)-*st*-(5-methacrylamido-1,2-benzoboroxole)-*st*-(*N*-isopropylacrylamide)],

viz. poly(AEMA-*st*-MAAmBo-*st*-NIPAM) or PAMN, on the flocculation and enhanced dewatering of fine particle suspensions. The temperature and pH responsive random copolymers PAMN are able to induce rapid settling rate of kaolin suspensions, resulting in released water with low turbidity, when compared to NIPAAm homopolymer and cationic random copolymers under neutral pH condition. Although cationic groups prevent the polymers from performing secondary condensation after reducing temperature, PAMN still work to break up the bulky flocs, attributing to pH responsive character. By changing pH from 7 to 11 at the secondary condensation phase, dramatically compact sediment can be obtained. Much more water can be released with the rearrangement of particle positions, which was achieved through the cationic/anionic switch of PAMN. The two-step solid-liquid separation method including two phases (i.e. settling and condensation) has proved efficient in enhancing the settling rate and condensing sediment of fine particle suspensions by using the temperature and pH responsive copolymer PAMN. Our results provide new insights into the development of novel polymer flocculants and dewatering technology.

3.5 References

(1) Allen, E.W. Process Water Treatment in Canada's Oil Sands Industry: I. Target Pollutants and Treatment Objectives. *J. Environ. Eng. Sci.* **2008**, *7*, 123-138.

(2) Alamgir, A., Harbottle, D., Masliyah, J., Xu, Z. Al-PAM Assisted Filtration System for Abatement of Mature Fine Tailings. *Chem. Eng. Sci.* **2012**, *80*, 91-99.

(3) Ji, Y., Lu, Q., Liu, Q., Zeng, H. Effect of Solution Salinity on Settling of Mineral Tailings by Polymer Flocculants. *Colloids Surf., A* **2013**, *430*, 29-38.

(4) Li, H.; O'Shea, J. P.; Franks, G. V. Effect of Molecular Weight of Poly (N-Isopropyl Acrylamide) Temperature-Sensitive Flocculants on Dewatering. *AlChE J.* **2009**, *55*, 2070-2080.

(5) Li, H., Long, J., Xu, Z., Masliyah, J. H. Masliyah. Flocculation of Kaolinite Clay Suspensions Using a Temperature-Sensitive Polymer. *AlChE J.* **2007**, *53*, 479-488.

(6) O'Shea, J. P., Qiao, G. G., Franks, G. V. Temperature Responsive Flocculation and Solid–Liquid Separations with Charged Random Copolymers of Poly (N-isopropyl acrylamide). *J. Colloid Interface Sci.* **2011**, *360*, 61-70.

(7) O'Shea, J. P., Qiao, G. G., Franks, G. V. Temperature-Responsive Solid-Liquid Separations with Charged Block-Copolymers of Poly(N-isopropyl acryamide). *Langmuir* **2012**, *28*, 905-913.

(8) Wang, Y., Kotsuchibashi, Y., Liu, Y., Narain, R. Temperature-Responsive Hyperbranched Amine-Based Polymers for Solid-Liquid Separation. *Langmuir* **2014**, *30*, 2360-2368.

(9) Burdukova, E., Ishida, N., Shaddick, T., Franks, G. V. The Size of Particle Aggregates Produced by Flocculation with PNIPAM as a Function of Temperature. *J. Colloid Interface Sci.* **2011**, *354*, 82-88.

(10) Franks, G.V. Stimulant Sensitive Flocculation and Consolidation for Improved Solid/Liquid Separation. *J. Colloid Interface Sci.* **2005**, *292*, 598-603.

(11) Sakohara, S., Kimura, T., Nishikawa, K. Flocculation Mechanism of Suspended Particles Utilizing Hydrophilic/Hydrophobic Transition of Thermosensitive Polymer. *Kagaku Kogaku Ronbun.* **2000**, *26*, 734-737.

(12) O'Shea, J. P., Qiao, G. G., Franks, G. V. Solid–Liquid Separations with a Temperature-Responsive Polymeric Flocculant: Effect of Temperature and Molecular Weight on Polymer Adsorption and Deposition. *J. Colloid Interface Sci.* **2010**, *348*, 9-23.

(13) Hogg, R. Flocculation and Dewatering. *Int. J. Miner. Process.* **2000**, *58*, 223-236.

(14) Sakohara, S., Ochiai, E., Kusaka, T. Dewatering of Activated Sludge by Thermosensitive Polymers. *Sep. Purif. Technol.* **2007**, *56*, 296-302.

(15) Franks, G. V.; O'Shea, J. P.; Forbes, E. Improved Solid-Liquid Separations with Temperature Responsive Flocculants: A Review. *Chemeca 2012: Quality of life through chemical engineering: 23-26 September 2012, Wellington, New Zealand* **2012**, 1062.

(16) Liu, H. Y., Zhu, X. X. Lower Critical Solution Temperatures of N-Substituted Acrylamide Copolymers in Aqueous Solutions. *Polymer* **1999**, *40*, 6985-6990.

(17) Cho, S. H., Jhon, M. S., Yuk, S. H. Temperature-Sensitive Swelling Behavior of Polymer Gel Composed of Poly N,N-Dimethylaminoethyl Methacrylate) and Its Copolymers. *Eur. Polym. J.* **1999**, *35*, 1841-1845.

(18) Cho, S. H., Jhon, M. S., Yuk, S. H. Effect of Comonomer Hydrophilicity and Ionization on The Lower Critical Solution Temperature of N-Isopropylacrylamide Copolymers. *Macromolecules* **1993**, *26*, 2496-2500.

(19) Kotsuchibashi, Y., Agustin, R. V. C., Lu, J. Y., Hall, D. G., Narain, R. Temperature, pH, and Glucose Responsive Gels via Simple Mixing of Boroxole-and Glyco-Based Polymers. *ACS Macro Letters* **2013**, *2*, 260-264.

(20) Kitano, S., Koyama, Y., Kataoka, K., Okano, T., Sakurai, Y. A Novel Drug Delivery System Utilizing a Glucose Responsive Polymer Complex between Poly (Vinyl Alcohol) and Poly (N-Vinyl-2-Pyrrolidone) with a Phenylboronic Acid Moiety. *J. Controlled Release* **1992**, *19*, 161-170.

(21) Shiino, D.; Murata, Y.; Kubo, A.; Kim, Y. J.; Kataoka, K.; Koyama, Y.; Kikuchi, A.; Yokoyama, M.; Sakurai, Y.; Okano, T. Amine Containing Phenylboronic Acid Gel for Glucose-Responsive Insulin Release under Physiological pH. *J. Controlled Release* **1995**, *37*, 269-276.

(22) Hall, D. G., Lee, J. C., Ding, J. Catalytic Enantioselective Transformations of Borylated Substrates: Preparation and Synthetic Applications of Chiral Alkylboronates. *Pure Appl. Chem.* **2012**, *84*, 2263-2277.

(23) Ma, R., Shi, L. Phenylboronic Acid-Based Glucose-Responsive Polymeric Nanoparticles: Synthesis and Applications in Drug Delivery. *Polym. Chem.* **2014**, *5*, 1503-1518.

(24) O'Day, P. A., Parks, G. A., Brown Jr, G. E. Molecular Structure and Binding Sites of Cobalt (ii) Surface Complexes on Kaolinite from X-Ray Absorption Spectroscopy. *Clays Clay Miner.* **1994**, *42*, 337-355.

(25) Giese, R. F. Hydroxyl Orientations in Gibbsite and Bayerite. *Acta Crystallogr., Sect. B: Struct. Sci.* **1976**, *32*, 1719-1723.

(26) Gupta, V., Miller, J. D. Miller. Surface Force Measurements at the Basal Planes of Ordered Kaolinite Particles. *J. Colloid Interface Sci.* **2010**, *344*, 362-371.

(27) Chan, M. C. W. A Novel Flocculant for Enhanced Dewatering of Oil Sands Tailings. *Master Thesis, University of Alberta, Edmonton,* **2011**.

(28) Michaels, A. S., Bolger, J. C. Settling Rates and Sediment Volumes of Flocculated Kaolin Suspensions. *Ind. Eng. Chem. Fundam.* **1962**, *1*, 24-33.

(29) Zbik, M. S., Smart, R. S. C., Morris, G. E. Kaolinite Flocculation Structure. *J. Colloid Interface Sci.* **2008**, *328*, 73-80.

(30) Nasser, M. S., James, A. E. The Effect of Polyacrylamide Charge Density and Molecular Weight on the Flocculation and Sedimentation Behaviour of Kaolinite Suspensions. *Sep. Purif. Technol.* **2006**, *52*, 241-252.

(31) Deng, Z., Bouchékif, H., Babooram, K., Housni, A., Choytun, N., Narain, R. Facile Synthesis of Controlled-Structure Primary Amine‑Based Methacrylamide Polymers via the Reversible Addition-Fragmentation Chain Transfer Process. *J. Polym. Sci., Part A: Polym. Chem.* **2008**, *46*, 4984-4996.

(32) Israelachvili, J., Min, Y., Akbulut, M., Alig, A., Carver, G., Greene, W., Kristansen, K., Meyer, E., Pesika, N., Rosenberg, K., Zeng, H. Recent Advances in the Surface Forces Apparatus (SFA) Technique. *Rep. Prog. Phys*. **2010**, *73*, 036601.

(33) Zeng, H., Hwang, D. S., Israelachvili, J. N., Waite, J. H. Strong Reversible Fe3+-Mediated Bridging between Dopa-Containing Protein Films in Water. *Proc. Natl. Acad. Sci. U. S. A*. **2010**, *107*, 12850-12853.

(34) Zeng, H., Tian, Y., Zhao, B., Tirrell, M., Israelachvili, J. Transient Surface Patterns and Instabilities at Adhesive Junctions of Viscoelastic Films. *Macromolecules* **2007**, *40*, 8409-8422.

(35) Lu, Q., Oh, D. X., Lee, Y., Jho, Y., Hwang, D. S., Zeng, H. Nanomechanics of Cation–Π Interactions in Aqueous Solution. *Angew. Chem*. **2013**, *125*, 4036-4040.

(36) Zeng, H., Tirrell, M., Israelachvili, J. Limit Cycles in Dynamic Adhesion and Friction Processes: A Discussion. *J. Adhes.* **2006**, *82*, 933-943.

(37) Zeng, H., Tian, Y., Anderson, T. H., Tirrell, M., Israelachvili, J. N. New SFA Techniques for Studying Surface Forces and Thin Film Patterns Induced by Electric Fields. *Langmuir* **2008**, *24*, 1173-1182.

(38) Hong, K., Zhang, H., Mays, J. W., Visser, A. E., Brazel, C. S., Holbrey, J. D., Reichert, W. M., Rogers, R. D. Conventional Free Radical Polymerization in Room Temperature Ionic Liquids: A Green Approach to Commodity Polymers with Practical Advantages. *Chem. Commun.* **2002**, 1368-1369.

(39) Zhang, H., Hong, K., Mays, J. W. Synthesis of Block Copolymers of Styrene and Methyl Methacrylate by Conventional Free Radical Polymerization in Room Temperature Ionic Liquids. *Macromolecules* **2002**, *35*, 5738-5741.

(40) Zhang, F., Wang, C. C. Preparation of P (NIPAM-Co-AA) Microcontainers Surface-Anchored with Magnetic Nanoparticles. *Langmuir* **2009**, *25*, 8255-8262.

(41) Mears, S. J., Deng, Y., Cosgrove, T., Pelton, R. Structure of Sodium Dodecyl Sulfate Bound to a Poly (NIPAM) Microgel Particle. *Langmuir* **1997**, *13*, 1901-1906.

(42) Kang, L., John L. C. Temperature Effects on Flocculation Kinetics Using Fe (iii) Coagulant. *J. Environ. Eng.* **1995**, 12, 893-901.

(43) Masliyah, J., Czarnecki, J., Xu, Z. Colloidal Science in Tailings Management. In *Handbook on Theory and Practice of Bitumen Recovery from Athabasca Oil Sands*. Kingsley Knowledge Publishing: Canada & United States, **2011**, Vol 1, 403-407.

(44) Franks, G., Burdukova, E., Li, H., Ishida, N., O'Shea, J. P. Mechanism Responsible for Flocculation in Poly (N-Isopropylacrylamide) Temperature Resposive Dewatering-Attractive Interaction Force Induced by Surface Hydrophobicity. *In 25th Int. Miner. Process. Congr*. Brisbane, Queensland, Australia, 4057-4067, **2011**.

(45) Franks, G. V., Li, H., O'Shea, J. P., Qiao, G. G. Temperature Responsive Polymers as Multiple Function Reagents in Mineral Processing. *Adv. Powder Technol.* **2009**, *20*, 273-279.

(46) Adam, W., Baeza, J., Liu, J. C. Stereospecific Introduction of Double Bounds via Thermolysis of Beta-Lactones. *J. Am. Chem. Soc.* **1972**, *94*, 2000-2006.

(47) Alidedeoglu, A. H., York, A. W., McCormick, C. L., Morgan, S. E. Aqueous Raft Polymerization of 2-Aminoethyl Methacrylate to Produce Well-Defined, Primary Amine Functional Homo-and Copolymers. *J. Polym. Sci., Part A: Polym. Chem.* **2009**, *47*, 5405-5415.

(48) Pauling, L. The Structure of the Micas and Related Minerals. *Proc. Natl. Acad. Sci.*

U. S. A. **1930**, 16, 123.

Chapter 4 Effect of Molecular Weight of Synthesized Poly (2-lactobionamidoethylmethacrylamide) on Flocculation and Dewatering

4.1 Introduction

Removing solid particles and recycling water are critical issues for mineral and oil sands industry for several decades since particles stabilized in the suspension can cause potentially serious environmental issues.[1-3] Inorganic salt and synthetic high molecular weight polyelectrolyte are widely applied to coagulate and flocculate particles in minerals industry and oil sands tailings.[2-12] However, inorganic flocculants like alumina and lime, and polymers like PNIPAAm are never considered to be eco-friendly due to the potential risk to environmental and health issues.[13] Several natural and synthetic polyelectrolytes have proved to be more effective and eco-friendly, such as chitosan ,[14] starch ,[15–17] poly (vinyl alcohol) (PVA) and poly (ethylene oxide) (PEO) etc.[18-21] A number of investigations about surface interaction of non-ionic linear polymer on the particles had been carried out from 1970s. Poly(vinyl alcohol) (PVA) and poly(ethylene oxide) (PEO) are the two most widely used examples to help researchers gain a deeper insight into the adsorption and flocculation mechanism.[22-32] From previously studies, the adsorption of non-ionic polymer like PVA was driven by hydrogen bonding of hydroxyl groups of PVA to the free silanol groups of silica particles, and influenced by pH value of the solution. At the point of zero

charge (pH 2) of silica, adsorption of PVA was the highest due to more undissociated silanol groups acted as adsorption site.[33]

Carbohydrate-based polymers are becoming extremely popular for the application of drug/gene delivery carrier and antibacterial/virus, due to their high biocompatibility, no cytotoxicity, and potential targeted delivery of cargo.[34,35] The synthesis, characterization and biochemical application of 2-lactobionamidoethyl methacrylamide (LAEMA) based polymer with different compositions and structures were widely investigated in the group of Narain.[36,37] However, their application in the solid-liquid separation field has not been explored. Carbohydrate-protein interaction was attributed to specific interaction of the protein with the sugar groups mediated by the hydroxyl groups, therefore, these hydroxyl groups can be exploited for the enhance flocculation as a non-ionic flocculant.[37] Due to the presence of pendant sugar residues, PLAEMA contains more hydroxyl groups than PVA with the same average number of repeating units (DP), contributing to larger attractive force (hydrogen bonding) to the silanol groups of particles. In addition, the wide applications of PLAEMA as gene and drug delivery carrier in biochemical field have proved its outstanding eco-friendly property. It is expected that PLAEMA is able to interact with silanol groups, improving flocculation of particles and water recycle.

In this work, LAEMA homopolymer with various molecular weight has been synthesized for the solid-liquid separation, viz. flocculation and enhanced dewatering of fine solid suspensions. To the best of our knowledge, this is the first report of using

76

glycopolymers containing galactose residues for solid-liquid separation in tailings water treatment. Kaolin particles used as model tailing in the study are the major component of oil sands tailing solid, consisting with alternating layers of silica tetrahedra and alumina octahedra, which are broken at the edge of crystal to expose silanol and aluminol groups, resulting in the pH-dependent charge property. Herrington, et al. have found the point of zero charge around pH 7,[19] which was used as the standard condition in this study. The initial settling rate, supernatant turbidity, sediment solid content, and mud-line position were investigated. Dynamic light scattering (DLS), surface forces apparatus (SFA), and atomic force microscopy (AFM) were also employed to characterize the intermolecular and surface interactions between the polymers and solid particles, providing insights into the flocculation mechanism.

4.2 Materials and Methods

4.2.1 Materials

The 2-lactobionamidoethyl methacrylamide (LAEMA) monomer was prepared in-house according to previously reported procedure.[38, 39] The ammonium persulfate A.C.S. reagent was purchased from Sigma-Aldrich Chemicals (Oakville, ON, Canada). N,N,N',N'-tetramethylenediamine (TEMED) was purchased from Fisher Scientific. All organic solvents were purchased from Caledon Laboratories Ltd. (Georgetown, ON, Canada). The specific surface area and particle size distribution of kaolin (Acros Organics)

were determined by laser diffraction (Mastersizer 2000, Malvern) and were shown in the Figure 1.

4.2.2 Synthesis of PLAEMA

The linear PLAEMA homopolymer was prepared according to previously reported procedures.[35] Typically, LAEMA (650 mg, 1.39 mM) was dissolved in 5 mL distilled deionized water in the presence of ammonium persulfate (5 mg, 0.02mM) and TEMED (20 μl, 0.063mM) as initiator and catalyst, respectively. The mixture was purged with nitrogen for 30 min in a sealed 10-mL Schlenk tube and the reaction was processing at room temperature for 24 h. The polymer was purified by dialysis against double distilled deionized water for 4 days. Then the solution was frozen by liquid nitrogen for 10 min and freeze-dried for 2 days. The number average molecular weight (Mn) and molecular weight dispersity (PDI) were determined by gel permeation chromatography (GPC) (Viscotek model 250 dual detectors system), using 0.5 M sodium acetate and 0.5 M acetic acid as eluent. The flow rate was set to 1.0 mL/min. The resulting polymers were characterized by a Varian 500 ^{1}H NMR using D_2O as solvent.

4.2.3 Settling test

The settling test followed the previously reported procedure.[4] In order for the complete dissolution of flocculant before mixing with the kaolin suspension, polymers (1, 2.5, 5, 10, 15 mg) were respectively dissolved in 10 mL distilled deionized water and kept for 24 h.

The kaolin suspension (5 wt%) was homogenized by a mechanical stirrer (IKA® Digital Stirrer RW20, Fisher Scientific). 90 mL kaolin suspension was transferred into a standard 250-mL baffled beaker and was stirred with a 4 blade stainless steel impeller (blade width 3 cm, Fisher Scientific) at 600 rpm for 2 min. polymer stock solution was then added to suspension in 1 min with a agitation speed of 200 rpm. The agitation was stopped immediately after complete addition of the polymers with desired amount. The mixture was transferred to a 100-mL cylinder. The cylinder was inverted for 5 times and then kept still stand for 24h at room temperature. The height of so called mud-line was monitored as a function of time. The mud-line position was determined as % mud-line= h_f/ H, h_f and H represent the height of sediment and the original suspension, respectively. The initials settling rate was determined by the initial slope of plot (normalized height vs time), the light transmittance of the supernatant at 500 nm wavelength was monitored by a UV-Vis spectrometer. Turbidity of the released water was calculated from the equation of NTU $\approx$ $0.191 + 926.1942 \times [-\log(\%T/100)]$, where the %T represents the value of transmittance of the supernatant. Solid content of sediment is derived from dividing the mass of solid clays (m_s) by the total mass of sediment (m_f).

4.2.4 Polymer sizes

The hydrodynamic radii of polymers in the bulk solution was determined by dynamic light scattering (DLS) using a Malvern Zetasizer Nano ZSP. In order for the complete dissolution, 100 ppm polymer solutions were prepared by dissolving desired amount of

polymers in the distilled deionized water in a 20-mL glass vials before the experiment. All of the tests were carried out at 25ºC.

4.2.5 Interaction force measurements between polymers and clay surfaces and imaging of adsorbed polymers

Surface forces apparatus (SFA 2000) was used to measure the interaction of polymer with the model mica clay surface, which has similar silicate structure and composition as kaolin. The morphology of adsorbed polymer coating was imaged by an atomic force microscopy (AFM, MFP-3D, Asylum, Santa Barbara, CA). The polymer films for AFM imaging were prepared by dipping the freshly cleaved mica sheets in 1000 ppm synthetic polymer solution (1 mg/mL in Milli-Q water) to allow adsorption for 1 h, followed by thoroughly rinsing the surfaces with Milli-Q water to remove the unbounded polymer chains for several times and then dried in vacuum. Surface topography of adsorbed polymer layer on mica was characterized using an AFM in tapping mode in the air. At least three images at different (>3) positions were measured and typical AFM images were presented.

SFA has been widely used to directly measure the intermolecular and surface forces of various materials, in both vapors and liquid media, with Angstrom resolution for separation distance and nanonewton force precision.[40-44] In a typical SFA experiment, two back-silvered mica sheets with the same thickness of 1-5μm were glued on two cylindrical

silica disks with radius (R) of 2 cm. If the separation distance D was much smaller than R ($D \ll R$), the interaction between two cross-cylindrical mounted mica surfaces is locally equal to two spheres of radius $2R$ or a sphere of radius R near a flat surface. The absolute distance between two mica surfaces was determined through multiple light beam interferometry employing fringes of equal chromatic order (FECO) and the surface forces were derived through Hooke's law by multiplying the spring constant.[32, 37] During the force measurements, the reference distance ($D = 0$) was measured at the adhesive contact between two bare mica surfaces in air. Then the prepared 10 ppm polymer solution was injected to the interval of two mica surfaces and incubated for 30 min. All experiments were conducted at room temperature (~23 ℃). For each sample, the surface forces measurements were repeated for at least three times for two different pairs of surfaces to ensure the reproducibility.

4.3 Result and discussion

4.3.1 Characterization of tailings and polymers

Particle size distribution is a critical factor that influences the flocculation and settling performance. As shown in Figure 3, the D_{10}, D_{50}, D_{90} of the kaolin particles were 1.94, 6.67, and 27.2 μm, respectively. The size distribution parameter D_m represent m wt% of the particle sample was smaller than the corresponding value of D_m (μm). In this study, 10 wt% of the kaolin particles were smaller than 1.94 μm. Similarly, 90 wt% and 50 wt% of the

particles were smaller than 27.2 and 6.67 µm, respectively. The specific surface area was calculated from the size distribution. LAEMA homopolymer with various molecular weights were synthesized via conventional free radical polymerization and their performance of aggregating particles were evaluated, as shown in Scheme 1. The average molecular weight (Mn), polydispersity (PDI), and compositions are listed in the Table 1. The adhesion of PLAEMA to the surface of kaolin particles was mainly caused by bridging force, attributed to van der Waals force and hydrogen bonding arisen from the large number of hydroxyl groups introduced by the galactose segment in the PLAEMA. The molecular weight distribution (PDI) is relatively large as expected via conventional free radical polymerization. PLAEMA with larger molecular weight suffered from broader PDI as shown in Figure 2, which lies in the fact that the viscosity of high molecular weight polymer solution was increasing seriously along with the polymerization, leading to insufficient homogenization.
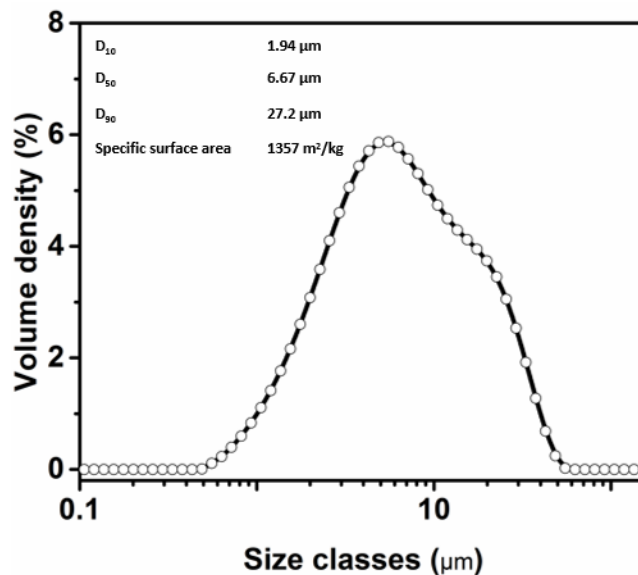
Figure 4.1. The particle size distribution of kaolin sample used in this study.
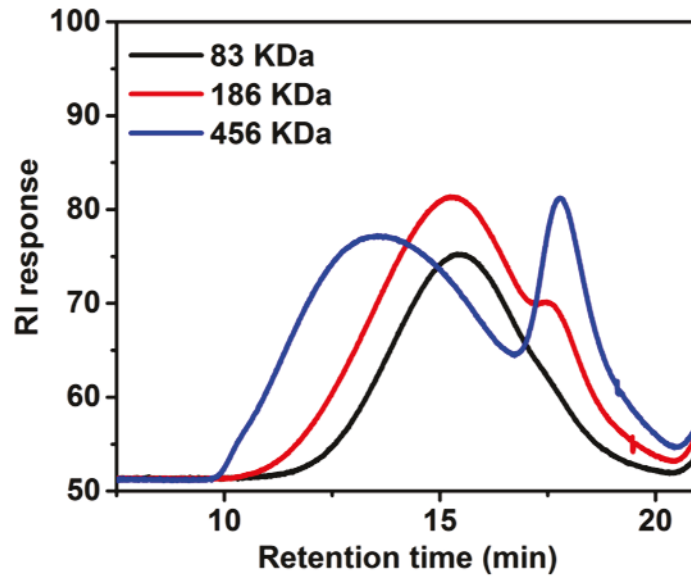
Figure 4.2. The molecular weight and polydispersity measured by gel permeation chromatogrophy (GPC), ▬ 83 kDa, ▬ 186 kDa, ▬ 456 kDa.
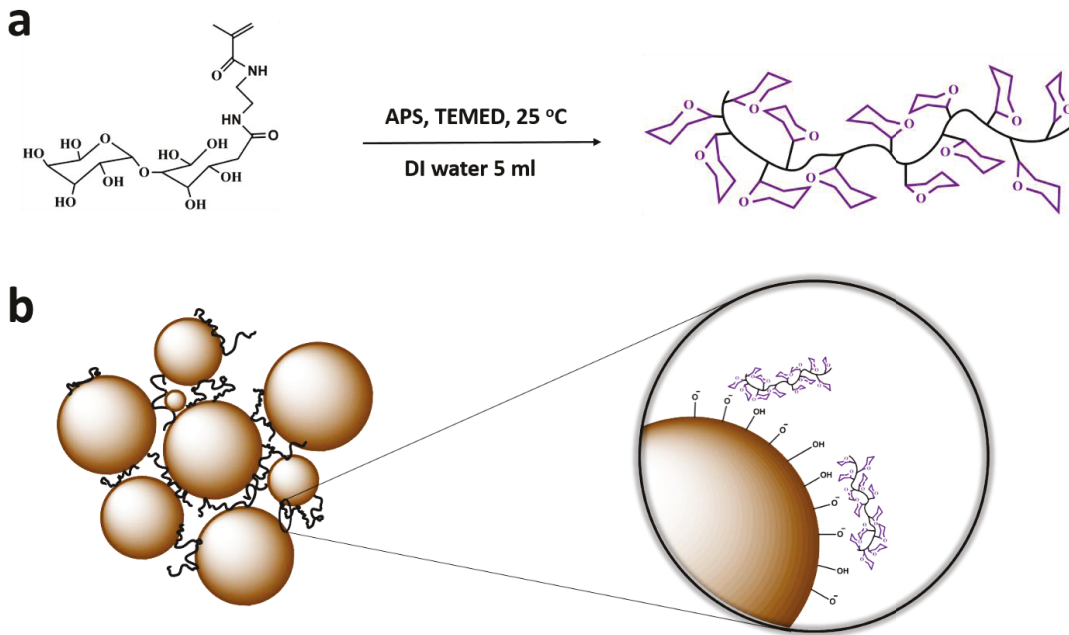
Figure 4.3. (a) Synthesis of LAEMA homopolymer via conventional free radical polymerization, (b) mechanism of the adhesion of polymer to the particle surface.

Table 4.1. Synthetic parameters, polymer compositions of PLAEMA.

Polymer Compositions	M_n (kDa)	M_w/M_n	Initiator (mg)
PLAEMA$_{177}$	83	2.61	APS, 5
PLAEMA$_{397}$	186	3.67	APS, 5
PLAEMA$_{975}$	456	3.35	APS, 5

4.3.2 Settling test

The flocculation performance of PLAEMA with different molecular weights as a function of dosage was investigated as shown in Figure 2a and b. As shown in Figure 2a, in the case of PLAEMA$_{975}$ (with molecular weight of 456 kDa), initials settling rate (ISR) reached the maximum values (1.26 m/h) at the dosage of 10 ppm. However, PLAEMA with lower molecular weights (186 and 83 kDa) showed negligible initial settling rate due to relatively smaller adhesive force of polymers to particle surface. The case of PLAEMA$_{397}$ (with molecular weight of 186 kDa) showed the highest settling rate (0.52 m/h) at the dosage of 25 ppm. In the case of PLAEMA$_{177}$ (with molecular weight of 83 kDa), settling rate kept increasing up to 0.49 m/h at the dosage of 150 ppm. Comparatively, in the cases of PLAEMA$_{975}$ and PLAEMA$_{397}$, settling rate reduced to nearly zero at 150 ppm, which is even lower than the settling rate of kaolin suspension without any polymer treatment. The gel-like formation of kaolin suspension was

observed at extremely high dosage, which was the result of over dose of polymer. The extra polymer chains covered on particle surface left less bare surface for the adsorption of polymers covered on other particles, leading to poor linkage of multiple particles and flocculation. The significance of controlling dosage of flocculant also lies in the fact that larger attractive force is necessary to overcome the steric force arisen from dehydration during the mutual penetration of thicker surface polymer layer.[45] PLAEMA with high molecular weight induced higher settling rate with less dosage as compared to low molecular weight case, suggesting the larger attractive forces (van der Waals force and hydrogen bonding) and stronger ability of aggregating particles. The longer polymer chains are more flexible to form hydrogen bond on particle surface, as compared with the short and stiff ones. The clearance of the released water was determined by testing turbidity of supernatant after 1 h of setting test. As shown in the Figure 2 (b), the turbidity of kaolin suspension with polymer treatment is reduced from 3179 to 2510, 1526, 750 Nephelometric Turbidity Units (NTU) at 10 ppm, for the cases of $PLAEMA_{177}$, $PLAEMA_{397,}$ $PLAEMA_{975}$. As the dosage increase up to 25 ppm, the turbidity of $PLAEMA_{975}$ (456 kDa) case was reduced to 95. In contrast, in the case of $PLAEMA_{177}$ (80 kDa), the reduction of turbidity was not obviously. At the dosage of 150 ppm, the turbidity of all cases was reduced to extremely low value (~ 20), showing negligible amount of kaolin particles exist in the supernatant. In high molecular weight case, the attractive force of polymer to the particle surface were sufficient at lower dosage, which

also suggests a stronger ability of providing more hydroxyl groups for flocculation. Figure 3a-c were the photos taken after 1 h of settling at room temperature, directly showing the supernatant clarity as functions of molecular weight and dosage. The cylinders from left to right represent polymer dosages of 10, 25, 50, 100, 150 ppm, respectively. In the case of PLAEMA$_{975}$, all samples showed the clearest supernatant. However, in the cases of PLAEMA$_{177}$ and PLAEMA$_{397}$, higher dosage cases induced clearer supernatant. The phenomenon showed in the photos were in good agreement with the result of Figure 2b.
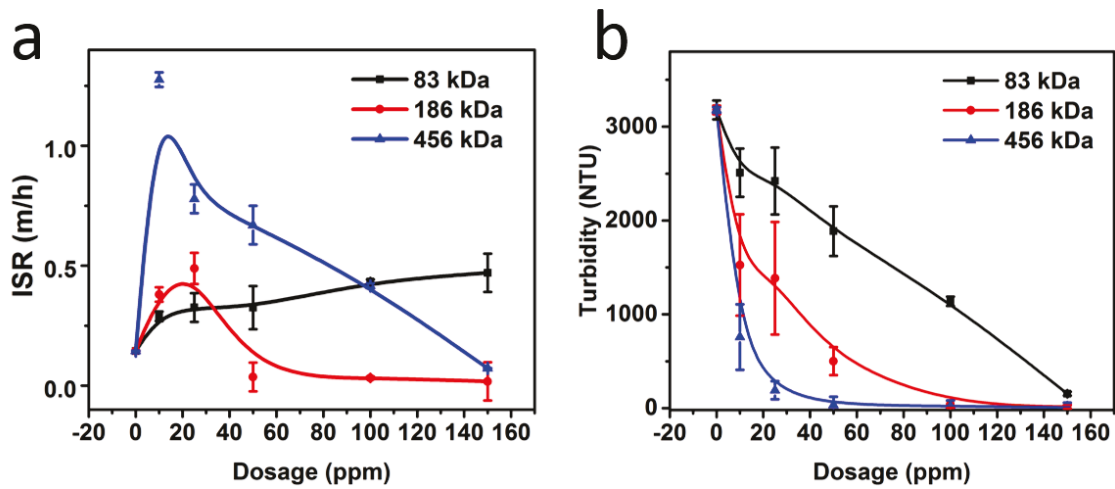
Figure 4.4. (a) Initial settling rate (ISR), (b) Supernatant turbidity of the PLAEMA treated model tailing (kaolin suspension) at 25 °C, ■83 kDa, ● 186 kDa, ▲ 456 kDa.
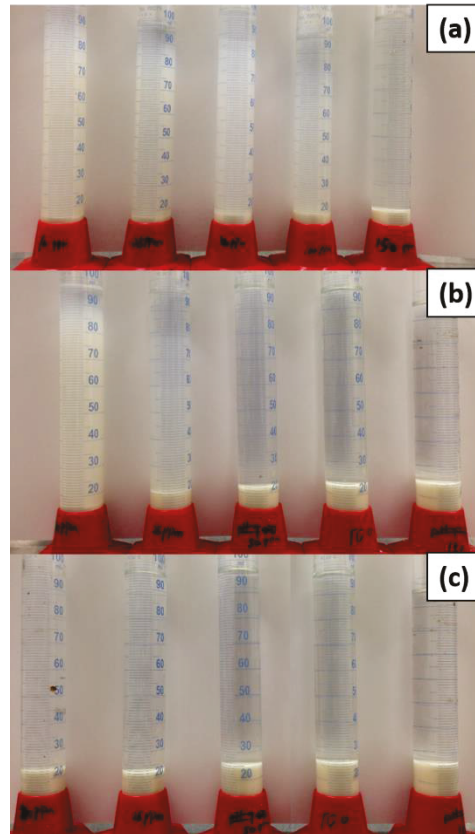
Figure 4.5. Photos show the effect of dosage and molecular weight on the turbidity of the supernatant, (a) 83 kDa, (b) 186 kDa, (c) 456 kDa. The dosages are 10, 25, 50, 100, 150 ppm (from left to right), respectively.

4.3.3 Condensation of sediment

The normalized height of liquid-solid interface (mud-line) and solid content of sediment both reflect the ratio of released water and water trapped in the sediment. As shown in Figure 5a, the mud-line of sediment treated with $PLAEMA_{177}$ was lowest among the three cases. With the increase of polymer dosage, mud-line of sediment became gradually higher in all three cases. Solid content of sediment was defined by the weight percent of solid in the sediment. As the result in the Figure 5b, 10 ppm is the optimal dosage to obtain the most compact sediment, and solid content of sediment was

decreasing with the increase of dosage, which suggested high dosage and molecular weight led to large amount of trapped water in the sediment. Although, high molecular weight polymer is beneficial for the aggregation of polymer and increase settling rate (Figure 1a), the stronger adhesion of polymer to the particle surface induce stronger sediment, which did not consolidate well.[8] In the high dosage case, the gel-like formation of suspension hindered the consolidation of particles due to steric force, which also led to a higher mud-line, in good agreement with the settling rate result. In the low dosage case, much more water was released from sediment due to more interval gaps was occupied by particles, also contributed to a more compact structure.
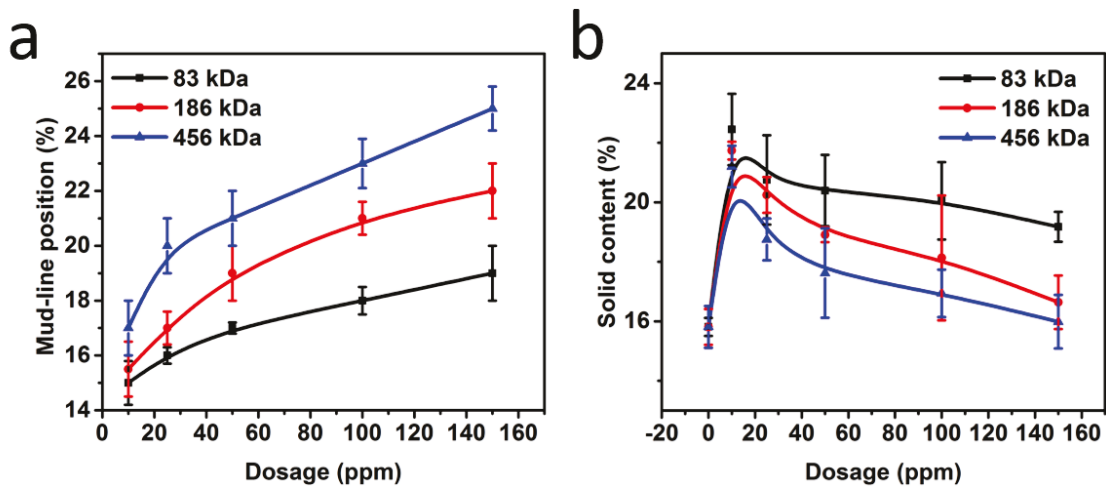
Figure 4.6. (a) Mud-line position %, and (b) Solid content of sediment of the PLAEMA treated model tailing (kaolin suspension) at 25 °C, ■83 kDa, ● 186 kDa, ▲ 456 kDa.

4.3.4 Polymer aggregation

The hydrodynamic radii of PLAEMA with various average molecular weight was

investigated at pH 7, as shown in Figure 6. The sizes of glycopolymer in the distilled

deionized water increased from 5 - 28 nm with the increase of molecular weight. The

increasing size with molecular weight of polymer in distilled deionized water suggests

the longer length of polymer chain or the aggregation of PLAEMA, which both proved

the existence of stronger capability to provide larger hydrogen bonding, agreed well with

the settling rate and consolidation result (Figure 3a and Figure 5a and b).
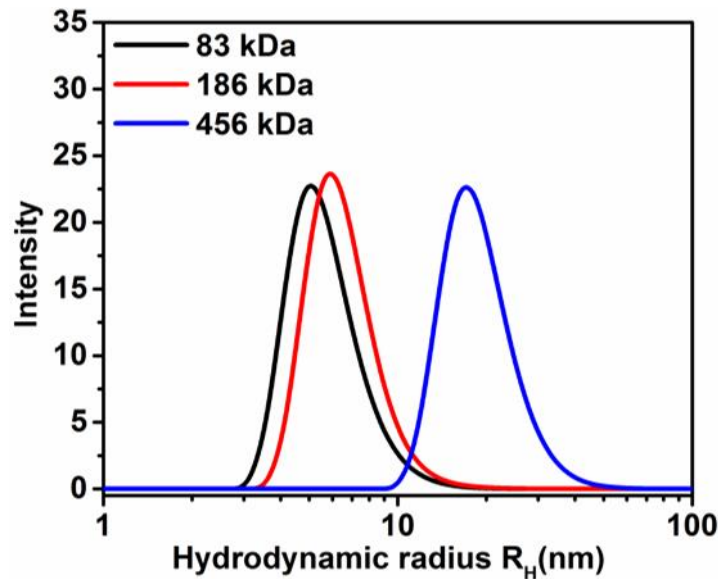
Figure 4.7. Hydrodynamic Radii (R_H) distribution of polymers with various average
molecular weight, ▬ 83 kDa, ▬ 186 kDa, ▬ 456 kDa.

4.3.5 Surface force measurement

To deeply understand the effect of molecular weight on the interaction of polymer on

kaolin particle surface, surface force measurement of two mica surfaces was carried out

in the 10 ppm PLAEMA water solution at neutral pH. The typical surface force vs

distance curves measured by SFA were shown in Figure 7a, b, and c, representing

PLAEMA$_{177}$, PLAEMA$_{397}$, PLAEMA$_{975}$, respectively. During the approaching of two mica surfaces, repulsive force was measured in all three cases resulting from that particle surface and polymer were both hydrated. Extra energy was necessary for the dehydration when polymer tried to adsorb on the particle surface. Adhesion (F_{ad}/R) was measured during the separation of two mica surfaces for all three cases, as shown in the red lines of Figure 7a, b, c. The adhesion results were ~3, 8, and 11 mN/m, which was increasing with molecular weight of the PLAEMA. Stronger hydrogen bonding was provided by PLAEMA$_{975}$ absorbed on kaolin particle surfaces due to more hydroxyl groups and more flexible polymer chain, resulting in the enhanced flocculation performance of polymer on kaolin particle suspension.
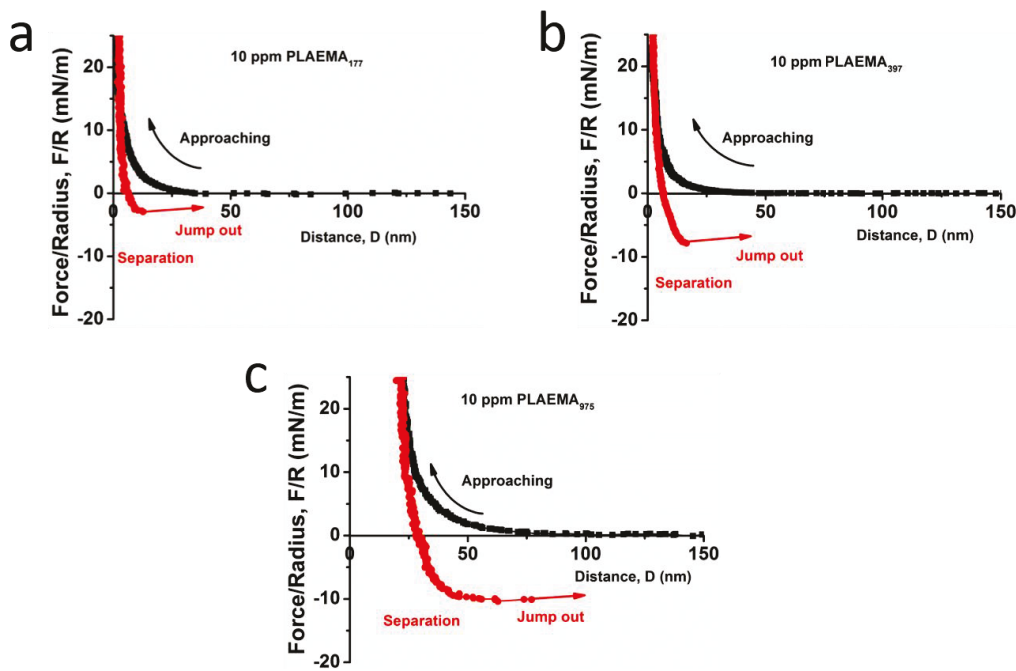
Figure 4.8. Force vs distance profile between two mica surfaces in 10 ppm (a)

PLAEMA$_{177}$, (b) PLAEMA$_{397}$, (c) PLAEMA$_{975}$ water solutions.

4.3.6 Topography of polymer adsorbed mica surface

In order to monitor the topographical changes with molecular weights of glycopolymers, PLAEMA$_{177}$, PLAEMA$_{397}$, PLAEMA$_{975}$ adsorbed on mica surfaces in Milli-Q water were imaged using an AFM and are shown in Figure 8a, b and c, respectively. The root-mean-square roughness determined by AFM was 0.1, 0.15, 0.23 nm for the cases of PLAEMA$_{177}$, PLAEMA$_{397}$, PLAEMA$_{975}$, respectively. The AFM images revealed that the amount of PLAEMA adsorbed on mica surface increased with molecular weight. The polymer-polymer and polymer-particle adhesive interaction results from hydrogen bonding, van der Waals force, hydrophobic force as previously reported.[45, 46] The dominant hydrogen bonding interactions was due to the large number of hydroxyl groups on the pendant sugars and the hydroxyl groups on particle surface. Since the large molecular weight PLAEMA$_{975}$ contains more functional sugar residues, combined with more flexible and longer polymer chains, a rapid and strong hydrogen bonding interactions with mica surface was possible and hence allowing rapid aggregation. The AFM results as shown Figure 8a, b and c are in agreement with the results from the settling test (Figure 3) and surface force measurements by SFA (Figure 7), that larger molecular weight PLAEMA contributed to stronger adhesion to kaolin particle and faster settling rate
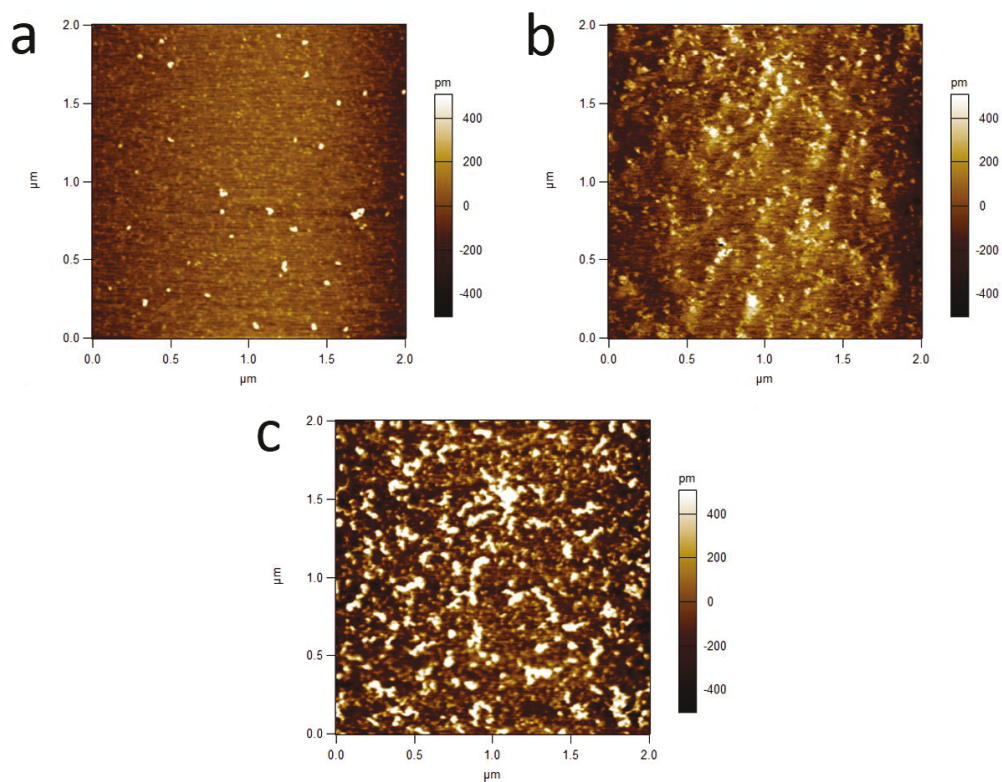
Figure 4.9. AFM images of (a) PLAEMA$_{177}$, (b) PLAEMA$_{397}$, (c) PLAEMA$_{975}$ coating absorbed on mica surfaces.

4.4 Conclusion

Glycopolymers, (PLAEMA), with different molecular weights were synthesized via conventional free radical polymerization. The flocculation performance and adhesion of PLAEMA were investigated through settling test, force measurement, and topography imaging. The influence of molecular weight on settling rate, released water clarity, solid content, and adhesive interaction were evaluated. High molecular weight of PLAEMA has a positive effect on rapid particle settling at low dosages, which results from the existence of larger amount of hydrogen bonds provided by galactose residues. The higher flexibility

of long polymer chains is also beneficial to the formation of hydrogen bonding with particle surface. Optimal dosage of 10 ppm was recorded during the process of flocculation. The surface force measurements and polymer coating images showed strong evidences of stronger intermolecular and polymer-particle adhesion for the case of PLAEMA$_{975}$, contributing to enhanced flocculation behavior..

4.5 Reference

(1) Allen, E. W. Process Water Treatment in Canada's Oil Sands Industry: I. Target Pollutants and Treatment Objectives. *J. Environ. Eng. Sci.* **2008**, *7* (2), 123–138.

(2) Alamgir, A.; Harbottle, D.; Masliyah, J.; Xu, Z. Al-PAM Assisted Filtration System for Abatement of Mature Fine Tailings. *Chemical Engineering Science* **2012**, *80*, 91–99.

(3) Nasim, T.; Bandyopadhyay, A. Introducing Different Poly (vinyl Alcohol) s as New Flocculant for Kaolinated Waste Water. *Separation and Purification Technology* **2012**, *88*, 87–94.

(4) Ji, Y.; Lu, Q.; Liu, Q.; Zeng, H. Effect of Solution Salinity on Settling of Mineral Tailings by Polymer Flocculants. *Colloids and Surfaces A: Physicochemical and Engineering Aspects* **2013**, *430*, 29–38.

(5) Wang, Y.; Kotsuchibashi, Y.; Liu, Y.; Narain, R. Temperature-Responsive Hyperbranched Amine-Based Polymers for Solid–Liquid Separation. *Langmuir* **2014**, *30* (9), 2360–2368.

(6) O'Shea, J.-P.; Qiao, G. G.; Franks, G. V. Temperature Responsive Flocculation and Solid–liquid Separations with Charged Random Copolymers of poly (N-Isopropyl Acrylamide). *Journal of Colloid and Interface Science* **2011**, *360* (1), 61–70.

(7) Li, H.; O'Shea, J.-P.; Franks, G. V. Effect of Molecular Weight of poly(N-Isopropyl Acrylamide) Temperature-Sensitive Flocculants on Dewatering. *AIChE J.* **2009**, *55* (8), 2070–2080.

(8) O'Shea, J.-P.; Qiao, G. G.; Franks, G. V. Temperature-Responsive Solid–Liquid Separations with Charged Block-Copolymers of Poly (N-Isopropyl Acryamide). *Langmuir* **2012**, *28* (1), 905–913.

(9) Burdukova, E.; Ishida, N.; Shaddick, T.; Franks, G. V. The Size of Particle Aggregates Produced by Flocculation with PNIPAM, as a Function of Temperature. *Journal of Colloid and Interface Science* **2011**, *354* (1), 82–88.

(10) Franks, G. V. Stimulant Sensitive Flocculation and Consolidation for Improved Solid/liquid Separation. *Journal of Colloid and Interface Science* **2005**, *292* (2), 598–603.

(11) Sakohara, S.; Kimura, T.; Nishikawa, K. Flocculation Mechanism of Suspended Particles Utilizing Hydrophilic/hydrophobic Transition of Thermosensitive Polymer. *Kagaku Kogaku Ronbunshu* **2000**, *26* (5), 734–737.

(12) Li, H.; Long, J.; Xu, Z.; Masliyah, J. H. Flocculation of Kaolinite Clay Suspensions Using a Temperature-Sensitive Polymer. *AIChE journal* **2007**, *53* (2), 479–488.

(13) Stauber, J. L.; Florence, T. M.; Davies, C. M.; Adams, M. S.; Buchanan, S. J. Bioavailability. **1999**.

(14) Yang, Z.; Shang, Y.; Lu, Y.; Chen, Y.; Huang, X.; Chen, A.; Jiang, Y.; Gu, W.; Qian, X.; Yang, H.; et al. Flocculation Properties of Biodegradable Amphoteric Chitosan-Based Flocculants. *Chemical Engineering Journal* **2011**, *172* (1), 287–295.

(15) Chen, Y.; Liu, S.; Wang, G. A Kinetic Investigation of Cationic Starch Adsorption and Flocculation in Kaolin Suspension. *Chemical Engineering Journal* **2007**, *133* (1), 325–333.

(16) Järnström, L.; Lason, L.; Rigdahl, M. Flocculation in Kaolin Suspensions Induced by Modified Starches 1. Cationically Modified Starch—effects of Temperature and Ionic Strength. *Colloids and Surfaces A: Physicochemical and Engineering Aspects* **1995**, *104* (2), 191–205.

(17) Bratskaya, S.; Schwarz, S.; Liebert, T.; Heinze, T. Starch Derivatives of High Degree of Functionalization: 10. Flocculation of Kaolin Dispersions. *Colloids and Surfaces A: Physicochemical and Engineering Aspects* **2005**, *254* (1), 75–80.

(18) Tadros, T. F. Adsorption of Polyvinyl Alcohol on Silica at Various pH Values and Its Effect on the Flocculation of the Dispersion. *Journal of Colloid and Interface Science* **1978**, *64* (1), 36–47.

(19) Sjöberg, M.; Bergström, L.; Larsson, A.; Sjöström, E. The Effect of Polymer and Surfactant Adsorption on the Colloidal Stability and Rheology of Kaolin Dispersions.

Colloids and Surfaces A: Physicochemical and Engineering Aspects **1999**, *159* (1), 197–208.

(20) Sakthivelu, S.; Manisha Vidyavathy, S.; Manohar, P. Effect of Polyvinyl Alcohol on Stability and Rheology of Nano Kaolinite Suspensions. *Transactions of the Indian Ceramic Society* **2012**, *71* (4), 175–180.

(21) Rubio, J.; Kitchener, J. A. The Mechanism of Adsorption of Poly (ethylene Oxide) Flocculant on Silica. *Journal of Colloid and Interface Science* **1976**, *57* (1), 132–142.

(22) Carasso, M. L.; Rowlands, W. N.; O'brien, R. W. The Effect of Neutral Polymer and Nonionic Surfactant Adsorption on the Electroacoustic Signals of Colloidal Silica. *Journal of colloid and interface science* **1997**, *193* (2), 200–214.

(23) Garvey, M. J.; Tadros, T. F.; Vincent, B. A Comparison of the Adsorbed Layer Thickness Obtained by Several Techniques of Various Molecular Weight Fractions of Poly (vinyl Alcohol) on Aqueous Polystyrene Latex Particles. *Journal of Colloid and Interface Science* **1976**, *55* (2), 440–453.

(24) Koopal, L. K.; Lyklema, J. Characterization of Adsorbed Polymers from Double Layer Experiments: The Effect of Acetate Groups in Polyvinyl Alcohol on Its Adsorption on Silver Iodide. *Journal of Electroanalytical Chemistry and Interfacial Electrochemistry* **1979**, *100* (1), 895–912.

(25) Garvey, M. J.; Tadros, T. F.; Vincent, B. A Comparison of the Volume Occupied by Macromolecules in the Adsorbed State and in Bulk Solution: Adsorption of Narrow

Molecular Weight Fractions of Poly (vinyl Alcohol) at the Polystyrene/water Interface. *Journal of Colloid and Interface Science* **1974**, *49* (1), 57–68.

(26) Joppien, G. R. Characterization of Adsorbed Polymers at the Charged Silica Aqueous Electrolyte Interface. *The Journal of Physical Chemistry* **1978**, *82* (20), 2210–2215.

(27) Brooks, D. E.; Seaman, G. V. F. The Effect of Neutral Polymers on the Electrokinetic Potential of Cells and Other Charged Particles: I. Models for the Zeta Potential Increase. *Journal of Colloid and Interface Science* **1973**, *43* (3), 670–686.

(28) Brooks, D. E. The Effect of Neutral Polymers on the Electrokinetic Potential of Cells and Other Charged Particles: II. A Model for the Effect of Adsorbed Polymer on the Diffuse Double Layer. *Journal of Colloid and Interface Science* **1973**, *43* (3), 687–699.

(29) Fleer, G. J.; Lyklema, J. Polymer Adsorption and Its Effect on the Stability of Hydrophobic Colloids. II. The Flocculation Process as Studied with the Silver Iodide-Polyvinyl Alcohol System. *Journal of Colloid and Interface Science* **1974**, *46* (1), 1–12.

(30) Van den Boomgaard, T.; King, T. A.; Tadros, T. F.; Tang, H.; Vincent, B. The Influence of Temperature on the Adsorption and Adsorbed Layer Thickness of Various Molecular Weight Fractions of Poly (vinyl Alcohol) on Polystyrene Latex Particles. *Journal of Colloid and Interface Science* **1978**, *66* (1), 68–76.

(31) Lambe, R.; Tadros, T. F.; Vincent, B. The Effect of Temperature, Particle Volume Fraction, and Polymer Concentration on the Stability of Aqueous Polystyrene Latex Dispersions in the Presence of Poly (vinyl Alcohol). *Journal of Colloid and Interface Science* **1978**, *66* (1), 77–84.

(32) Barker, M. C.; Garvey, M. J. The Effect of Solvency on the Adsorption of Poly (vinyl Alcohol) onto Polystyrene Latex. *Journal of Colloid and Interface Science* **1980**, *74* (2), 331–340.

(33) Tadros, T. F. The Interaction of Cetyltrimethylammonium Bromide and Sodium Dodecylbenzene Sulfonate with Polyvinyl Alcohol. Adsorption of the Polymer—surfactant Complexes on Silica. *Journal of Colloid and Interface Science* **1974**, *46* (3), 528–540.

(34) Ahmed, M.; Lai, B. F.; Kizhakkedathu, J. N.; Narain, R. Hyperbranched Glycopolymers for Blood Biocompatibility. *Bioconjugate chemistry* **2012**, *23* (5), 1050–1058.

(35) Deng, Z.; Li, S.; Jiang, X.; Narain, R. Well-Defined Galactose-Containing Multi-Functional Copolymers and Glyconanoparticles for Biomolecular Recognition Processes. *Macromolecules* **2009**, *42* (17), 6393–6405.

(36) Ahmed, M.; Narain, R. The Effect of Molecular Weight, Compositions and Lectin Type on the Properties of Hyperbranched Glycopolymers as Non-Viral Gene Delivery Systems. *Biomaterials* **2012**, *33* (15), 3990–4001.

(37) Wang, Y.; Narain, R.; Liu, Y. Study of Bacterial Adhesion on Different Glycopolymer Surfaces by Quartz Crystal Microbalance with Dissipation. *Langmuir* **2014**, *30* (25), 7377–7387.

(38) Deng, Z.; Ahmed, M.; Narain, R. Novel Well-Defined Glycopolymers Synthesized via the Reversible Addition Fragmentation Chain Transfer Process in Aqueous Media. *Journal of Polymer Science Part A: Polymer Chemistry* **2009**, *47* (2), 614–627.

(39) Deng, Z.; Bouchékif, H.; Babooram, K.; Housni, A.; Choytun, N.; Narain, R. Facile Synthesis of Controlled-Structure Primary Amine-Based Methacrylamide Polymers via the Reversible Addition-Fragmentation Chain Transfer Process. *Journal of Polymer Science Part A: Polymer Chemistry* **2008**, *46* (15), 4984–4996.

(40) Zeng, H., Hwang, D. S., Israelachvili, J. N., & Waite, J. H. Strong reversible Fe^{3+}-mediated bridging between dopa-containing protein films in water. *Pro*c. Natl. Acad. Sci. **2010,** *107*, 12850-12853.

(41) Israelachvili, J., Min, Y., Akbulut, M., Alig, A., Carver, G., Greene, W., Kristansen, K., Meyer, E., Pesika, N., Rosenberg, K., & Zeng, H. Recent advances in the surface forces apparatus (SFA) technique. *Rep. Prog. Phys*. **2010**, *73*, 036601.

(42) Lu, Q., Oh, D. X., Lee, Y., Jho, Y., Hwang, D. S., & Zeng, H. Nanomechanics of Cation–π Interactions in Aqueous Solution. *Angew.   Chem*. **2013**, *125*, 4036-4040.

(43) Zeng, H., Tian, Y., Zhao, B., Tirrell, M., & Israelachvili, J. Transient surface patterns and instabilities at adhesive junctions of viscoelastic films. *Macromolecules* **2007**, *40*, 8409-8422.

(44) Zeng, H., Tirrell, M., & Israelachvili, J. Limit cycles in dynamic adhesion and friction processes: A discussion. J. Adhes. **2006,** *82*, 933-943.

(45) Masliyah, J.; Czarnecki, J.; Xu, Z. Handbook on Theory and Practice of Bitumen Recovery from Athabasca Oil Sands. *Vol. I. Theoretical basis* **2010**.

(46) Lim, C.; Lee, D. W.; Israelachvili, J. N.; Jho, Y.; Hwang, D. S. Contact Time-and pH-Dependent Adhesion and Cohesion of Low Molecular Weight Chitosan Coated Surfaces. *Carbohydrate polymers* **2015**, *117*, 887–894.

(47) Lee, D. W.; Lim, C.; Israelachvili, J. N.; Hwang, D. S. Strong Adhesion and Cohesion of Chitosan in Aqueous Solutions. *Langmuir* **2013**, *29* (46), 14222–14229.

Chapter 5 Conclusion and Future work

5.1 Major conclusions

In this thesis, several types of homopolymers and copolymers were synthesized via conventional free radical polymerization for investigation of the settling performance of fine particles. In addition, the effects of various functional groups, temperature, pH, and molecular weight on flocculation of fine particles were investigated using various techniques. Gel permeation chromatography (GPC) and nuclear magnetic resonance (NMR) were used to characterize polymers. UV-Vis spectrometer was used to measure the clarity of the supernatant and lower critical solution temperature (LCST) of polymer. Zeta

potential measurements and settling tests were used to investigate the flocculation performance of polymers. Dynamic light scattering was used to determine the particle sizes in solution. The adhesion strength of the polymers on particle surfaces was determined by SFA, and the surface topography of polymers adsorbed on eparticle surface was determined by AFM.

1. Temperature and pH responsive random copolymers P(AEMA$_{51}$-*st*-MAAmBo$_{76}$-*st*-NIPAM$_{381}$) (PAMN) and glycopolymer poly (2-lactobionamidoethylmethacrylamide) (PLAEMA) have been synthesized via conventional free radical polymerization. NMR spectra were used to determine the composition of benzoboroxole groups (MAAmBo), amino-groups (AEMA), and NIPAAm in the polymer chains. GPC results were used to determine the molecular weight and polydispersity of polymers.

2. In the kaolin suspension (model tailings), the maximum initial settling rate (ISR) was found to be higher with low turbidity of supernatant recorded for PAMN at neutral pH, as compared to that of PAN and PNIPAAm. However, the solid content of the sediment treated by PAMN is lower due to the rigid structure arisen from strong attractive forces as compared to other two polymers.

3. The introduction of hydrophobic benzoboroxole groups in the PAMN contributed to the reduction of LCST, resulting in stronger hydrophobic interactions at high temperature,

which also overcomes the limited aspect that the incorporation of cationic segment leads to higher LCST as the case of PAN.

4. Increasing the temperature has a positive impact on ISR of the kaolin suspension for the cases of PAMN, PAN, PNIPAAm. However, the clarity of supernatant was less satisfactory as compared to the case of low temperature.

5. At pH 9, the suspension treated with PAMN showed the highest settling rate at a dosage of 25 ppm, resulting from the complexation of the negatively charged form of benzoboroxole groups and the hydroxyl groups on the particles surface. At pH 7, the adhesive interaction induced by PAMN was found to be relatively small due to the neutral form of benzoboroxole groups which was only able to provide hydrogen bonding to adsorb on the particle surface. At pH 11, anionic polymer was incapable to adsorb on fully negatively charged particle surface due to the strong and long-range electrostatic repulsion.

6. After high rate of settling at high temperature and pH 9, the secondary consolidation was achieved through increasing pH to 11. The charge transfer of PAMN allowed the reduction of strong adhesion between polymers and particles, contributing to the breakup of big flocs and enhanced consolidation.

7. The maximum of ISR and the lowest turbidity were achieved when the kaolin suspension was treated with the PLAEMA$_{975}$. However, the solid content of sediment in this case is relatively lower as compared to the cases of the other two smaller

molecular weight polymers. The strong adhesion between the galactose residue and hydroxyl groups prevent the sediment from consolidating well.

8. The adhesive interaction of PLAEMA and the kaolin particles increased with molecular weight, contributing to the formation of big flocs and high ISR. The surface topography obtained using AFM also proved that the polymer-polymer and polymer-particle adhesion increased with molecular weight of PLAEMA, attributed to larger amount of hydrogen bonding and high flexibility of long polymer chain.

5.2 The original contributions

In previous studies, incorporation of cationic segment to the temperature responsive NIPAAm based statistical copolymer was investigated to evaluate the flocculation behavior. For the non-ionic polymer case, the interaction of poly(vinyl alcohol) (PVA) and poly (ethylene oxide) (PEO) with kaolin and silica particles were widely studied. However, the research of using glycopolymer and the introduction of benzoboroxole groups in the copolymers to induce aggregation of particles is novel and for the first time. Since monomer LAEMA and MAAmBo were used to synthesize copolymer for the application in biomedical field due to their biocompatibility, they can be used as flocculants for water treatment with negligible harm to environment and health. The study of the interaction of galactose and benzoboroxole residues with kaolin particles provides new insights into the development of novel polymer flocculants and dewatering technology.

5.3 Future work

For the study of the flocculation behavior of benzoboroxole groups, fast initial settling rate and compact sediment can be achieved through controlling temperature and pH in the model settling test. However, several deeper issues need to be further investigated.

1. The molecular weight of PAMN used in this study is low for the commercial utilization. New polymerization procedure is necessary to synthesize benzoboroxole based copolymers with higher molecular weight for the development of commercial polymer flocculant.

2. The adhesion of PAMN to the mica surface was measured only at neutral pH by surface forces apparatus (SFA). The interaction mechanism can be further studied through force measurements at various pH conditions.

Only the effects of molecular weight and polymer dosage were shown in the flocculation study of PLAEMA.

1. Although the charge property of non-ionic polymers can hardly be influenced by changing solution pH, several studies with respect to the effect of pH on the interaction between non-ionic polymers such as poly (vinyl alcohol) (PVA) and poly (ethylene oxide) (PEO) and kaolin particles have shown that the surface charges of particles

could be changed at different pH conditions. Thus the pH effect on the flocculation of PLAEMA on kaolin particles can be further investigated.

2. The molecular weight distribution of PLAEMA$_{975}$ was very broad due to the poor homogeneity of solution, resulting from the sharply increased viscosity along with the polymerization. The polymerization protocol can be optimized to narrow the polydispersity.

All the settling tests were conducted with kaolin suspension, rather than real tailings. The settling tests using process water to prepare model tailings and settling tests on real tailings with synthesized polymers can be investigated in the future.

Bibliography

(1) Timilsina, G. R.; Prince, J. P.; Czamanski, D.; LeBlanc, N. Impacts of Crude Oil Production from Alberta Oil Sands on the Canadian Economy. In *EcoMod 2005 International Conference on Policy Modeling, Istanbul, June*; 2005.

(2) Berkowitz, N.; Speight, J. G. The Oil Sands of Alberta. *Fuel* **1975**, *54* (3), 138–149.

(3) Masliyah, J.; Zhou, Z. J.; Xu, Z.; Czarnecki, J.; Hamza, H. Understanding Water-Based Bitumen Extraction from Athabasca Oil Sands. *Can. J. Chem. Eng.* **2004**, *82* (4), 628–654.

(4) Söderbergh, B.; Robelius, F.; Aleklett, K. A Crash Programme Scenario for the Canadian Oil Sands Industry. *Energy Policy* **2007**, *35* (3), 1931–1947.

(5) Kelly, E. N.; Schindler, D. W.; Hodson, P. V.; Short, J. W.; Radmanovich, R.; Nielsen, C. C. Oil Sands Development Contributes Elements Toxic at Low Concentrations to the Athabasca River and Its Tributaries. *PNAS* **2010**, *107* (37), 16178–16183.

(6) Kelly, E. N.; Short, J. W.; Schindler, D. W.; Hodson, P. V.; Ma, M.; Kwan, A. K.; Fortin, B. L. Oil Sands Development Contributes Polycyclic Aromatic Compounds to the

Athabasca River and Its Tributaries. *Proceedings of the National Academy of Sciences* **2009**, *106* (52), 22346–22351.

(7) Rogers, V. V.; Wickstrom, M.; Liber, K.; MacKinnon, M. D. Acute and Subchronic Mammalian Toxicity of Naphthenic Acids from Oil Sands Tailings. *Toxicol. Sci.* **2002**, *66* (2), 347–355.

(8) El-Din, M. G.; Fu, H.; Wang, N.; Chelme-Ayala, P.; Pérez-Estrada, L.; Drzewicz, P.; Martin, J. W.; Zubot, W.; Smith, D. W. Naphthenic Acids Speciation and Removal during Petroleum-Coke Adsorption and Ozonation of Oil Sands Process-Affected Water. *Science of the Total Environment* **2011**, *409* (23), 5119–5125.

(9) Beynon, B. M.; Pemberton, S. G.; Bell, D. D.; Logan, C. A. Environmental Implications of Ichnofossils from the Lower Cretaceous Grand Rapids Formation, Cold Lake Oil Sands Deposit. **1988**.

(10) Liu, J.; Xu, Z.; Masliyah, J. Interaction between Bitumen and Fines in Oil Sands Extraction System: Implication to Bitumen Recovery. *The Canadian Journal of Chemical Engineering* **2004**, *82* (4), 655–666.

(11) Humphreys, R. D. *Tar Sands Extraction Process*; Google Patents, 1999.

(12) Filby, J.; Aviezer, S.; Tannenbaum, E. *Oil Sands Extraction*; Google Patents, 2010.

(13) Shin, H.; Polikar, M.; others. Optimizing the SAGD Process in Three Major Canadian Oil-Sands Areas. In *SPE Annual Technical Conference and Exhibition*; Society of Petroleum Engineers, 2005.

(14) Butler, R.; others. SAGD Comes of Age! *Journal of Canadian Petroleum Technology* **1998**, *37* (07).

(15) Masliyah, J.; Czarnecki, J.; Xu, Z. Handbook on Theory and Practice of Bitumen Recovery from Athabasca Oil Sands. *Vol. I. Theoretical basis* **2010**.

(16) Kasperski, K. L. A Review of Properties and Treatment of Oil Sands Tailings. *AOSTRA Journal of Research* **1992**, *8*, 11–11.

(17) Allen, E. W. Process Water Treatment in Canada's Oil Sands Industry: I. Target Pollutants and Treatment Objectives. *Journal of Environmental Engineering and Science* **2008**, *7* (2), 123–138.

(18) Xu, Y.; Dabros, T.; Kan, J. Filterability of Oil Sands Tailings. *Process Safety and Environmental Protection* **2008**, *86* (4), 268–276.

(19) Revington, A. P.; Omotoso, O.; Wells, P. S.; Hann, T. C.; Weiss, M. H.; Bugg, T.; Eastwood, J.; Young, S. J.; O'neill, H. R.; Sanchez, A. C.; et al. *Process for Flocculating and Dewatering Oil Sand Mature Fine Tailings*; Google Patents, 2010.

(20) Penner, T. J.; Foght, J. M. Mature Fine Tailings from Oil Sands Processing Harbour Diverse Methanogenic Communities. *Can. J. Microbiol.* **2010**, *56* (6), 459–470.

(21) Powter, C. B.; Biggar, K. W.; Silva, M. J.; McKenna, G. T.; Scordo, E. B. Review of Oil Sands Tailings Technology Options. In *Tailings and Mine Waste*; 2011; Vol. 10.

(22) Permien, T.; Lagaly, G. The Rheological and Colloidal Properties of Bentonite Dispersions in the Presence of Organic Compounds V. Bentonite and Sodium Montmorillonite and Surfactants. *Clays and Clay Minerals* **1995**, *43* (2), 229–236.

(23) Oster, J. D.; Shainberg, I.; Wood, J. D. Flocculation Value and Gel Structure of Sodium/calcium Montmorillonite and Illite Suspensions. *Soil Science Society of America Journal* **1980**, *44* (5), 955–959.

(24) McFarlane, A.; Bremmell, K.; Addai-Mensah, J. Improved Dewatering Behavior of Clay Minerals Dispersions via Interfacial Chemistry and Particle Interactions Optimization. *Journal of colloid and interface science* **2006**, *293* (1), 116–127.

(25) Allen, E. W. Process Water Treatment in Canada's Oil Sands Industry: II. A Review of Emerging Technologies. *Journal of Environmental Engineering and Science* **2008**, *7* (5), 499–524.

(26) Renault, S.; Lait, C.; Zwiazek, J. J.; MacKinnon, M. Effect of High Salinity Tailings Waters Produced from Gypsum Treatment of Oil Sands Tailings on Plants of the Boreal Forest. *Environmental Pollution* **1998**, *102* (2), 177–184.

(27) Chalaturnyk, R. J.; Scott, J. D.; Özüm, B. Management of Oil Sands Tailings. *Petroleum Science and Technology* **2002**, *20* (9-10), 1025–1046.

(28) Murray, H. H. Applied Clay Mineralogy Today and Tomorrow. *Clay minerals* **1999**, *34* (1), 39–39.

(29) Hu, Y.; Liu, X.; Xu, Z. Role of Crystal Structure in Flotation Separation of Diaspore from Kaolinite, Pyrophyllite and Illite. *Minerals Engineering* **2003**, *16* (3), 219–227.

(30) Ji, Y.; Lu, Q.; Liu, Q.; Zeng, H. Effect of Solution Salinity on Settling of Mineral Tailings by Polymer Flocculants. *Colloids and Surfaces A: Physicochemical and Engineering Aspects* **2013**, *430*, 29–38.

(31) Zhu, X.; Yan, C.; Winnik, F. M.; Leckband, D. End-Grafted Low-Molecular-Weight PNIPAM Does Not Collapse above the LCST. *Langmuir* **2007**, *23* (1), 162–169.

(32) Ohya, S.; Nakayama, Y.; Matsuda, T. Thermoresponsive Artificial Extracellular Matrix for Tissue Engineering: Hyaluronic Acid Bioconjugated with Poly (N-Isopropylacrylamide) Grafts. *Biomacromolecules* **2001**, *2* (3), 856–863.

(33) Lutz, J.-F.; Akdemir, Ö.; Hoth, A. Point by Point Comparison of Two Thermosensitive Polymers Exhibiting a Similar LCST: Is the Age of Poly (NIPAM) Over? *Journal of the American Chemical Society* **2006**, *128* (40), 13046–13047.

(34) Kawaguchi, H.; Fujimoto, K.; Mizuhara, Y. Hydrogel Microspheres III. Temperature-Dependent Adsorption of Proteins on Poly-N-Isopropylacrylamide Hydrogel Microspheres. *Colloid and Polymer Science* **1992**, *270* (1), 53–57.

(35) de las Heras Alarcón, C.; Farhan, T.; Osborne, V. L.; Huck, W. T.; Alexander, C. Bioadhesion at Micro-Patterned Stimuli-Responsive Polymer Brushes. *Journal of Materials Chemistry* **2005**, *15* (21), 2089–2094.

(36) Derjaguin, B. V.; Voropayeva, T. N. Surface Forces and the Stability of Colloids and Disperse Systems. *Journal of Colloid Science* **1964**, *19* (2), 113–135.

(37) Tabor, D.; Winterton, R. H. S. The Direct Measurement of Normal and Retarded van Der Waals Forces. In *Proceedings of the Royal Society of London A: Mathematical, Physical and Engineering Sciences*; The Royal Society, 1969; Vol. 312, pp 435–450.

(38) Israelachvili, J. N.; Adams, G. E. Measurement of Forces between Two Mica Surfaces in Aqueous Electrolyte Solutions in the Range 0–100 Nm. *Journal of the Chemical Society, Faraday Transactions 1: Physical Chemistry in Condensed Phases* **1978**, *74*, 975–1001.

(39) Israelachvili, J. N.; McGuiggan, P. M. Adhesion and Short-Range Forces between Surfaces. Part I: New Apparatus for Surface Force Measurements. *Journal of Materials Research* **1990**, *5* (10), 2223–2231.

(40) Israelachvili, J. N.; Adams, G. E. Direct Measurement of Long Range Forces between Two Mica Surfaces in Aqueous KNO3 Solutions. *Nature* **1976**, *262*, 774–776.

(41) Israelachvili, J. Direct Measurements of Forces between Surfaces in Liquids at the Molecular Level. *Proceedings of the National Academy of Sciences of the United States of America* **1987**, *84* (14), 4722.

(42) Israelachvili, J. N. Techniques for Direct Measurements of Forces between Surfaces in Liquids at the Atomic Scale. *Chemtracts Anal. Phys. Chem* **1989**, *1* (1).

(43) Israelachvili, J.; Min, Y.; Akbulut, M.; Alig, A.; Carver, G.; Greene, W.; Kristiansen, K.; Meyer, E.; Pesika, N.; Rosenberg, K.; et al. Recent Advances in the Surface Forces Apparatus (SFA) Technique. *Reports on Progress in Physics* **2010**, *73* (3), 036601.

(44) Chen, Y. L.; Helm, C. A.; Israelachvili, J. N. Measurements of the Elastic Properties of Surfactant and Lipid Monolayers. *Langmuir* **1991**, *7* (11), 2694–2699.

(45) Alig, A. R. G.; Gourdon, D.; Israelachvili, J. Properties of Confined and Sheared Rhodamine B Films Studied by SFA-FECO Spectroscopy. *The Journal of Physical Chemistry B* **2007**, *111* (1), 95–106.

(46) Luengo, G.; Tsuchiya, M.; Heuberger, M.; Israelachvili, J. Thin Film Rheology and Tribology of Chocolate. *Journal of food science* **1997**, *62* (4), 767–812.

(47) Israelachvili, J. N. Thin Film Studies Using Multiple-Beam Interferometry. *Journal of Colloid and Interface Science* **1973**, *44* (2), 259–272.

(48) Heuberger, M.; Luengo, G.; Israelachvili, J. Topographic Information from Multiple Beam Interferometry in the Surface Forces Apparatus. *Langmuir* **1997**, *13* (14), 3839–3848.

(49) Cantow, M. J. R. *Polymer Fractionation*; Elsevier, 2013.

(50) Giger, W.; Schaffner, C. Determination of Polycyclic Aromatic Hydrocarbons in the Environment by Glass Capillary Gas Chromatography. *Analytical Chemistry* **1978**, *50* (2), 243–249.

(51) Cazes, J. Gel Permeation chromatography—Part 1. *J. Chem. Educ.* **1966**, *43* (7), A567.

(52) Revil, A.; Pezard, P. A.; Glover, P. W. J. Streaming Potential in Porous Media: 1. Theory of the Zeta Potential. *Journal of Geophysical Research: Solid Earth (1978–2012)* **1999**, *104* (B9), 20021–20031.

(53) Eaton, D. R. Outer Sphere Complexes as Intermediates in Coordination Chemistry. *Reviews of chemical intermediates* **1988**, *9* (3), 201–232.

(54) Brar, S. K.; Verma, M. Measurement of Nanoparticles by Light-Scattering Techniques. *TrAC Trends in Analytical Chemistry* **2011**, *30* (1), 4–17.

(55) Apetz, R.; Van Bruggen, P. B. Transparent Alumina: A Light Scattering Model. *Journal of the American Ceramic Society; authors version* **2003**.

(56) Alamgir, A., Harbottle, D., Masliyah, J., Xu, Z. Al-PAM Assisted Filtration System for Abatement of Mature Fine Tailings. *Chem. Eng. Sci.* **2012**, *80*, 91-99.

(57) Li, H.; O'Shea, J. P.; Franks, G. V. Effect of Molecular Weight of Poly (N-Isopropyl Acrylamide) Temperature-Sensitive Flocculants on Dewatering. *AlChE J.* **2009**, *55*, 2070-2080.

(58) Li, H., Long, J., Xu, Z., Masliyah, J. H. Masliyah. Flocculation of Kaolinite Clay Suspensions Using a Temperature-Sensitive Polymer. *AlChE J.* **2007**, *53*, 479-488.

(59) O'Shea, J. P., Qiao, G. G., Franks, G. V. Temperature Responsive Flocculation and Solid–Liquid Separations with Charged Random Copolymers of Poly (N-isopropyl acrylamide). *J. Colloid Interface Sci.* **2011**, *360*, 61-70.

(60) O'Shea, J. P., Qiao, G. G., Franks, G. V. Temperature-Responsive Solid-Liquid Separations with Charged Block-Copolymers of Poly(N-isopropyl acryamide). *Langmuir* **2012**, *28*, 905-913.

(61) Wang, Y., Kotsuchibashi, Y., Liu, Y., Narain, R. Temperature-Responsive Hyperbranched Amine-Based Polymers for Solid-Liquid Separation. *Langmuir* **2014**, *30*, 2360-2368.

(62) Burdukova, E., Ishida, N., Shaddick, T., Franks, G. V. The Size of Particle Aggregates Produced by Flocculation with PNIPAM as a Function of Temperature. *J. Colloid Interface Sci.* **2011**, *354*, 82-88.

(63) Franks, G.V. Stimulant Sensitive Flocculation and Consolidation for Improved Solid/Liquid Separation. *J. Colloid Interface Sci.* **2005**, *292*, 598-603.

(64) Sakohara, S., Kimura, T., Nishikawa, K. Flocculation Mechanism of Suspended Particles Utilizing Hydrophilic/Hydrophobic Transition of Thermosensitive Polymer. *Kagaku Kogaku Ronbun.* **2000**, *26*, 734-737.

(65) O'Shea, J. P., Qiao, G. G., Franks, G. V. Solid–Liquid Separations with a Temperature-Responsive Polymeric Flocculant: Effect of Temperature and Molecular Weight on Polymer Adsorption and Deposition. *J. Colloid Interface Sci.* **2010**, *348*, 9-23.

(66) Hogg, R. Flocculation and Dewatering. *Int. J. Miner. Process.* **2000**, *58*, 223-236.

(67) Sakohara, S., Ochiai, E., Kusaka, T. Dewatering of Activated Sludge by Thermosensitive Polymers. *Sep. Purif. Technol.* **2007**, *56*, 296-302.

(68) Franks, G. V.; O'Shea, J. P.; Forbes, E. Improved Solid-Liquid Separations with Temperature Responsive Flocculants: A Review. *Chemeca 2012: Quality of life through chemical engineering: 23-26 September 2012, Wellington, New Zealand* **2012**, 1062.

(69) Liu, H. Y., Zhu, X. X. Lower Critical Solution Temperatures of N-Substituted

Acrylamide Copolymers in Aqueous Solutions. *Polymer* **1999**, *40*, 6985-6990.

(70) Cho, S. H., Jhon, M. S., Yuk, S. H. Temperature-Sensitive Swelling Behavior of

Polymer Gel Composed of Poly N,N-Dimethylaminoethyl Methacrylate) and Its

Copolymers. *Eur. Polym. J.* **1999**, *35*, 1841-1845.

(71) Cho, S. H., Jhon, M. S., Yuk, S. H. Effect of Comonomer Hydrophilicity and

Ionization on The Lower Critical Solution Temperature of N-Isopropylacrylamide

Copolymers. *Macromolecules* **1993**, *26*, 2496-2500.

(72) Kotsuchibashi, Y., Agustin, R. V. C., Lu, J. Y., Hall, D. G., Narain, R. Temperature,

pH, and Glucose Responsive Gels via Simple Mixing of Boroxole-and Glyco-Based

Polymers. *ACS Macro Letters* **2013**, *2*, 260-264.

(73) Kitano, S., Koyama, Y., Kataoka, K., Okano, T., Sakurai, Y. A Novel Drug Delivery

System Utilizing a Glucose Responsive Polymer Complex between Poly (Vinyl Alcohol)

and Poly (N-Vinyl-2-Pyrrolidone) with a Phenylboronic Acid Moiety. *J. Controlled*

Release **1992**, *19*, 161-170.

(74) Shiino, D.; Murata, Y.; Kubo, A.; Kim, Y. J.; Kataoka, K.; Koyama, Y.; Kikuchi, A.; Yokoyama, M.; Sakurai, Y.; Okano, T. Amine Containing Phenylboronic Acid Gel for Glucose-Responsive Insulin Release under Physiological pH. *J. Controlled Release* **1995**, *37*, 269-276.

(75) Hall, D. G., Lee, J. C., Ding, J. Catalytic Enantioselective Transformations of Borylated Substrates: Preparation and Synthetic Applications of Chiral Alkylboronates. *Pure Appl. Chem.* **2012**, *84*, 2263-2277.

(76) Ma, R., Shi, L. Phenylboronic Acid-Based Glucose-Responsive Polymeric Nanoparticles: Synthesis and Applications in Drug Delivery. *Polym. Chem.* **2014**, *5*, 1503-1518.

(77) O'Day, P. A., Parks, G. A., Brown Jr, G. E. Molecular Structure and Binding Sites of Cobalt (ii) Surface Complexes on Kaolinite from X-Ray Absorption Spectroscopy. *Clays Clay Miner.* **1994**, *42*, 337-355.

(78) Giese, R. F. Hydroxyl Orientations in Gibbsite and Bayerite. *Acta Crystallogr., Sect. B: Struct. Sci.* **1976**, *32*, 1719-1723.

(79) Gupta, V., Miller, J. D. Miller. Surface Force Measurements at the Basal Planes of Ordered Kaolinite Particles. *J. Colloid Interface Sci.* **2010**, *344*, 362-371.

(80) Chan, M. C. W. A Novel Flocculant for Enhanced Dewatering of Oil Sands Tailings. *Master Thesis, University of Alberta, Edmonton,* **2011**.

(81) Michaels, A. S., Bolger, J. C. Settling Rates and Sediment Volumes of Flocculated Kaolin Suspensions. *Ind. Eng. Chem. Fundam.* **1962**, *1*, 24-33.

(82) Zbik, M. S., Smart, R. S. C., Morris, G. E. Kaolinite Flocculation Structure. *J. Colloid Interface Sci.* **2008**, *328*, 73-80.

(83) Nasser, M. S., James, A. E. The Effect of Polyacrylamide Charge Density and Molecular Weight on the Flocculation and Sedimentation Behaviour of Kaolinite Suspensions. *Sep. Purif. Technol.* **2006**, *52*, 241-252.

(84) Deng, Z., Bouchékif, H., Babooram, K., Housni, A., Choytun, N., Narain, R. Facile Synthesis of Controlled-Structure Primary Amine‐Based Methacrylamide Polymers via the Reversible Addition-Fragmentation Chain Transfer Process. *J. Polym. Sci., Part A: Polym. Chem.* **2008**, *46*, 4984-4996.

(85) Zeng, H., Hwang, D. S., Israelachvili, J. N., Waite, J. H. Strong Reversible Fe3+-Mediated Bridging between Dopa-Containing Protein Films in Water. *Proc. Natl. Acad. Sci. U. S. A.* **2010**, *107*, 12850-12853.

(86) Zeng, H., Tian, Y., Zhao, B., Tirrell, M., Israelachvili, J. Transient Surface Patterns and Instabilities at Adhesive Junctions of Viscoelastic Films. *Macromolecules* **2007**, *40*, 8409-8422.

(87) Lu, Q., Oh, D. X., Lee, Y., Jho, Y., Hwang, D. S., Zeng, H. Nanomechanics of Cation–Π Interactions in Aqueous Solution. *Angew.   Chem*. **2013**, *125*, 4036-4040.

(88) Zeng, H., Tirrell, M., Israelachvili, J. Limit Cycles in Dynamic Adhesion and Friction Processes: A Discussion. *J. Adhes.* **2006**, *82*, 933-943.

(89) Zeng, H., Tian, Y., Anderson, T. H., Tirrell, M., Israelachvili, J. N. New SFA Techniques for Studying Surface Forces and Thin Film Patterns Induced by Electric Fields. *Langmuir* **2008**, *24*, 1173-1182.

(90) Hong, K., Zhang, H., Mays, J. W., Visser, A. E., Brazel, C. S., Holbrey, J. D., Reichert, W. M., Rogers, R. D. Conventional Free Radical Polymerization in Room

Temperature Ionic Liquids: A Green Approach to Commodity Polymers with Practical

Advantages. *Chem. Commun.* **2002**, 1368-1369.

(91) Zhang, H., Hong, K., Mays, J. W. Synthesis of Block Copolymers of Styrene and

Methyl Methacrylate by Conventional Free Radical Polymerization in Room

Temperature Ionic Liquids. *Macromolecules* **2002**, *35*, 5738-5741.

(92) Zhang, F., Wang, C. C. Preparation of P (NIPAM-Co-AA) Microcontainers

Surface-Anchored with Magnetic Nanoparticles. *Langmuir* **2009**, *25*, 8255-8262.

(93) Mears, S. J., Deng, Y., Cosgrove, T., Pelton, R. Structure of Sodium Dodecyl

Sulfate Bound to a Poly (NIPAM) Microgel Particle. *Langmuir* **1997**, *13*, 1901-1906.

(94) Kang, L., John L. C. Temperature Effects on Flocculation Kinetics Using Fe (iii)

Coagulant. *J. Environ. Eng.* **1995**, 12, 893-901.

(95) Franks, G., Burdukova, E., Li, H., Ishida, N., O'Shea, J. P. Mechanism Responsible

for Flocculation in Poly (N-Isopropylacrylamide) Temperature Resposive

Dewatering-Attractive Interaction Force Induced by Surface Hydrophobicity. *In 25th Int.*

Miner. Process. Congr. Brisbane, Queensland, Australia, 4057-4067, **2011**.

(96) Franks, G. V., Li, H., O'Shea, J. P., Qiao, G. G. Temperature Responsive Polymers as Multiple Function Reagents in Mineral Processing. *Adv. Powder Technol.* **2009**, *20*, 273-279.

(97) Adam, W., Baeza, J., Liu, J. C. Stereospecific Introduction of Double Bounds via Thermolysis of Beta-Lactones. *J. Am. Chem. Soc.* **1972**, *94*, 2000-2006.

(98) Alidedeoglu, A. H., York, A. W., McCormick, C. L., Morgan, S. E. Aqueous Raft Polymerization of 2-Aminoethyl Methacrylate to Produce Well-Defined, Primary Amine Functional Homo-and Copolymers. *J. Polym. Sci., Part A: Polym. Chem.* **2009**, *47*, 5405-5415.

(99) Pauling, L. The Structure of the Micas and Related Minerals. *Proc. Natl. Acad. Sci. U. S. A.* **1930**, 16, 123.

(100) Nasim, T.; Bandyopadhyay, A. Introducing Different Poly (vinyl Alcohol) s as New Flocculant for Kaolinated Waste Water. *Separation and Purification Technology* **2012**, *88*, 87–94.

(101) O'Shea, J.-P.; Qiao, G. G.; Franks, G. V. Temperature Responsive Flocculation and Solid–liquid Separations with Charged Random Copolymers of poly (N-Isopropyl Acrylamide). *Journal of Colloid and Interface Science* **2011**, *360* (1), 61–70.

(102) Stauber, J. L.; Florence, T. M.; Davies, C. M.; Adams, M. S.; Buchanan, S. J. Bioavailability. **1999**.

(103) Yang, Z.; Shang, Y.; Lu, Y.; Chen, Y.; Huang, X.; Chen, A.; Jiang, Y.; Gu, W.; Qian, X.; Yang, H.; et al. Flocculation Properties of Biodegradable Amphoteric Chitosan-Based Flocculants. *Chemical Engineering Journal* **2011**, *172* (1), 287–295.

(104) Chen, Y.; Liu, S.; Wang, G. A Kinetic Investigation of Cationic Starch Adsorption and Flocculation in Kaolin Suspension. *Chemical Engineering Journal* **2007**, *133* (1), 325–333.

(105) Järnström, L.; Lason, L.; Rigdahl, M. Flocculation in Kaolin Suspensions Induced by Modified Starches 1. Cationically Modified Starch—effects of Temperature and Ionic Strength. *Colloids and Surfaces A: Physicochemical and Engineering Aspects* **1995**, *104* (2), 191–205.

(106) Bratskaya, S.; Schwarz, S.; Liebert, T.; Heinze, T. Starch Derivatives of High Degree of Functionalization: 10. Flocculation of Kaolin Dispersions. *Colloids and Surfaces A: Physicochemical and Engineering Aspects* **2005**, *254* (1), 75–80.

(107) Tadros, T. F. Adsorption of Polyvinyl Alcohol on Silica at Various pH Values and Its Effect on the Flocculation of the Dispersion. *Journal of Colloid and Interface Science* **1978**, *64* (1), 36–47.

(108) Sjöberg, M.; Bergström, L.; Larsson, A.; Sjöström, E. The Effect of Polymer and Surfactant Adsorption on the Colloidal Stability and Rheology of Kaolin Dispersions. *Colloids and Surfaces A: Physicochemical and Engineering Aspects* **1999**, *159* (1), 197–208.

(109) Sakthivelu, S.; Manisha Vidyavathy, S.; Manohar, P. Effect of Polyvinyl Alcohol on Stability and Rheology of Nano Kaolinite Suspensions. *Transactions of the Indian Ceramic Society* **2012**, *71* (4), 175–180.

(110) Rubio, J.; Kitchener, J. A. The Mechanism of Adsorption of Poly (ethylene Oxide) Flocculant on Silica. *Journal of Colloid and Interface Science* **1976**, *57* (1), 132–142.

(111) Carasso, M. L.; Rowlands, W. N.; O'brien, R. W. The Effect of Neutral Polymer and Nonionic Surfactant Adsorption on the Electroacoustic Signals of Colloidal Silica. *Journal of colloid and interface science* **1997**, *193* (2), 200–214.

(112) Garvey, M. J.; Tadros, T. F.; Vincent, B. A Comparison of the Adsorbed Layer Thickness Obtained by Several Techniques of Various Molecular Weight Fractions of Poly (vinyl Alcohol) on Aqueous Polystyrene Latex Particles. *Journal of Colloid and Interface Science* **1976**, *55* (2), 440–453.

(113) Koopal, L. K.; Lyklema, J. Characterization of Adsorbed Polymers from Double Layer Experiments: The Effect of Acetate Groups in Polyvinyl Alcohol on Its Adsorption on Silver Iodide. *Journal of Electroanalytical Chemistry and Interfacial Electrochemistry* **1979**, *100* (1), 895–912.

(114) Garvey, M. J.; Tadros, T. F.; Vincent, B. A Comparison of the Volume Occupied by Macromolecules in the Adsorbed State and in Bulk Solution: Adsorption of Narrow Molecular Weight Fractions of Poly (vinyl Alcohol) at the Polystyrene/water Interface. *Journal of Colloid and Interface Science* **1974**, *49* (1), 57–68.

(115) Joppien, G. R. Characterization of Adsorbed Polymers at the Charged Silica Aqueous Electrolyte Interface. *The Journal of Physical Chemistry* **1978**, *82* (20), 2210–2215.

(116) Brooks, D. E.; Seaman, G. V. F. The Effect of Neutral Polymers on the Electrokinetic Potential of Cells and Other Charged Particles: I. Models for the Zeta Potential Increase. *Journal of Colloid and Interface Science* **1973**, *43* (3), 670–686.

(117) Brooks, D. E. The Effect of Neutral Polymers on the Electrokinetic Potential of Cells and Other Charged Particles: II. A Model for the Effect of Adsorbed Polymer on the Diffuse Double Layer. *Journal of Colloid and Interface Science* **1973**, *43* (3), 687–699.

(118) Fleer, G. J.; Lyklema, J. Polymer Adsorption and Its Effect on the Stability of Hydrophobic Colloids. II. The Flocculation Process as Studied with the Silver Iodide-Polyvinyl Alcohol System. *Journal of Colloid and Interface Science* **1974**, *46* (1), 1–12.

(119) Van den Boomgaard, T.; King, T. A.; Tadros, T. F.; Tang, H.; Vincent, B. The Influence of Temperature on the Adsorption and Adsorbed Layer Thickness of Various

Molecular Weight Fractions of Poly (vinyl Alcohol) on Polystyrene Latex Particles. *Journal of Colloid and Interface Science* **1978**, *66* (1), 68–76.

(120) Lambe, R.; Tadros, T. F.; Vincent, B. The Effect of Temperature, Particle Volume Fraction, and Polymer Concentration on the Stability of Aqueous Polystyrene Latex Dispersions in the Presence of Poly (vinyl Alcohol). *Journal of Colloid and Interface Science* **1978**, *66* (1), 77–84.

(121) Barker, M. C.; Garvey, M. J. The Effect of Solvency on the Adsorption of Poly (vinyl Alcohol) onto Polystyrene Latex. *Journal of Colloid and Interface Science* **1980**, *74* (2), 331–340.

(122) Tadros, T. F. The Interaction of Cetyltrimethylammonium Bromide and Sodium Dodecylbenzene Sulfonate with Polyvinyl Alcohol. Adsorption of the Polymer—surfactant Complexes on Silica. *Journal of Colloid and Interface Science* **1974**, *46* (3), 528–540.

(123) Ahmed, M.; Lai, B. F.; Kizhakkedathu, J. N.; Narain, R. Hyperbranched Glycopolymers for Blood Biocompatibility. *Bioconjugate chemistry* **2012**, *23* (5), 1050–1058.

(124) Deng, Z.; Li, S.; Jiang, X.; Narain, R. Well-Defined Galactose-Containing Multi-Functional Copolymers and Glyconanoparticles for Biomolecular Recognition Processes. *Macromolecules* **2009**, *42* (17), 6393–6405.

(125) Ahmed, M.; Narain, R. The Effect of Molecular Weight, Compositions and Lectin Type on the Properties of Hyperbranched Glycopolymers as Non-Viral Gene Delivery Systems. *Biomaterials* **2012**, *33* (15), 3990–4001.

(126) Wang, Y.; Narain, R.; Liu, Y. Study of Bacterial Adhesion on Different Glycopolymer Surfaces by Quartz Crystal Microbalance with Dissipation. *Langmuir* **2014**, *30* (25), 7377–7387.

(127) Deng, Z.; Ahmed, M.; Narain, R. Novel Well-Defined Glycopolymers Synthesized via the Reversible Addition Fragmentation Chain Transfer Process in Aqueous Media. *Journal of Polymer Science Part A: Polymer Chemistry* **2009**, *47* (2), 614–627.

(128) Deng, Z.; Bouchékif, H.; Babooram, K.; Housni, A.; Choytun, N.; Narain, R. Facile Synthesis of Controlled-Structure Primary Amine-Based Methacrylamide Polymers via the Reversible Addition-Fragmentation Chain Transfer Process. *Journal of Polymer Science Part A: Polymer Chemistry* **2008**, *46* (15), 4984–4996.

(129) Lim, C.; Lee, D. W.; Israelachvili, J. N.; Jho, Y.; Hwang, D. S. Contact Time-and pH-Dependent Adhesion and Cohesion of Low Molecular Weight Chitosan Coated Surfaces. *Carbohydrate polymers* **2015**, *117*, 887–894.

(130) Lee, D. W.; Lim, C.; Israelachvili, J. N.; Hwang, D. S. Strong Adhesion and Cohesion of Chitosan in Aqueous Solutions. *Langmuir* **2013**, *29* (46), 14222–14229.